UNIVERSITY OF ALBERTA

The developmental effects of dominant *invected* and *vestigial* mutations in *Drosophila melanogaster*

BY

Andrew Simmonds ©

A thesis submitted to the Faculty of Graduate Studies and Research in partial
fulfillment of the requirements for the degree of Doctor of Philosophy

IN

MOLECULAR BIOLOGY AND GENETICS

DEPARTMENT OF BIOLOGICAL SCIENCES

Edmonton Alberta

Spring, 1997

National Library
of Canada

Acquisitions and
Bibliographic Services

395 Wellington Street
Ottawa ON K1A 0N4
Canada

Bibliothèque nationale
du Canada

Acquisitions et
services bibliographiques

395, rue Wellington
Ottawa ON K1A 0N4
Canada

Your file Votre référence

Our file Notre référence

The author has granted a non-exclusive licence allowing the National Library of Canada to reproduce, loan, distribute or sell copies of his/her thesis by any means and in any form or format, making this thesis available to interested persons.

The author retains ownership of the copyright in his/her thesis. Neither the thesis nor substantial extracts from it may be printed or otherwise reproduced with the author's permission.

L'auteur a accordé une licence non exclusive permettant à la Bibliothèque nationale du Canada de reproduire, prêter, distribuer ou vendre des copies de sa thèse de quelque manière et sous quelque forme que ce soit pour mettre des exemplaires de cette thèse à la disposition des personnes intéressées.

L'auteur conserve la propriété du droit d'auteur qui protège sa thèse. Ni la thèse ni des extraits substantiels de celle-ci ne doivent être imprimés ou autrement reproduits sans son autorisation.

0-612-21636-5

Canada

UNIVERSITY OF ALBERTA

RELEASE FORM

NAME OF AUTHOR: Andrew Simmonds

TITLE OF THESIS: The developmental effects of dominant *invected* and *vestigial* mutations in *Drosophila melanogaster*

DEGREE: Doctor of Philosophy

YEAR THIS DEGREE GRANTED: 1997

Permission is hereby granted to the University of Alberta Library to reproduce single copies of this thesis and to lend or sell such copies for private, scholarly or scientific research purposes only.

The author reserves all other publication and other rights in association with the copyright of the thesis, and except as hereinbefore provided neither the thesis nor any substantial portion thereof may be printed or otherwise reproduced in any material form whatever without the author's prior written permission.

Andrew Simmonds
#202 8015 106 St.
Edmonton, Alberta
Canada
T6E 5P1
March 27, 1997

UNIVERSITY OF ALBERTA

FACULTY OF GRADUATE STUDIES AND RESEARCH

The undersigned certify that they have read, and recommended to the Faculty of Graduate Studies and Research for acceptance, a thesis entitled "The developmental effects of dominant *invected* and *vestigial* mutations in *Drosophila melanogaster*" submitted by Andrew Simmonds in partial fulfillment of the requirements for the degree of Doctor of Philosophy in Molecular Biology and Genetics.

John B Bell
Dr. John Bell

Dr. David Nash

Dr. David Pilgrim

Paul F Lasko
Dr. Paul Lasko

Charlotte Spencer
Dr. Charlotte Spencer

This thesis is dedicated to my family, who, while not quite sure exactly what it is that I do, care enough to be proud of me anyway.

Abstract

The *vestigial* (*vg*) gene product is required for the proper formation of the wing and haltere appendages of *Drosophila melanogaster*. The absence of significant expression of *vg* protein within the primordia wing cells of the larval wing imaginal disc has been correlated with the apoptotic death of these cells and the subsequent loss of elements of the adult wing. Thus, it is likely that *vg* represents an important element required for the patterning and formation of the *Drosophila* wing. The easily detectable phenotype associated with *vg* mutations has meant that an extremely large collection of mutants of this gene has been examined. However, of all mutations within *vg*, only two fully dominant alleles, vg^{W} and vg^{U} are currently known to exist. This study outlines a revertant analysis of vg^{W} and vg^{U} showing that the *vg* sequences associated with the dominant alleles are critical for mediating dominance. The dominant effect associated with vg^{W} and vg^{U} is not due to suppression of *vg* expression within all cells of the organism. Rather the dominant *vg* phenotype stems from specific disruption of *vg* patterning during the late third larval instar within the portion of the wing disc fated to form the wing. A homeotic transformation of anterior to posterior fate within the wing associated with vg^{W} is independent of the wing loss phenotype and is instead due to ectopic expression of the *invected* (*inv*) protein driven by control elements of *vg*. This allele, inv^{D}, was used to show that *inv* can confer posterior identity without affecting establishment of the anterior-posterior compartment boundary within the wing. Finally, a possible function for the *vg* is suggested by the presence of significant *in vitro* affinity of the *vg* protein to the

scalloped (*sd*) protein, a *Drosophila* transcription factor. Interaction of *vg* and *sd* protein can be eliminated by removing a segment of the C-terminal portion of the Vg. This suggests a model in which the expression of *vg* is established from a number of patterning systems to specify wing identity within the wing compartment through the activity of *sd*.

Acknowledgements

I would like to acknowledge some of the people that helped make this work possible. First, thanks to Dr. John Bell, for providing a wonderful environment to research whatever it was that I saw fit. Many times, when I was focused upon some petty annoyance, he would help provide perspective and advice as to what was truly important. That, and perhaps the occasional beer or two as well. I also was lucky to have excellent technical help within the lab from Tove and Matt Reece, as well as Sandra O'Keefe, Denise Adams, Effie Woloshyn and Bill Clark who patiently answered many of my questions. Other graduate students within the Bell lab deserve special mention including Audrey Atkin, Ali Riazi and especially Kelly Soanes, who made the last few years in the lab a very pleasant and enjoyable time. Within the Genetics wing, the "Drosophila group" was always an invaluable resource. Thanks to Millan Patel, Michelle Schouls, Tim Heslip, Bill Brook and Eugene Chomey who were not only excellent sources of information and fly stocks, but often interesting roommates at conferences. Special thanks as well to Nancy Nesslinger, Petra Jackle-Baldwin, Rosanna Baker and Mark Hicks, both fellow graduate students and good friends. I also wish to thank Dr. Henry Krause at the University of Toronto, who let me work in his lab for a summer and to the residents of the C.H. Best Institute who had to put up with my many questions and boisterous personality.

Last and most importantly, I want to thank Sarah Hughes, my best friend, fellow fly-pusher, proofreader, hiking partner, collaborator and M.K.W for everything.

Table of Contents

Chapter I - Introduction **1**

Chapter II - Reversion analysis of the dominant *vg*^{W} and *vg*^{U} alleles **29**

Introduction 29

Results 38

Discussion 76

Chapter III - Distinguishable functions for the *engrailed* and *invected* genes of *Drosophila* **85**

Introduction 85

Results 90

Discussion 115

Chapter IV - *In vitro* interactions between the *vg* and *sd* protein **122**

Introduction 122

Results 126

Discussion 135

Chapter V - General Discussion **140**

Chapter VI - Materials and Methods **152**

Origin and Maintenance of Drosophila stocks 152

Immunohistochemistry 152

Southern Hybridizations 161

PCR analysis of genomic DNA 163

Western blot analysis 163

RT-PCR detection of *vg* transcripts 165

Acridine orange staining of imaginal discs 165

β-galactosidase staining of imaginal discs 152

Mounting adult tissues 166

Preparation of specific anti-sense RNA probes and whole mount *in-situ* hybridization to imaginal discs 167
Cloning of the *vg* and *sd* ORF into the pET 16b bacterial expression vector 174
Preparation of plasmid DNA 176
Far-Western Blot Analysis 182
Bibliography 85

List of Tables

Table II -1. Summary of the revertant strains produced from mutagenesis of the vg^U and vg^W dominant alleles. 43

Table III -1 The phenotypes of inv^D heterozygous to alleles of *en*, *inv* and *vg*. 112

Table VI -1 Genotypes of stocks used in this study. 155

Table VI -2 Antibodies and conjugates used for immunohistochemical studies 160

Table VI -3 Primers used for analysis of revertant alleles 164

Table VI -4Primers used to create expression constructs of *vg* and *sd*. 177

List of Figures

Figure I-1 The location of the imaginal discs within the *Drosophila* larva. 3

Figure I-2 A fate map of the late third instar wing imaginal disc 7

Figure I-3 Expression of *vg* within the wing pouch of the wing imaginal disc is established by the activity of multiple patterning pathways. 14

Figure I-4 The structure of the *Drosophila melanogaster* wing. 18

Figure I-5 The structure of the *Drosophila melanogaster* haltere. 20

Figure I-6 Classification of the severity of the loss of wing phenotype associated with *vg* mutations. 23

Figure II-1 A diagram illustrating the chromosomal inversions that produce the dominant alleles vg^W and vg^U 31

Figure II-2 Wing phenotypes produced by revertants of vg^W and vg^U. 39

Figure II-3 The localization of *vg* expression within third instar wing discs. 46

Figure II-4 Alterations within the *vg* portion of the revertant alleles of vg^W and vg^U alleles are associated with a partial revertant phenotype. 50

Figure II-5 A physical map of revertants affecting the *vg* region of the vg^W and vg^U alleles. 52

Figure II-6 Western blot analysis of *vg* protein expression in the presence of dominant *vg* alleles. 55

Figure II-7 RNA transcripts containing *vg* sequences can be detected from the vg^W dominant allele and its derivatives. 60

Figure II-8 The presence of dominant *vg* alleles does not affect early *vg* expression. 62

Figure II-9 Altered patterns of apoptotic cell death associated with the dominant *vg* activity. 66
Figure II-10 The expression of *wg, sd* the *vg* intron-2, and the intron-4
Figure II-11 Dual antibody detection of *vg* and *wg* protein in vg^W and vg^U......... 73
Figure III-1. Wings from inv^P flies show a homeotic transformation of anterior to posterior wing. 92
Figure III-2 Alterations are seen in the localization of *vg* and *inv* / *en* protein in late third instar wing imaginal discs derived from inv^P/+ larvae. 95
Figure III-3 In situ analysis with specific *inv* or *en* probes indicates that only *inv* is ectopically expressed in the anterior compartment. 98
Figure III-4 A deletion in the 3' end of the *vg* coding region of vg^W causes the inv^P phenotype. 100
Figure III-5 Dual confocal immunofluorescent images showing expression of A/P and D/V patterning genes in larval wing discs from inv^P third instar larvae. 104
Figure III-6 The inv^P allele shows a temperature dependent phenotype. 109
Figure III-7 The inv^P phenotype is enhanced by alleles of *en* and *ph* but not by *inv*. 113
Figure IV-1 The *vg* and *sd* ORFs cloned into the pET16b expression vector allows the production of full length *vg* and *sd* proteins. 128
Figure IV-2 A strong *in vitro* interaction is detected between full-length *vg* and *sd* proteins. 131

Figure IV-3 A 78 amino acid region within the *vg* protein is necessary for binding Sd.. 133

Figure VI-1 Mutagenesis of vg^W and vg^U to obtain revertant alleles................. 153

Figure VI-2 *vg* cDNA-1 in pBluescriptSK+ for making full-length anti-sense *vg* RNA probes.. 168

Figure VI-3 A plasmid for making *inv* RNA anti-sense probes that will recognize *inv* but not *en* transcripts *in-situ*. 170

Figure VI-4 Constructs containing the *vg* ORF that allow for bacterial or *in vitro* expression of full-length *vg* protein. 178

Figure VI-5 Constructs containing the *sd* ORF to allow for bacterial or *in vitro* expression of *sd* protein.. 180

List of Abbreviations

A/P	anterior-posterior
AEL	after egg laying
AP	alkaline phosphatase
BCIP	5'-bromo-chloro-indol-phosphate
bp	base pair
BSA	bovine serum albumin
Cy3	Indocarbocyanine
D/V	dorsal-ventral
DAB	diamino-benzine
DABCO	1,4-Diazabicyclo [2.2.2] octane
Df	deficiency
DIG	digoxigenin
DMSO	dimethyl-sulfoxide
DNA	deoxyribonucleic acid
DNase	deoxyribonuclease
DTT	dithiothreitol
ATP	adenosine-triphosphate
dNTPs	deoxy-nucleotide-triphospates
dUTP	deoxy-uracil-triphosphate
EDTA	ethylenediaminetetracetic acid
FITC	fluorescein isothiocyanate
GAL4	*Gal4* binding domain of yeast
Gy	gray
HRP	horse radish peroxidase
In	inversion
LB	Luria Broth
mRNA	messenger ribonucleic acid
NaOH	sodium hydroxide
NBT	nitro-blue tetrazolium
NP-40	Nonidet P-40
ORF	open reading frame
P/D	proximal-distal
PAGE	polyacrylamide gel electrophoresis
PBS	phosphate buffered saline
PBT	1 x phosphate buffered saline + 0.1% Tween 20
PBN	1 x phosphate buffered saline, 0.5% NP-40
PBNB	phosphate buffered saline + 0.5% NP-40 + 1% BSA
PBTB	phosphate buffered saline + 0.1% Tween-20 + 1% BSA
PCR	polymerase chain reaction
Pfu	*Pyrococcus fumerensis*
RNA	ribonucleic acid
RNase	ribonuclease
rpm	rotations per minute
RT	reverse transcriptase
SDS	sodium dodecyl sulphate

SSC	3M NaCl, 0.3M Sodium Citrate, pH 7.0
T1	first thoracic segment
T2	second thoracic segment
T3	third thoracic segment
Taq	*Thermus aquaticus*
TGF-β	transforming growth factor β
TIFF	tagged image file format
Tris-HCl	tris-hydroxmethyl aminomethane hydrochloride
TR	Texas Red Sulfonyl Chloride
tRNA	transfer ribonucleic acid
UAS	upstream activation sequence

List of Symbols

α	alpha
β	beta
°C	degree Celsius
γ	gamma
μ	micro
f	femto
g	gram
g	gravitational force
k	kilo
l	litre
m	milli
M	molar
n	nano
N	normal
p	pico
s	second
V	volts
W	watts

List of *Drosophila* Genetic Symbols

al	*aristaless*
ap	*apterous*
Antp	*Antennapedia*
Ant-C	*Antennapedia gene complex*
Bc	*Black cell*
bx	*bithorax*
Bx-C	*Bithorax gene complex*
Cbx	*Contrabithorax*
ci	*cubitus interruptus*
ct	*cut*
Cy	*Curly*
CyO	*Curly of Oster*, second chromosome balancer
dac	*dachshund*
Dfd	*Deformed*
Dl	*Delta*
Dll	*Distalless*
dpp	*decapentaplegic*
Dw	*Dorsal wing*
Elp	*Ellipse (EGFR)*
en	*engrailed*
esg	*escargot*
ey	*eyeless*
fng	*fringe*
Gla	*Glazed*
hh	*hedgehog*
inv	*invected*
lab	*labial*
mam	*mastermind*
N	*Notch*
omb	*optomotor-blind*
OR	*Oregon R* (wild type strain)
PkA	*Protein kinase A*
PkC	*Protein kinase C*
ptc	*patched*
Pc	*Polycomb*
ph	*polyhomeotic*
Roi	*Rough ocelli*, second chromosome balancer
ry	*rosy*
Sb	*Stubble*
Scr	*Sex combs reduced*
sd	*scalloped*
Ser	*Serrate*
sgg/zw3	*shaggy/zeste-white3*
sna	*snail*
Su(H)	*Supressor of Hairless*
tkv	*thick veined*
Ubx	*Ultrabithorax*
Ubl	*Ultrabithorax-like*
vg	*vestigial*

w	*white*
wg	*wingless*
y	*yellow*
z	*zeste*

Chapter I - Introduction

The study of patterned gene expression within the imaginal discs of *Drosophila melanogaster* provides basic insight into a hierarchy of gene function responsible for creating an organized structure from undifferentiated epithelia. In recent years, investigation into *Drosophila* development has been focused largely upon the subdivision of the embryo into the basic segmented structure that characterizes the remaining stages of the *Drosophila* life cycle. To date, a large number of the genes critical to embryonic patterning have been identified and much progress has been made toward understanding how each gene function and interact with other embryonic patterning elements (Lawrence and Sampedro, 1993). In addition to these primary embryonic patterning elements, additional genes have been found that are involved exclusively in the formation of adult structures such as the wings. It appears that with the advent of complex tissue types characteristic of the adult, there has evolved a corresponding class of genes that are specific to development of these tissues (Williams et al., 1993). An example of this second class of patterning genes is *vestigial* (*vg*), which appears to be primarily active in patterning the adult wing and haltere (Williams et al., 1991). The *Drosophila* wing is well suited to the study of these secondary-patterning genes as subtle alterations within the wing structure can be correlated with specific gene mutations. Further, mutations affecting only wing development can be easily detected and maintained as the loss of the wing has little effect on the viability of the fly (Morgan, 1911).

The life cycle of *Drosophila* is divided into a number of distinct stages including the embryo, three larval instars, pupal and the imago (adult) (Demerec, 1965). When raised at 25°C the first instar larva emerges from the embryo approximately 24 hours after fertilization. Larvae have few external appendages and show little resemblance to the adult. However, the primordia of the wing and other adult epidermal tissues are set aside as small discrete clusters of 10-40 epithelial cells during embryonic development (Blair, 1995). Within the larva, these cell clusters continue to divide in an organized manner forming large epithelial sacs, each of characteristic shape and size (Cohen, 1993). Some of these cell clusters form nine pairs of larval imaginal discs which ultimately form the majority of the adult head, thorax and the thoracic appendages (Anderson, 1972; Cohen, 1993). The abdomen and other posterior structures are formed from the abdominal histoblast nests. The external genitalia develop from a single posterior genital imaginal disc and the internal organs of the gut, salivary glands and trachea develop from their respective imaginal rings (Hartenstein, 1993). The location of each of the imaginal primordia within the late third instar larva is shown in Figure I-1. Note the close apposition of the haltere and wing imaginal discs to the metathoracic and mesothoracic leg discs. It has been proposed that both the dorsal wing and haltere and ventral leg imaginal discs arise from a common set of precursor cells in the embryo that separate during germ band retraction (Cohen et al., 1993). The imaginal primordia have been shown to exist by late embryogenesis by indirect means such as gynandromorphic induction, clonal analysis or cellular ablation (Garcia Bellido and Merriam, 1969; Lohs-Schardin et al., 1979; Wieschaus and Gehring, 1976).

During the first larval instar, the imaginal discs can be directly observed as discrete cell clusters (Madhavan and Schneiderman, 1978). Each of the imaginal discs is composed of a layer of apparently identical epithelial cells that become arranged into specific folds. Within this epithelial layer, there are no morphological indications of the various adult structures that will be ultimately

Figure I-1 The location of the imaginal discs within the *Drosophila* larva.

Each imaginal disc can be found in a characteristic segmental location within the developing larva. A late third instar larva is shown with T1-T3 representing the three thoracic segments and A1-A8 the 8 abdominal segments ultimately found within the adult fly. The wing and haltere imaginal discs are intimately associated with the T2 and T3 thoracic segments, which correspond to their ultimate position within the adult. Histoblast nests are smaller groups of cells that also contribute to the adult structures. In this drawing both sexual structures and a single copy of each pair of imaginal discs are shown within one larva for simplicity. Dorsally located structures are shown on the right while ventral structures are shown on the left. The structures of the gut and salivary glands are shown outside of the larval body for ease of illustration only (Modified from Bryant (1975).

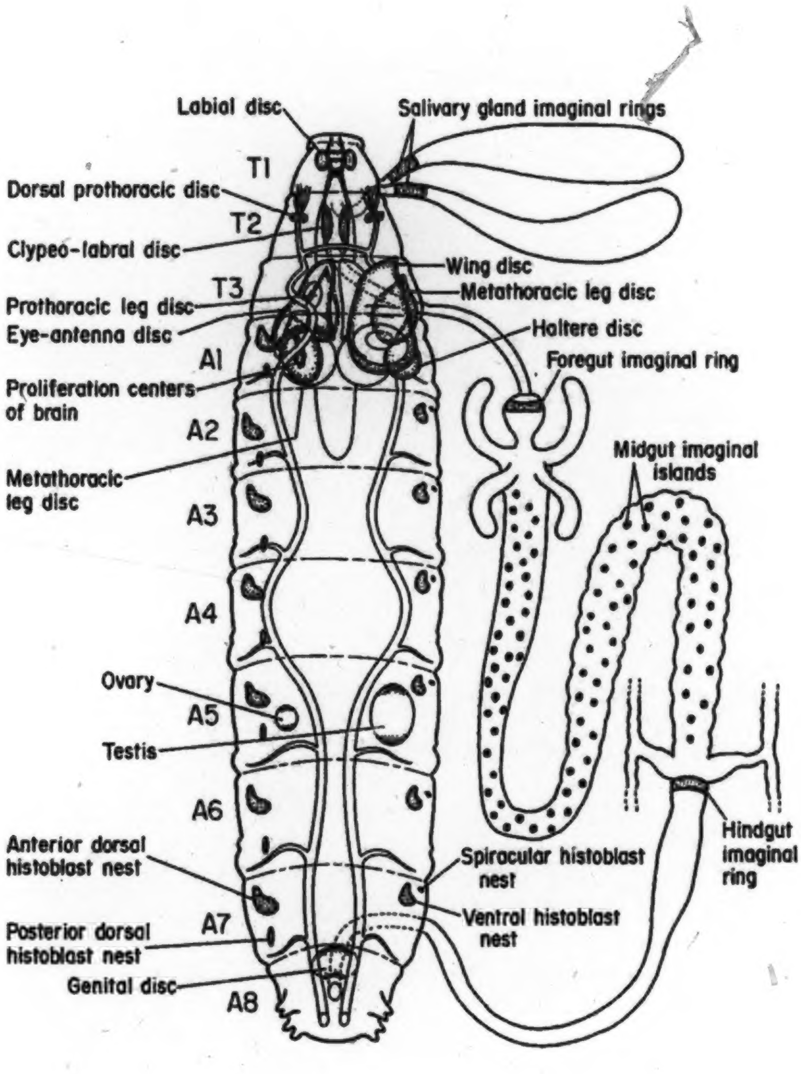
Labial disc
Salivary gland imaginal rings
T1
Dorsal prothoracic disc
T2
Clypeo-labral disc
Wing disc
T3
Metathoracic leg disc
Prothoracic leg disc
Eye-antenna disc
Haltere disc
A1
Foregut imaginal ring
Proliferation centers of brain
A2
Midgut imaginal islands
Metathoracic leg disc
A3
A4
Ovary
A5
Testis
A6
Hindgut imaginal ring
Anterior dorsal histoblast nest
Spiracular histoblast nest
A7
Ventral histoblast nest
Posterior dorsal histoblast nest
Genital disc
A8

formed (Brower et al., 1982; Bryant, 1978; Nöthiger, 1972). During the third larval instar, the imaginal discs increase in size dramatically. After approximately 120 hours, the larva pupariates and the cells of the imaginal discs proliferate rapidly and begin to form their respective adult tissues (Anderson, 1972; Hartenstein, 1993). The specific appendage formed by each of the imaginal discs is defined by the segment in which they are located (Garcia Bellido, 1975; Garcia Bellido, 1977). For example, the dorsal imaginal discs found within the second thoracic (T2) segment of the larva produce the characteristic wing and dorsal thoracic cuticle structures while those found in the third thoracic segment (T3) differentiate into the halteres (Figure I-1) (Demerec, 1965). Mutations that alter segment identity like the *bx* allele of *Ultrabithorax* (*Ubx*), affect the global pattern of disc development, in this case causing the haltere imaginal discs in the T3 segment to develop into wings characteristic of T2 (Lewis, 1978). Even when segment identity has been properly specified, the identity of imaginal discs in long term culture can change spontaneously to that of another in an event labeled transdetermination (Hadorn, 1978). The molecular basis of transdetermination is now thought to be a function of abnormal gene expression within the imaginal disc cells. If ectopic *wingless (wg)*-expressing clones are induced within cells of a leg disc this can produce transdetermination to wing (Maves and Schubiger, 1995).

Mutations, which produce an alteration to the overall developmental fate of a Drosophila segment, are described as homeotic. Characteristically, most homeotic genes in *Drosophila* include sequences called the homeobox which encode a DNA binding element (Morata, 1993). Loss of function mutations in homeotic genes cause a loss of morphological diversity between tissues, often causing them to revert to a basic "ground" identity (Morata, 1993). A number of homeotic genes interact to specify the embryonic segments upon which most of the development of *Drosophila* is patterned (Wilkins and Gubb, 1991). Each imaginal disc derives positional information from the specific pattern of homeotic gene products that specify the segment where the disc is located. However, while the overall identity of a single imaginal disc is defined by its segmental identity, the imaginal disc is not the smallest unit of specification. During the metamorphosis of a larva into an adult each imaginal disc produces a number of distinct and highly specialized adult structures (Bryant, 1978). A fate map illustrating the structures formed from the wing imaginal disc is shown in Figure I-2. Each of the various structures formed from a single disc can be independently transformed to a different developmental fate by mutations within specific patterning genes (Cohen, 1993). Therefore, it appears that specification of the developmental fate of both the entire imaginal disc and the subsequent patterning of structures defined by that disc is a dynamic process ultimately controlled by patterned gene expression.

Cells fated to form the wing and haltere discs can first be detected during embryonic stage 12. The primordial wing discs appear as small clusters of cells that segregate dorsally from the ventral leg disc primordia located in the second and third thoracic segments (Cohen et al., 1993; Williams et al., 1991). The restriction of wing and haltere development to the T2 and T3 segments is regulated by a number of homeotic genes. The formation of the wing imaginal discs within the abdomen is suppressed by expression of genes of the bithorax complex (Bx-C) (Bate and Martinez Arias, 1991; Simcox et al., 1991; Vachon et al., 1992). Similarly, mutations within either labial (lab) or Deformed (Dfd) causes transformations of head structures to those resembling the thorax(Merrill et al., 1989; Merrill et al., 1987). This indicates that these gene products are involved in suppressing a thoracic identity in the head region. Within the

Figure I-2 A fate map of the late third instar wing imaginal disc

The regions of the imaginal disc that produce major body structures were determined by Bryant(1975). The regions of the wing compartment that form the wing blade are located in the larger ventral portion of the disc (top). These are surrounded by the region fated to form the structures of the wing hinge and the pleura. The regions located at the dorsal end the wing disc (bottom) will form the notum, which represents the portion of the body wall where the wing is attached. The regions labeled in the wing disc correspond to the structures illustrated in (Figure I-4). The fate map of the haltere disc (not shown) is similar to that of the wing although fewer structures are formed in the haltere (Figure I-5)

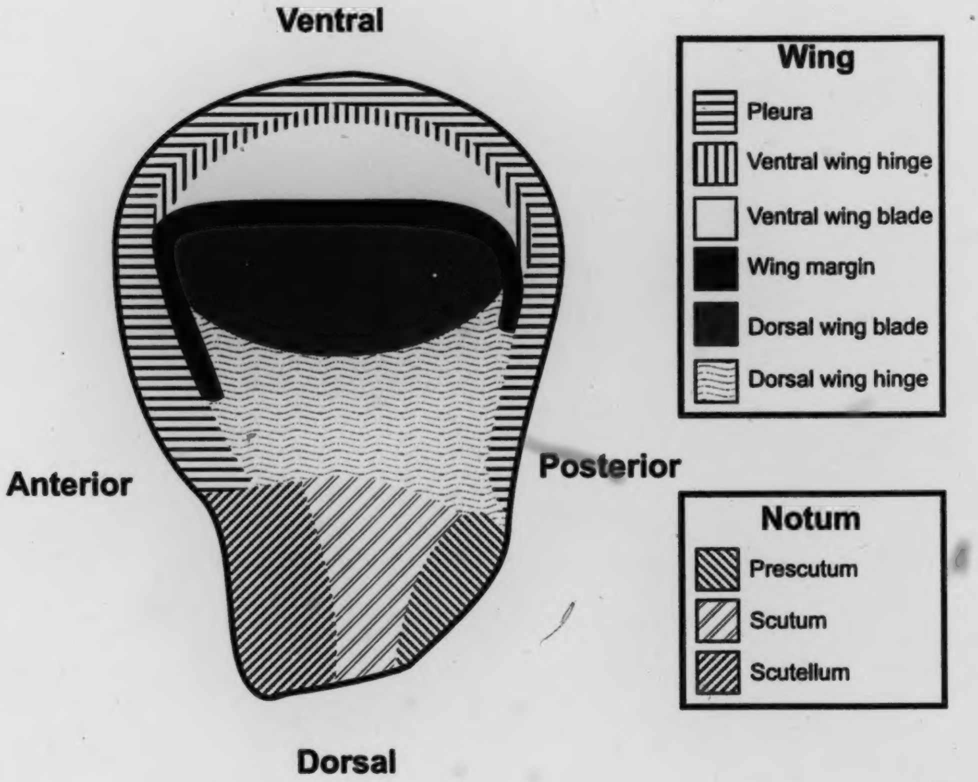
Ventral
Anterior
Posterior
Dorsal
Wing
Pleura
Ventral wing hinge
Ventral wing blade
Wing margin
Dorsal wing blade
Dorsal wing hinge
Notum
Prescutum
Scutum
Scutellum

thorax itself formation of wing in the first thoracic (T1) segment is repressed by the expression of the homeotic gene, *Sex combs reduced* (*Scr*) which is part of the Antennapedia complex (Ant-C) (Carroll et al., 1995). This is illustrated by mutations of another Ant-C gene, *Antennapedia (Antp),* which removes this repression leading to ectopic formation of wing primordia in T1 (Carroll et al., 1995). Within the T2 and T3 embryonic segments, the specification of the wing and haltere primordia appears to be controlled in part by two similar zinc-finger proteins, produced by the *escargot* (*esg*) and *snail* (*sna*) genes (Fuse et al., 1996). A two step model for wing fate determination has been proposed by Fuse et al. (1996). In their model, *esg* and *sna* are necessary for the maintenance of wing imaginal disc fate in the embryo following the partitioning of the wing disc cells from the leg disc cells during stage 12 of embryogenesis. The phenotype of *esg* and *sna* mutants suggests that they regulate the expression of themselves and each other to maintain a wing cell fate (Fuse et al., 1996). In the absence of either *esg* or *sna* the expression of genes that are specific to wing cell fate is lost in all three thoracic segments during embryonic stage 13. The restoration of expression of either *esg* or *sna* in corresponding mutant embryos by employing heat-shock constructs of these genes preserves proper wing cell identity (Fuse et al., 1996).

The specification of cells of the wing and haltere primordia in T2 and T3 by the activity of *esg* and *sna* is also associated with initial expression of *vg*. Within normally developing embryonic wing and haltere imaginal disc primordia cells a high level of *vg* expression that can be detected by an anti-Vg antibody (Williams et al., 1991). It appears unlikely that *vg* is the primary determinant of the wing and haltere disc primordia at this stage as wing and haltere imaginal discs appear in homozygous *vg* null mutant embryos (Cohen et al., 1993).

However, the proper expression of *vg* is required later during later larval development of the wing and haltere following the compartmentalization of the imaginal disc tissue (Williams et al., 1991).

As a group, the imaginal discs bear more resemblance to each other than the various tissue types that they will ultimately form. However, examination of genetically marked cell lineages has revealed the presence of specific boundaries that sequentially divide each imaginal disc into a series of developmental compartments (Garcia Bellido et al., 1976). Within the imaginal disc, a compartment has been defined historically as a group of cells whose descendants remain within specific developmental boundaries and possess an alternative developmental fate from neighbouring compartment cells. Within any compartment, a given cell can form any portion of the structure developed from that compartment (Garcia Bellido et al., 1973). Cells located along the boundaries between these compartments are thought to act as organizing centres for further patterning of the sub-domains defined by that border (Blair, 1995; Meinhardt, 1982). The first compartmentalization within all of the thoracic imaginal discs is the division of anterior from posterior (Garcia Bellido et al., 1976). Within the wing and haltere imaginal disc this is later followed by a dorsal-ventral (D/V) and finally a proximal-distal (P/D) division (Blair, 1995). Early during imaginal disc development, the initial A/P division is established by the selective expression of the *engrailed* (*en*) gene in the posterior compartment (Brower, 1986). The specific expression pattern of *en* is derived from embryonic *en* patterning (Wilkins and Gubb, 1991). However, this posterior specific expression pattern must be maintained in a stable fashion within the imaginal discs to properly establish the A/P compartment border (Kornberg et al., 1985). The expression of the *en* gene causes cells to actively secrete the Hedgehog, (Hh) protein (Tabata et al., 1992). Cells that are actively expressing the *hh* gene are not themselves receptive to the Hh signal. In this manner, Hh protein acts a short-range signal received by cells immediately anterior to the posterior compartment. The anterior compartment cells responding to Hh begin expressing the secreted protein produced by the *decapentaplegic* (*dpp*) gene (Gúillen et al., 1995; Sanicola et al., 1995; Tabata and Kornberg, 1994; Zecca et al., 1995). The Dpp protein then diffuses from the A/P boundary cells across the entire width of the wing disc and controls subsequent patterning along the A/P axis (Lecuit et al., 1996; Nellen et al., 1996; Zecca et al., 1995).

Although *en* is critical for early establishment of the A/P border, it appears that this activity of *en* may not be solely responsible for the identity of the posterior compartment. By late third larval instar, the expression pattern of *en* appears to broaden to encompass cells in the anterior compartment adjacent to the A/P boundary. The presence of additional cells expressing *en* outside the posterior compartment does not seem to affect either the A/P compartment border nor the compartment identity of the anterior cells (Blair, 1992). Further it appears that the *en* gene is not the only determinant of posterior identity. When *en* expression is removed from the posterior compartment either by mutation or by induction of mitotic *en*$^-$ clones, cells show an indeterminate transformation with characteristics of both posterior and anterior cell fate (Hidalgo, 1994; Kornberg, 1981b). There exists a second homeobox containing gene, *invected* (*inv*), that mirrors the expression of *en* in the imaginal discs but the expression of which remains posteriorly localized throughout development (Blair, 1992; Coleman et al., 1987). As will be discussed later, the product of this gene appears be able to specify posterior compartment identity while having no apparent role in the establishment of the A/P border.

During later wing imaginal disc development, D/V restrictions are created in a similar fashion to that of the A/P compartment border by the dorsal-specific localization of the *apterous* (*ap*) protein (Diaz-Benjumea and Cohen, 1993). Interactions between *ap* expressing and non-expressing cells at this margin serve to establish the D/V compartment boundary (Diaz-Benjumea and Cohen, 1993; Kim et al., 1995). This expression of *ap* mediates the ventrally restricted expression of other patterning genes including *fringe* (*fng*), *Dorsal wing* (*Dw*). Finally the expression of the signaling molecules *Notch* (*N*) and *Serrate* (*Ser*) is induced in the cells located along the D/V border (Figure I-3) (Doherty et al., 1996; Irvine and Wieschaus, 1994; Kim et al., 1995; Tiong et al., 1995). The activation of *vg* along the D/V axis by *N* is thought to be mediated by a direct interaction with the transcription factor *Suppressor of Hairless* (*Su*(*H*)) (de Cellis et al., 1996a; Kim et al., 1996). The activation of *vg* expression along the D/V margin during the third larval instar seems to occur by a two step process. An enhancer element located in the second intron of *vg* has been shown to be responsible for binding the *Su*(*H*) protein and activating *vg* expression immediately along the D/V border and to a lesser extent along the A/P margin (Figure I-3) (Kim et al., 1995; Williams et al., 1994). A second element in the fourth intron of *vg* activates *vg* expression in the four quadrants of the wing compartment responding to cues from both the D/V and A/P compartment boundaries (Kim et al., 1995). P/D compartmentalization occurs late in imaginal disc development and is thought to be controlled by the selector genes *Distalless*, (*Dll*) and *aristaless* (*al*) (Campbell et al., 1993; Cohen et al., 1989; Panganiban et al., 1994). Ectopic expression of small clones of *al* within the wing disc will cause ectopic P/D outgrowths from the wing (Campbell et al., 1993). The P/D axis, although formed late, appears to have a critical role in regeneration of imaginal disc tissue. Cut fragments cultured within the abdomen of a female host exhibit regeneration in a polar coordinate fashion along the P/D axis (Bryant et al., 1981; French et al., 1976). The polar coordinate values are thought to be established by the activity of the compartments but may function independently thereafter (Blair, 1995).

Each wing imaginal disc forms a number of different tissues including the wing, hinge and the region of dorsal notum where the wing attaches to the body (Figure I-4) (Bryant, 1975). While initial *vg* activity is associated with the entire wing imaginal disc, during third instar the expression of *vg* is restricted to the ventral regions of the wing disc (Williams et al., 1991). By late third instar, the majority of *vg* expression within wing discs corresponds to those cells fated to become the wing blade and hinge, with weaker expression in pleura and notum (Figure I-2). Early genetic studies indicated that the portion of the imaginal disc fated to form the wing is compartmentalized immediately before the third larval instar (Garcia Bellido et al., 1973). Two models have been proposed as to how the various genes are involved in the specification of wing specific tissues within the wing imaginal disc. Couso et al. (1995) propose that interactions between ventrally expressed *wg* and dorsally expressed *Ser* proteins along the D/V margin ultimately induce symmetric expression of the signal receptor *N*. This leads to the activation of D/V specific *vg* expression and subsequently defines the wing pouch region of the wing imaginal disc. However, the complete expression pattern of *vg* in the late third instar wing imaginal disc is not limited to the wing compartment but also extends into the hinge and notum regions (Williams et al., 1991). Separate experiments in which the *wg* gene is ectopically expressed in wing disc cells outside its normal expression pattern suggest that *wg* has a dual role in patterning the wing disc. Early expression of *wg* defines the wing specific compartment during the latter part of the second larval instar while later *wg* is responsible for patterning along the D/V axis

Figure I-3 Expression of *vg* within the wing pouch of the wing imaginal disc is established by the activity of multiple patterning pathways.

The establishment of cells fated to form the wing pouch within the wing disc is controlled via early *wg* expression (Ng et al., 1996). The initial pattern of elevated *vg* expression within the wing disc is controlled by signals emanating from the D/V compartment border. Establishment of the D/V compartment boundary in the wing compartment is controlled by activity of the *ap* gene. The juxtaposition of *ap* expressing and non-expressing cells activates *fng* within cells of the ventral compartment and subsequently leads to activation of other ventral-specific genes including *Dw*. The establishment of the D/V boundary establishes expression of *Ser, Dl, N* and *wg* along the D/V boundary (Cohen, 1993; Cohen, 1996). The *vg* intron-2 element responds to cues from the D/V boundary ultimately effected by the binding of the *Su*(*H*) protein (Kim et al., 1996). This establishes initial *vg* expression in a thin stripe along the D/V compartment border (Williams et al., 1994). The *vg* intron-4 enhancer responds to signals from both the D/V pathway and a second A/P mediated signal established by *en*, *ptc*, *hh* and *dpp*. This is ultimately controlled via the action of the *dpp* receptor protein encoded by *thick vein* (*tkv*) to establish graded *vg* expression within the cells of the remaining quadrants of the wing compartment (Kim et al., 1996). This gradient of *vg* expression is thought to be controlled by the activity of the *wg* protein which is secreted from cells along the D/V boundary (Neumann and Cohen, 1996b).

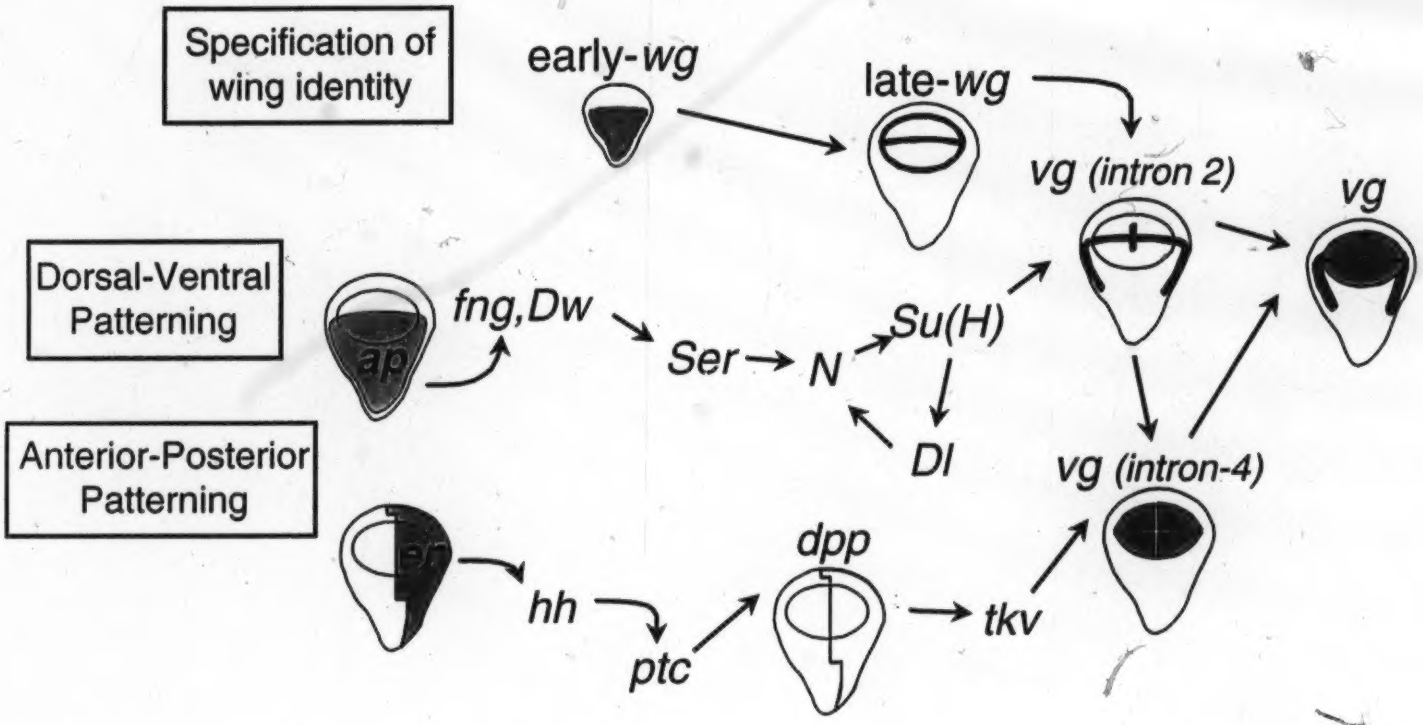
Specification of wing identity
Dorsal-Ventral Patterning
Anterior-Posterior Patterning
early-wg
late-wg
vg (intron 2)
vg
ap
fng,Dw
Ser
N
Su(H)
Dl
vg (intron-4)
en
hh
ptc
dpp
tkv

(Figure I-3)(Ng et al., 1996). In this second model *N* is activated by dorsally restricted *Ser* and in ventral cells by the activity of *Delta* (*Dl*) which is expressed in a pattern complementary to that of *Ser* (de Cellis et al., 1996b; Doherty et al., 1996). The role of *vg* in this model is the promotion of growth and development of wing tissues in a wing compartment pre-specified by early *wg* expression (Kim et al., 1996; Ng et al., 1996). This model is supported by the observation that ectopic activation of the *wg* pathway in mitotic clones of cells mutant for *shaggy/zeste-white* 3 (*sgg/zw-*3) also causes activation of *vg*. (Blair, 1994). Therefore it is likely that *wg* signaling coupled with activation of *vg* along the D/V compartment border is required for the subsequent activation of the *vg* intron-4 element to establish the full *vg* expression pattern (Figure I-3) (Cohen, 1996). The promotion of wing-specific gene expression by the *vg* protein can be illustrated by the ectopic expression of *vg* in other imaginal discs. When *vg* expression is targeted to portions of leg, eye and antennal imaginal discs using synthetic GAL4/UAS constructs, the presence of ectopic Vg induces the transformation of cells to produce wing like bristles (Kim et al., 1996). In this manner *vg* acts like the *eyeless* (*ey*) gene which can induce the transformation of a portion of any imaginal disc to form a complete ectopic eye (Halder et al., 1995). However, unlike *ey, which* controls the formation of a complete eye, expression of *vg* does not induce a complete ectopic wing to form (Kim et al., 1996). Instead, it appears that *vg* can provide a wing cell identity to cells within a pre-defined compartment but does not create a wing compartment *de novo* when expressed in other imaginal discs. This supports the second model, outlined above, in which *vg* is required for wing identity and cellular proliferation but does not itself define the wing compartment within the wing imaginal disc. The role for *vg* in promoting wing cell proliferation is illustrated best by the observation that disc overgrowth mutants such as *lethal* (2) *giant discs* or *fat* can partially compensate for reduced *vg* expression (Agrawal et al., 1995).

The *vg* mutation was characterized genetically early in the study of *Drosophila melanogaster* (Morgan, 1911). The easily discerned loss of wing phenotype associated with *vg* has meant that a comparatively large collection of *vg* alleles has been examined (Lasko and Pardue, 1988; Lindsley and Zimm, 1992; Williams and Bell, 1988). The phenotype of flies homozygous for recessive *vg* mutations is the failure to form variable amounts of the wing margin and interior of the wing blade. The severity of wing loss associated with *vg* alleles can be ordered from complete wing loss to slight nicks appearing in the wing margin (Figure I-6) (Nakashima-Tanaka, 1968). Genetically, a single functional copy of the *vg* locus appears to be sufficient for proper development of all structures of the adult wing blade (Figure I-4). A complete deficiency of the *vg* locus Df(vg^B) heterozygous to vg^+, produces only slight nicking in the extreme distal portion of the wing (Figure I-6-Class II) in approximately 30% of the adult flies (Lindsley and Zimm, 1992). However, Green (1946) found that the presence of duplications of *vg* mutations or of vg^+ will occasionally enhance the *vg* phenotype, which suggests the possibility that a weak autoregulatory activity can be associated with *vg*. Other non-wing phenotypes have also been attributed to some but not all alleles of *vg*. The capitelium of the haltere, a balance organ thought to represent a reduced second wing (Figure I-5), is often smaller in the presence of severe *vg* mutations (Green and Oliver, 1940; Lindsley and Zimm, 1992). However since no margin structures are seen in the haltere like those formed in the wing, the severity of haltere deletions associated with *vg* is hard to examine (Bownes and Roberts, 1981a). Other ancillary phenotypes associated with *vg* mutations may include; female sterility, pupal lethality, reduced adult size and erect bristles on the scutellum. These

Figure I-4 The structure of the *Drosophila melanogaster* wing.

A) A dorsal view of the adult wing, redrawn from Bryant (1975) (TR) the triple row of anterior specific bristles, (DR) a double row of bristles characteristic of the distal tip of the wing, (PR) a single row of posterior specific bristles. The areas of the notum, hinge and wing blade are derived from different regions of the wing imaginal disc (Figure I-2). Within the wing blade, each wing vein (vII-vV) has a characteristic position and structure that can be used to determine the developmental fate of a specific region. Further, the vIII vein that runs adjacent the A/P border can be identified by the presence of capaniform sinsillae (cs). The prescutum (Ps), scutum (Sc) and scutellum, (Scl) structures of the dorsal notum formed by the wing imaginal disc correspond to those identified in the fate map shown in Figure I-2.

B) Ventral view: The ventrally located pleural regions including the mesopleura (MP), pteropleura (PtP), postpleura (PP) and postnotum (PN) derived from the ventral regions of the wing imaginal disc can be observed.

C) A detailed view showing the complex structure of the wing hinge. The (Al)-alula, (Ac) axillary cord and (Teg) tegula represent wing hinge specific structures that show anterior-posterior asymmetry. Within this region, the structures of the costa (Co) are often retained even in the strongest *vg* mutants. (Scu) refers to the characteristic scutellar bristles that can be used to identify identity of each region of the notum.

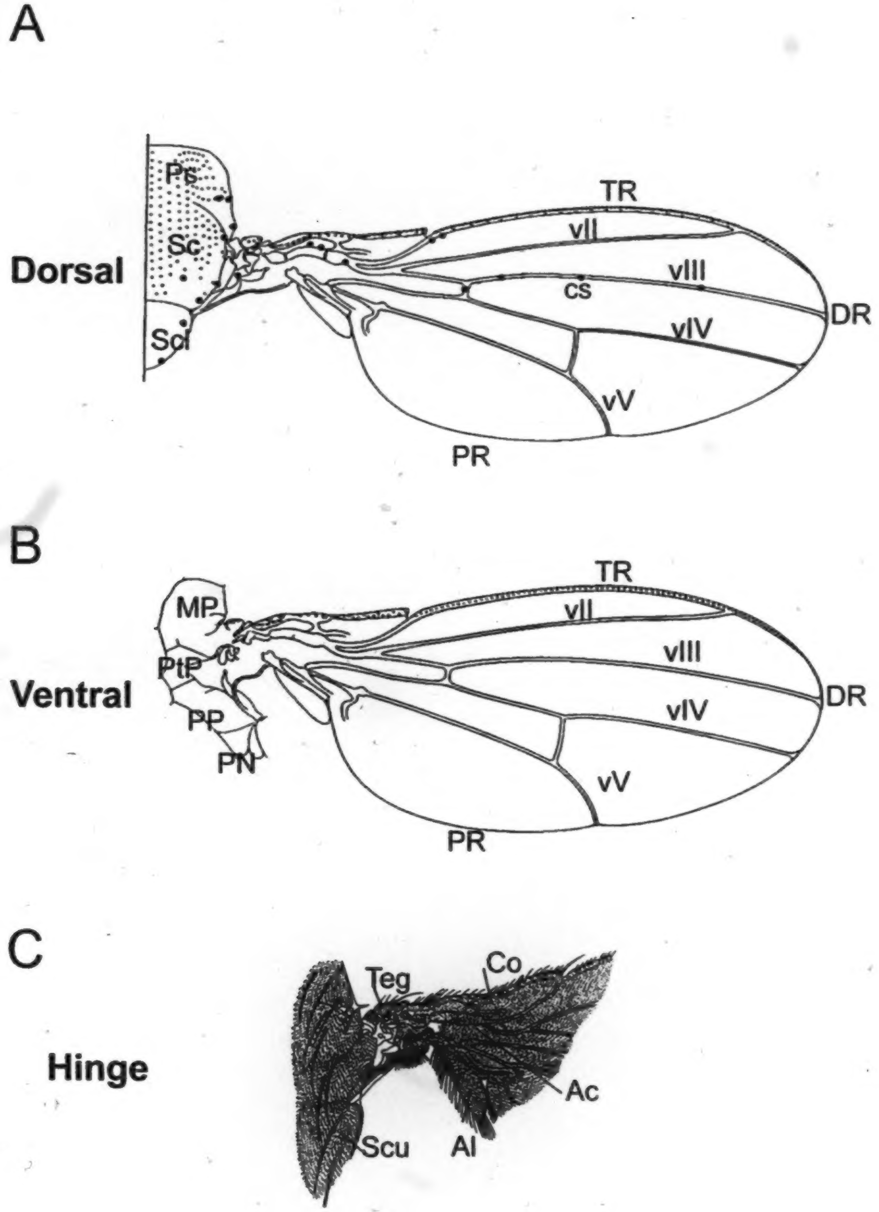
A
Dorsal
Ps
Sc
Scl
TR
vII
vIII
cs
DR
vIV
vV
PR
B
Ventral
MP
PtP
PP
PN
TR
vII
vIII
DR
vIV
vV
PR
C
Hinge
Teg
Co
Ac
Scu
Al

Figure I-5 The structure of the *Drosophila melanogaster* haltere.

The haltere is thought to represent a residual second wing found in other insects that is adapted for balance in *Drosophila*. The wing blade is reduced to the structures of the capitelium. A/P differentiation is difficult to examine in the haltere as only a few capitellar sensilla are formed in the capitelium compared to the specific bristle pattern found in the wing. The corresponding hinge region of the haltere is much simpler than the wing. The pedicel joins the capitellum to the notum body wall. There are a number of characteristic patches of sensilla located on the ventral and dorsal sides of the pedicel. The various portion of the dorsal notum and ventral pleura and the adjoining abdominal segments are also labeled (Bryant, 1975).

Dorsal

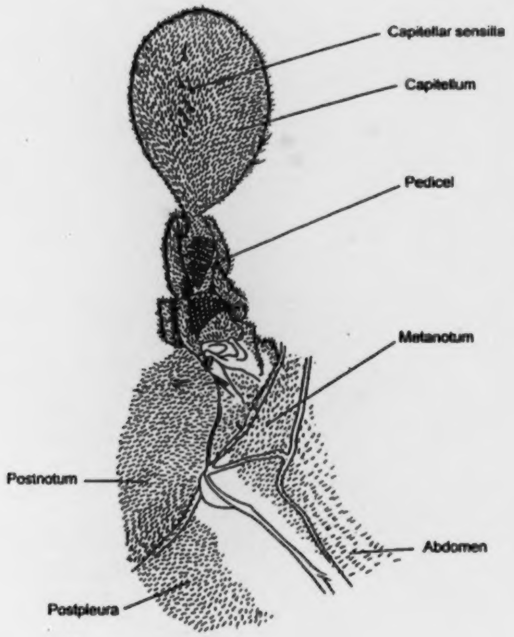

Ventral

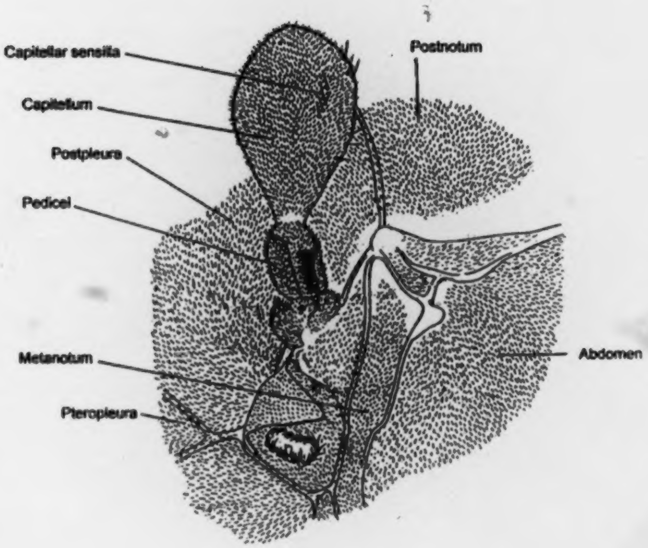

secondary *vg* phenotypes are most often associated with mutations that also show a strong reduction of wing formation (Lindsley and Zimm, 1992). Thus, mutational analysis suggests a primary role for *vg* in the specification of the wing although a secondary role in the neuronal development is suggested by the wing bristle and notum phenotypes caused by *vg* mutations.

The *vg* locus was cloned by P-element tagging and has been shown to encompass a 16-19kb span at cytological position 49D2-E1 (Williams et al., 1990a; Williams and Bell, 1988). The *vg* gene produces a single 3.8kb mRNA from eight exons that is first detected in the developing embryo within the cells fated to become the wing and haltere imaginal discs (Williams et al., 1990a, 1991). The 453 amino acid protein encoded by the *vg* mRNA shows no homology to other known proteins except for a small region of weak similarity to *paired* at the C terminal end (Williams et al., 1991). There is a high degree of sequence conservation between the *Drosophila melanogaster* and *Drosophila virilis* Vg amino acid sequence at the amino- and carboxy-terminal region of the protein and in the regions derived from exon-4 (Williams et al., 1991). An antibody directed against the C-terminal portion of the *vg* protein detects expression in the wing and haltere imaginal discs. Further *vg* protein is detected transiently within the ventral nerve cord and possibly the progenitors of the sensory organs of the peripheral nervous system (Williams et al., 1991). The patterning of *vg* expression during wing imaginal disc development begins with expression of *vg* within the entire wing and haltere imaginal discs. By the second larval instar, *vg* expression is suppressed in the most ventral portions of the wing and haltere discs. During early third instar, the pattern of *vg* expression in the wing disc begins to resolve into a stripe positioned approximately along the D/V border in the region that will form the wing blade (Williams et al., 1993). As mentioned above, the late larval expression of *vg* is controlled by enhancer

Figure I-6 Classification of the severity of the loss of wing phenotype associated with *vg* mutations.

A numbering system was established by Nakashima-Tanaka (1968) to classify the severity of the wing loss associated with *vg* mutations. The relative wing loss associated with *vg* alleles can be graded from none (1) to a complete loss of the entire wing blade (30). The various *vg* mutant phenotypes can be grouped into ten broad classes based upon the amount and location of the tissue that is deleted from the wing margin. Class I (1-2) represents wild type or *vg* alleles that have no effect on wing development. Class II (3-5) represents a slight loss of the margin specific bristles that is most commonly observed at the P/D wing tip. Class III (6-8) is characterized by nicks missing from the distal tip of the wing. Classes IV (9-12) and V (13-14) represent more severe nicking of the wing blade while VI (15-19) and VII (20-21) are associated with complete deletion of the anterior and posterior margin of the wing. Mutants of class VIII (22-24) or IX (25-28) produce only a small portion of the wing although either of the anterior or posterior cross veins may be observed. The most severe *vg* mutants of class X (29-30) produce no significant wing and the regions of the wing hinge are often affected in these mutants. The original drawings of each wing phenotype were modified from Nakashima-Tanaka (1968).

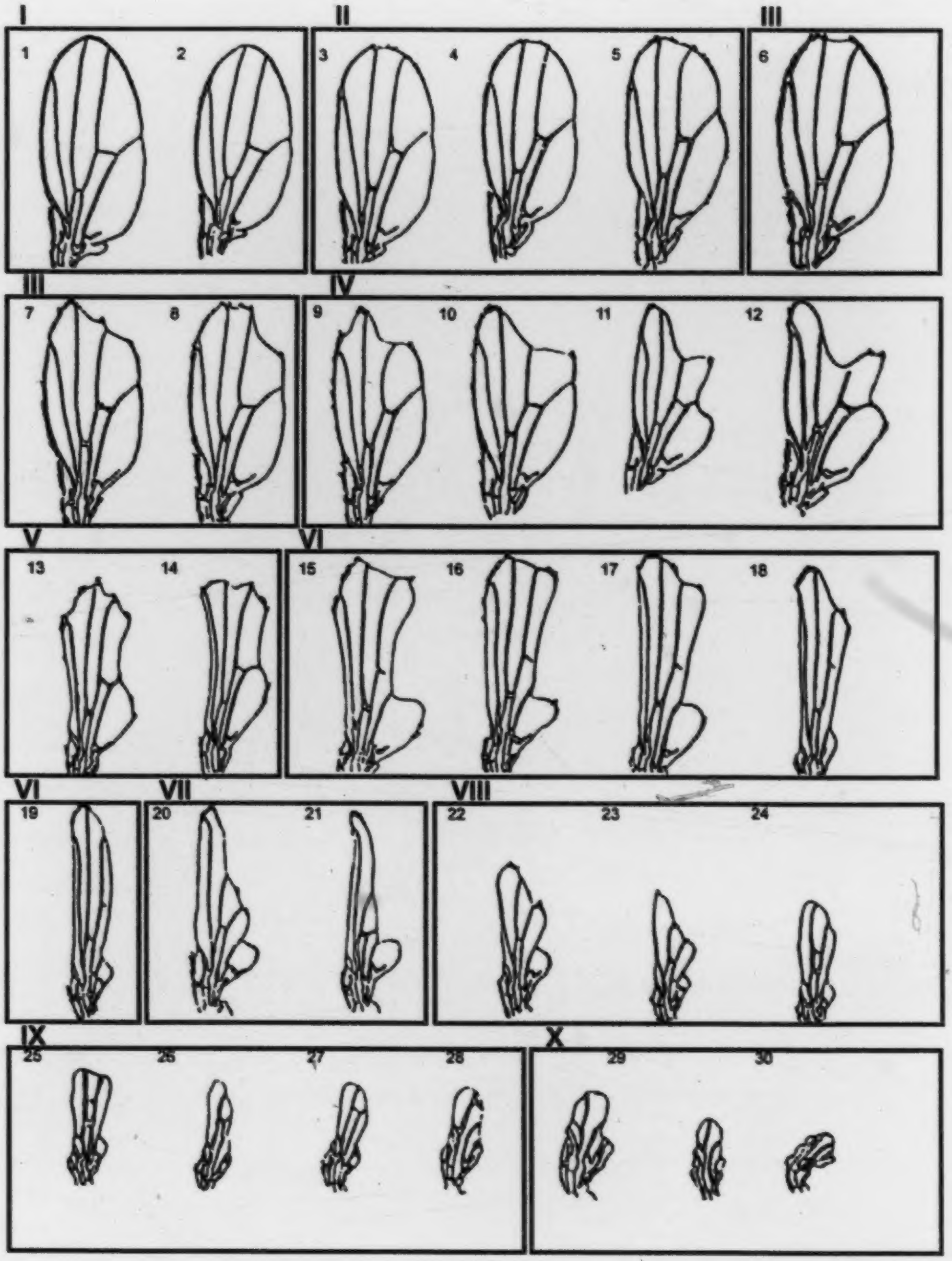
I
II
III
III
IV
V
VI
VI
VII
VIII
IX
X

elements located in the *vg* introns (Kim et al., 1996; Williams et al., 1994). Evidence for this control mechanism was first suggested by a second complementation group that maps to the second intron and thus is completely contained within the *vg* locus (Alexandrov and Alexandrova, 1988). The intragenic complementation associated with the second *vg* intron is due to the presence of an intron-2 enhancer element that directs initial *vg* expression along the D/V margin during the third larval instar (Williams et al., 1994).

The loss of wing tissue associated with *vg* alleles can be correlated with an increased amount of cell death found in the wing discs. In larvae, wing imaginal discs lacking *vg* expression contain elevated numbers of dying cells during the late third instar compared to that seen during normal wing development (Fristrom, 1969). When imaginal discs are recovered from *vg* mutant larvae, they are not able to form wing structures even when transplanted into a vg^+ host (Bownes and Roberts, 1981b). Therefore, cell death associated with *vg* mutants is caused by a cell-autonomous loss of wing cell fate within those regions of the wing imaginal disc as the remaining cells are no longer competent to produce wing margin. Analysis of vg^-/vg^- mitotic clones within the wing imaginal disc has proven to be extremely difficult as cells within these clones do not proliferate (Simpson et al., 1981). This lack of cellular proliferation is not a ubiquitous property of cells within the wing imaginal disc as clones can be readily induced in the portion fated to form the notum (Kim et al., 1996). This suggests that in the absence of *vg* expression, cells within the imaginal disc either fail to proliferate or do not become competent to form wing structures and instead enter the apoptotic pathway by default. A number of other mutations associated with wing development also produce specific patterns of cell death within the developing wing imaginal disc including *wg*, *ap* and *scalloped* (*sd*) (Williams et al., 1993). However the cell death associated with both *wg* and *ap* mutants occurs during the second or early third instar suggesting that these genes are required to act before *vg* (Williams et al., 1993). The roles of *wg* and *ap* appear to be in the initial specification of the wing compartment (Figure I-3) (Cohen, 1996). In contrast to the early cell death associated with alleles of *wg* and *ap*, larvae homozygous for either *vg* or *sd* recessive alleles manifest elevated cell death in the wing imaginal discs later in the third larval instar (O'Brochta, 1980; Williams et al., 1993). By late third instar, wing discs mutant for either *sd* or *vg* show a vastly reduced number of cells (60-70%) compared to wild type (James and Bryant, 1981). Many viable *sd* mutations also produce a wing margin loss phenotype, and both *vg* and *sd* show mirror image duplications of notum and ventral hinge when wing tissue is lost (Campbell et al., 1991; Williams et al., 1993). The wing phenotypes produced by comparable alleles of *vg* and *sd* appear identical except that posterior notum is deleted more often in *sd* (James and Bryant, 1981). Thus, in this respect the two mutants are similar in their secondary roles in wing development. The complete larval expression pattern of *sd* includes the central and peripheral nervous system and all imaginal discs except for the labial disc (Campbell et al., 1992). Expression of *sd* is required for early expression of *vg* and subsequently *vg* is then required for maintaining later *sd* expression (Williams et al., 1993). The *sd* locus covers a 14kb region at position 13F on the X chromosome that contains 12 exons and encodes both a 3.3kb and a 4.5 kb mRNA transcript. However, both of these *sd* mRNAs contain the same ORF with the alternative splicing affecting the 5' untranslated region (Campbell et al., 1991). The *sd* protein is a transcription factor containing a TEA DNA binding domain (Campbell et al., 1992). The TEA domain represents a novel, conserved DNA-binding motif named for the three genes in which it was originally found, human *TEF*-1, yeast *TEC*-1 and *abaA* from *Aspergillus nidulans* (Bürglin, 1991). The early expression of *sd* has not been well studied but in mutant clones of *sgg/zw-3* both *vg* and *sd* are activated simultaneously (Blair, 1994). Examination of early wing disc patterning in *vg* and *sd* mutants led Williams et al. (1993) to suggest that *sd* may act as an activator of *vg* expression in the wing disc. Finally, both *vg* and *sd* interact with the *cut* (*ct*) gene (Goldschmidt, 1937; Jack and DeLotto, 1992). The ct^{6} allele can produce a wing nicking phenotype in a *vg/+* background when coupled with other unknown *vg* modifiers (Goldschmidt, 1937). The same synergistic phenotypic interaction with *ct* is seen with weak alleles of *sd* (Jack and DeLotto, 1992).

The following chapters deal with analysis of the role of the *vg*, *sd* and *inv* genes during wing development. The starting point for much of this work was the analysis of two extraordinary dominant mutations of *vg*, vg^{W} and vg^{U}, which produce the loss of wing normally associated with recessive *vg* homozygotes. These mutations affect not only the *vg* region, but also two other loci associated with wing development; *inv*, and *mastermind* (mam) involved in neurogenesis and bristle formation both in the embryo and imaginal discs (Coleman et al., 1987; Smoller et al., 1990; Williams et al., 1990b). The reason why other genes are affected is that the dominant alleles are each associated with a cytologically detectable chromosomal inversion the fuses *vg* sequences with *mam* in the case of vg^{U} and *inv* in the case of vg^{W}. The phenotype of vg^{W} also includes a suspected homeotic transformation of the remaining wing and haltere to an altered developmental fate (Bownes and Roberts, 1981a). Thus, these mutations represent extraordinary alleles of *vg*. Chapter 2 deals with the analysis of the development effects associated with vg^{U} and vg^{W}. In an attempt to determine the mechanism by which these dominant alleles suppress wild type *vg* function, a mutagenesis screen to detect phenotypic revertants of both vg^{W} and vg^{U} was performed. By obtaining mutations within the *vg* portion of the chimeric gene fusions that are associated with these dominant alleles, it was hoped to determine the role of *vg* sequences in creating the dominant effect. Further, the regions of *vg* that are important for mediating dominance would also likely have a role in the normal function of *vg*. It appears that the dominant effect of *vg*^{W} and *vg*^{U} is an interaction between the fusion partner *inv* and *mam* genes, respectively, with the captured *vg* sequences. The third chapter deals with the analysis of one particular reversion mutant of *vg*^{W}, which restored formation of the wing but retained a homeotic transformation of anterior to posterior wing. This transformation is caused by the mis-expression of *inv* by the *vg* enhancers. This mutation provides evidence that the homeotic phenotype of *vg*^{W} is genetically separable from the dominant wing loss. The correlation of the mis-expression of *inv* to the homeotic transformation of anterior to posterior wing has provided evidence for a distinguishable role for *inv* in controlling the identity of posterior compartment cells within the wing disc, an activity previously attributed solely to *en*. The fourth chapter deals with a direct protein-protein mediated interaction between the *vg* protein with the transcription factor encoded by *sd*. The *vg* and *sd* proteins show a strong affinity *in vitro* and this may indicate a possible direct *vg-sd* interaction controlling the expression of developmentally downstream patterning genes required for wing formation or for general cellular proliferation. Finally, a summary and discussion of the mechanisms that mediate the dominant activity of both *vg* and *inv* and the role of *vg*, *inv* and *sd* in patterning the *Drosophila* wing is presented in chapter five.

Chapter II - Reversion analysis of the dominant *vg*^{W} and *vg*^{U} alleles

Introduction

Since the discovery of the first *vg* mutation, (Bridges and Morgan, 1919; Morgan, 1911), a comparatively large number of *vg* alleles have been recovered (Lasko and Pardue, 1988; Williams and Bell, 1988). However, of over 500 alleles of *vg* catalogued by Lindsley and Zimm (1992) only two, Df(2R)*vg*^{Ultravestigial} (*vg*^{U})and Df(2R)*vg*^{Wingless} (*vg*^{W}) produce a dominant loss of wing phenotype in the presence of a *vg*$^{+}$ allele (Ives, 1956; Shukla, 1980; Williams et al., 1990b). As dominant *vg* alleles appear to represent an extremely rare phenomenon, it is perhaps not surprising that they are associated with specific chromosomal aberrations. Both dominant alleles result from inversions that place the majority of the *vg* coding region into proximity with *inv* in the case of *vg*^{W} and within the coding region of *mastermind* (*mam*) in the case of *vg*^{U} (Williams and Bell, 1988; Williams et al., 1990b). Specifically, the inversion that creates *vg*^{W} has one breakpoint 8 kb upstream of the *inv* transcriptional start site and the other within the first exon of *vg*. In *vg*^{U}, a breakpoint in the 5' portion of the *vg* second intron, immediately after the intron/exon boundary, is joined to polymorphic repetitive DNA in the 5' portion of the *mam* gene (Figure II-1) (Williams et al., 1990b). Like *vg*, both *inv* and *mam* are involved in patterning the developing wing and haltere imaginal discs and are expressed in these tissues during larval development (Coleman et al., 1987; Smoller et al., 1990). The specific molecular activity of *mam* is not known, but examination of the *mam* mutant phenotype suggests a role in neurogenesis (Smoller et al., 1990). The *inv* gene was discovered not by mutation but by virtue of a high degree of similarity to the A/P patterning element *en* (Coleman et al., 1987). The *inv* protein is expressed in a pattern identical to *en* and like *en*, *inv* contains a homeodomain but mutations of *inv* do not seem to produce any observable phenotype(Coleman et al., 1987; Tabata et al., 1995). However, the activity of the *inv* protein can define posterior compartment identity within the developing wing imaginal disc(Chapter-III; Gúillen et al., 1995).

Although vg^W and vg^U produce wing phenotypes similar to those associated with recessive *vg* alleles they possess unique properties as well. The basic loss of wing phenotype of a recessive vg^1 homozygote and the vg^U/+ heterozygote is identical in flies reared at 25°C. This phenotype includes a total loss of the wing margin and majority of the wing blade leaving only the hinge regions. However, the portion of the wing and hinge that remains contains the tegula, sensilae campanoformia, axillary cord, axillary sclerites and costal structures (Figure I-4) (O'Brochta, 1980). vg^U corresponds to the most severe class of alleles shown in Figure I-3. Both vg^1/vg^1 and vg^U/+ genotypes cause the surface area of the haltere to be reduced in size, although no other part of the fly appears to be affected (O'Brochta, 1980). The wings of vg^W/+ heterozygotes are reduced to a similar degree, but the vg^W allele also produces a duplication of the remaining posterior structures. This transformation phenotype is most often observed as small duplications of axillary cord and alar lobe (Bownes and Roberts, 1981a). Even in rare vg^W adults that produce a small amount of wing blade, no anterior bristles are ever observed nor are anterior specific costal structures.(Figure I-1 B,J) (Bownes and Roberts, 1981a). One additional phenotype observed in vg^W flies is occasional abnormalities of the thorax including both duplications and loss of these tissues (Bownes and Roberts, 1981a). Further, both vg^W and vg^U are recessive for the erect postscutellar

Figure II-1 A diagram illustrating the chromosomal inversions that produce the dominant alleles vg^W and vg^U

Top) The organization of the region of the right arm of the second chromosome containing the *en, inv, vg and mam* genes. The centromere is to the left of the diagram. Each gene is represented by an arrow that indicates the direction of transcription. The *inv* and *en* genes are located at cytological position 48A and the transcriptional orientation of these two genes is such that they are in opposing directions (Coleman et al., 1987). The *vg* gene is located at position 49D and is transcribed in a centromere proximal to distal direction (Williams et al., 1990a).

Bottom-right) A large part of the *vg* coding sequence is located within the vg^U inversion. One breakpoint lies within the second intron of *vg* while the second breakpoint is within the coding region of *mam.*

Bottom-left) vg^W is established by an inversion that breaks 8kb upstream of the *inv* start site and within the first exon of *vg* (Williams et al., 1990b). The inv^D allele is associated with a reversion of the dominant loss of wing phenotype but retention of the homeotic transformation associated with vg^W. The dominant loss of wing activity of vg^W is eliminated by a removal of sequences including the distal portion and the 3' UTR of the *vg* coding region (arrow).

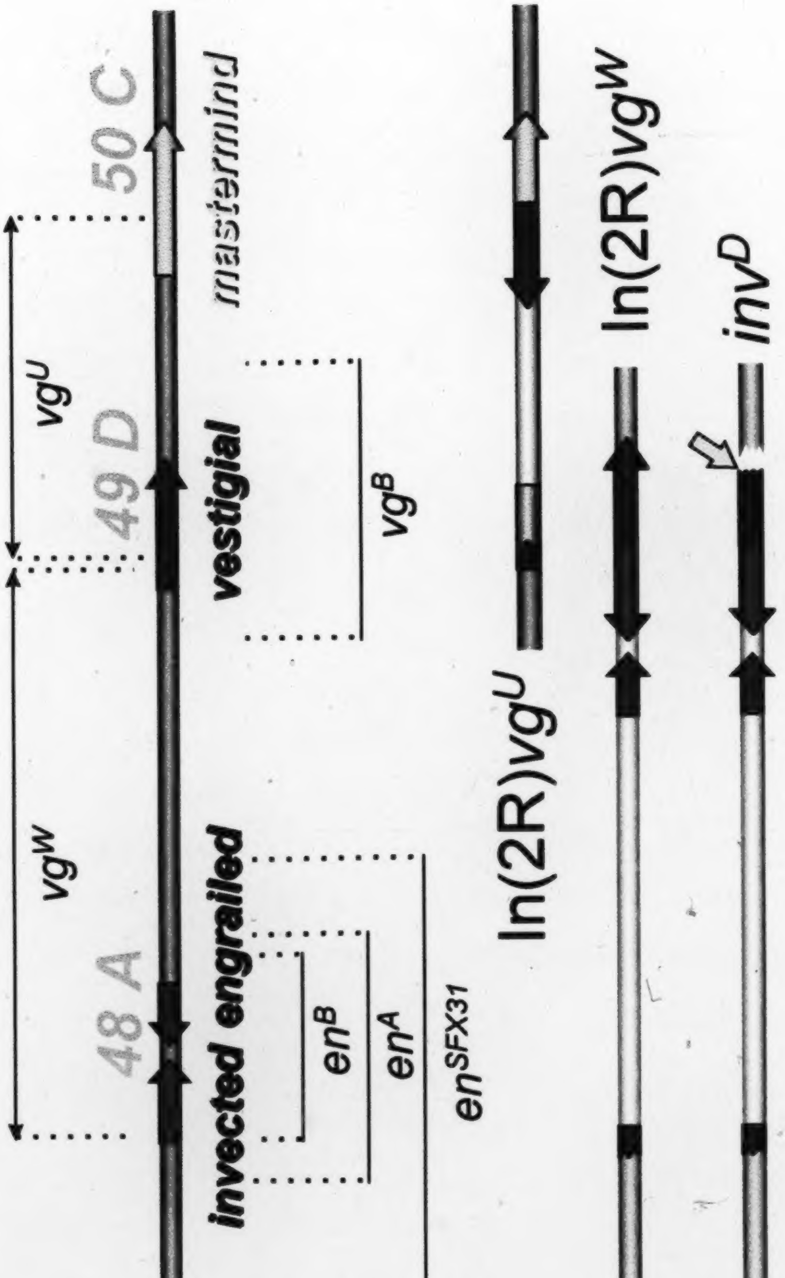
48 A
49 D
50 C
invected engrailed
vestigial
mastermind
vg^W
vg^U
vg^B
en^B
en^A
en^SFX31
In(2R)vg^U
In(2R)vg^W
inv^D

bristle and female sterility phenotypes commonly associated with correspondingly severe recessive *vg* alleles. The survival associated with the dominant alleles also differentiates them from most other *vg* alleles as both the vg^{W}/vg^{W} and vg^{U}/vg^{U} homozygotes are unconditionally lethal. The vg^{U} homozygote shows a neuralized embryonic lethal phenotype that is similar to that produced by homozygous null *mam* alleles or vg^{U}/mam (Williams et al., 1990b). The vg^{W} homozygote is also an embryonic lethal, acting prior to formation of the syncytial blastoderm (Bownes and Roberts, 1981a). Extensive previous analysis has shown that all aspects of vg^{W}, including the embryonic lethal phenotype, are attributable to defects in the *vg* region of the second chromosome (Bownes and Roberts, 1981a). This was determined by systematically substituting each chromosome other than that containing vg^{W} with marked chromosomes. Further, Bownes and Roberts (1981a), also examined the remainder of the second chromosome outside the vg^{W} inversion by recombination with genetic markers adjacent to the *vg-en* region. Therefore, unless there is a gene in very close proximity to the vg^{W} inversion there is little possibility of second site mutations causing any aspects of the phenotype. The lethality associated with homozygous vg^{W} and vg^{U} alleles is a specific property associated with vg^{U} or vg^{W}, as homozygous *vg* null alleles are completely viable (Williams et al., 1993; Williams et al., 1990b). Because of this lethality, the genotypes vg^{W} and vg^{U} referred to hereafter represent the vg^{W}/vg^{+} and vg^{U}/vg^{+} heterozygotes.

Previous characterization of vg^{W} and vg^{U} determined that the transcriptional orientation of both the *inv* and *mam* genes is opposite to that of the remaining *vg* coding region (Figure II-1) (Williams and Bell, 1988; Williams et al., 1990b). This eliminates the possibility of a hybrid fusion transcript of *vg* and either *inv* or *mam* sequences beginning from either of the normal transcriptional start sites of the two fused genes. Northern blot analysis of RNA from either vg^{W} or vg^{U} detects no transcripts other than the normal 3.8 kb *vg* transcripts arising from the vg^{+} allele on the heterozygous wild type chromosome (Williams et al., 1990b). As part of this initial characterization, Williams et al. (1990b) also recovered four full wing phenotypic revertant alleles of vg^{W} and one of vg^{U}. The single revertant allele of vg^{U}, vg^{UR2}, can partially complement classical *vg* alleles and thus represents the conversion of the dominant vg^{U} allele into a *vg* hypomorph (Williams et al., 1990b). vg^{UR2} is the result of an insertion into the *mam* sequences located near the inversion breakpoint that is closest to the majority of the *vg* coding region (Williams et al., 1990b). Similarly, each of the four vg^{W} revertants vg^{WR1} - vg^{WR4} completely suppressed both the dominant loss of wing phenotype and the homeotic transformation of the wing (Williams et al., 1990b). The vg^{WR1} allele is a deletion that removes the entire *vg* coding region and a large portion of *inv*. Analysis of the vg^{WR2}-vg^{WR4} alleles indicated that they are the product of insertions within upstream *inv* sequences that move the fused *vg* and *inv* sequences further apart, converting them to recessive *vg* alleles (Williams et al., 1990b). These revertants also show that the *inv* or *mam* sequences fused to *vg* are playing a role in causing the lethality associated with vg^{W} and vg^{U}. While the combination of vg^{U}/vg^{W} is unconditionally lethal, specific combinations of the phenotypic revertants with these alleles or themselves, including vg^{W}/vg^{UR2}; vg^{U}/vg^{WR2} and vg^{UR2}/vg^{WR2} are viable but produce a strong *vg* phenotype (Williams et al., 1990b). Therefore, the lethality associated with vg^{W} and vg^{U} is likely a property of the gene fusions caused by the inversions and is not a property of any other lethal mutations closely linked to the dominant alleles (Williams et al., 1990b). Further, these revertant alleles also illustrate the importance of the *inv* and *mam* sequences in mediating the dominant wing phenotype of vg^W and vg^U as lesions within those sequences cause complete phenotypic reversion.

Genetic analysis of vg^W and vg^U further illustrates that the mechanism for the dominant activity of these alleles is highly complex. vg^B is a *vg* null allele associated with the removal of a large genomic region that completely encompasses the *vg* coding sequence and flanking regions (Morgan et al., 1938). vg^U is viable when heterozygous with vg^B and produces a phenotype similar to that of vg^U/+ (Williams et al., 1990b). A similar combination of vg^W/vg^B causes a more extreme phenotype including complete loss of the notum in the majority of the flies (Bownes and Roberts, 1981a). However, a similar heterozygote of vg^W with a smaller deficiency, vg^C , does not remove the thorax (Bownes and Roberts, 1981a). When vg^U or vg^W are heterozygous with recessive *vg* hypomorphs a phenotype intermediate between that associated with the respective recessive *vg* homozygotes and either vg^W/ vg^B or vg^U/ vg^B is observed (Williams et al., 1990b). However, it is difficult to characterize these intermediate phenotypes except on gross morphological differences as both the dominant and recessive *vg* phenotype possess inherent variability (Bownes and Roberts, 1981a; Nakashima-Tanaka, 1968; O'Brochta and Bryant, 1983; Williams et al., 1990b). This is illustrated best by the minor differences observed in the expressivity of the vg^W and vg^U phenotype at various temperatures. When grown at 29°C slightly larger wings are formed in the presence of either of the dominant alleles (Williams et al., 1990b). However, despite this variability, the homozygous lethality and variable notum phenotypes suggest a complex interaction between *vg* and the fused *inv* and *mam* sequences that is distinct from the phenotype produced by recessive *vg* mutants. Complex interactions with the homeotic phenotype associated with vg^W have also been observed. The *Contrabithorax* (*Cbx*), allele of *Ubx* produces transformations of wing to haltere that occur most often in the posterior compartment. However, in the presence of *vg*^{W}, the transformations only remove the original posterior wing structures and do not alter the transformed posterior structures in the anterior of the wing (Bownes and Roberts, 1981a). Finally, since the *inv* gene is located in close proximity to the *en* locus, any consideration of the *vg*^{W} allele must include possible alterations to *en* function. However, it appears that the inversion associated with *vg*^{W} affects only the *inv* locus and not the *en* gene. When *vg*^{W} is crossed to *en*^{LI301} (a lethal *en* point mutation) these flies survive. This indicates that while *vg* sequences are moved closer to *en* by the inversion, there is no effect upon wild type *en* expression (Bownes and Roberts, 1981a; Williams et al., 1990b).

In normally developing wing discs, the cell number increases slowly but steadily throughout embryonic and larval development. Homozygous recessive mutations of *vg* show reduced numbers of cells within the wing imaginal disc, approximately 60-70% of wild type measured just before pupariation (James and Bryant, 1981). This cell loss is thought to result almost exclusively from cell death, which occurs during the late third larval instar (Fristrom, 1969; James and Bryant, 1981; O'Brochta, 1980). It appears that recessive *vg* mutants induce no significant amounts of cell death in the second or early third larval instar (Fristrom, 1969). Within wild type wing discs, there is a low level of cell death associated with normal development with peak levels observed at approximately 72 hours AEL. However, in no case do significant amounts of patterned cell death occur in wild type wing discs compared to discs from *vg* mutants (James and Bryant, 1981). In the presence of the *vg*^{W} allele, the pattern of cell death in the wing imaginal disc changes significantly both temporally and spatially. In *vg*^{W} wing discs, an extremely high amount of cell death occurs before the late third instar (Bownes and Roberts, 1981a). At the same time, the haltere discs of *vg*^{W}

show an increase in size in addition to altered patterns of cell death. The increased cell number may, however, be due to the anterior of the haltere being transformed to wing (Bownes and Roberts, 1981a). By the late third larval instar, no significant amount of cell death is observed in *vg*^{W} wing discs although by this stage they are significantly reduced in size (Bownes and Roberts, 1981a). In a similar fashion, the elevated amount of cell death observed in *vg*^{U} wing discs occurs during the early third instar (O'Brochta, 1980). Accompanying *vg*^{U}-mediated cell death, there is a significant number of degenerating cells that remain within the epithelial layers of the wing disc whereas in recessive *vg* mutants the dead cells accumulate along the basal epithelia (O'Brochta, 1980). By late third instar, *vg*^{U} wing discs stained with trypan blue do not exhibit elevated levels of cell degeneration. Further, the overall morphology of the *vg*^{U} wing imaginal disc indicates that the cell loss leading to the *vg*^{U} phenotype has already taken place (O'Brochta, 1980). Thus, the differences in timing and patterns of cell death represent a significant difference in the activity of dominant *vg* alleles versus their recessive counterparts. The differences in patterns of cell death observed with the dominant *vg* alleles is significant, as cell death early in the third larval instar wing disc is associated with other wing patterning genes. These include *wg* and *ap*, whereas cell death in late third instar is a phenotype associated with recessive mutants of *vg* and *sd* (Fristrom, 1969; James and Bryant, 1981). The presence of cell death early in the third instar suggests that the mechanism mediating the dominant *vg* activity may involve interaction with the earlier patterning genes *wg* or *ap*.

In an attempt to determine the mechanisms involved in producing a dominant *vg* phenotype we further mutagenised *vg*^{W} and *vg*^{U}, screening for the restoration of a wing size greater than that associated with the original dominant alleles. Since any role for the *vg* portion of the respective fusions was previously undefined, it was hoped that additional mutations would map to the *vg* sequences. From this new screen, a number of full wing revertants and two classes of new alleles that partially eliminate the dominant *vg* activity were recovered. Unlike previous revertants, many of these new alleles contain alterations to specific regions of the *vg* portion of the gene fusions. Examination of protein expression within the wing imaginal discs in the presence of dominant *vg* alleles shows limited *vg* expression within the remaining tissue. This reappearance of some but not all of *vg* expression in the partial revertants suggests a mechanism for the dominant *vg* activity. It appears that the presence of the dominant alleles is interfering with the establishment of a complete *vg* expression pattern in the wing imaginal disc. The partial revertant alleles also provide an opportunity to observe the consequence of removing discrete portions of *vg* expression within the wing disc.

Results

γ-ray mutagenesis of vg^U and vg^W flies produced 21 additional independent phenotypically revertant lines that eliminated some or all of the dominant *vg* phenotype. Each of these produces more wing tissue when heterozygous to vg^+ than is found in adult flies harboring the progenitor dominant alleles. Based upon the size and shape of the resulting wing, these revertant lines grouped into three distinguishable phenotypic classes (Table II-1). Reversion mutations that restore full adult wing formation represent the majority (Figure II-2 E, I) with an overall size corresponding to the full wing classes I-III listed in Figure I-3. Occasionally these flies show nicks at the distal end of the wings similar to what is seen in flies containing a single vg^+ allele heterozygous

Figure II-2 Wing phenotypes produced by revertants of vg^{W} and vg^{U}.

The scale bars at lower right indicate 5 mm for A-I,L and 1 mm for J-K. A) A wild type wing showing normal size and morphology. B) Wings from vg^{W}/+ flies are extremely reduced in size compared to wild type although a complete margin surrounds the reduced wing. C) A slightly larger wing produced by a weak revertant (vg^{WRK4}/+) of vg^{W}. These wings have some vein patterning within the interior of the incomplete wing but margin specific bristles are not seen. Some structures of the wing hinge are produced in these flies but many abnormalities are seen compared to wild type (open arrowhead). D) vg^{WRK6}/+, an example of a vg^{W} strap wing revertant. The wings of these flies are between 20% to 60% the size of wild type wings (Class VI-VII). Additional wing veins are seen compared to the wings produced by weak revertants, and in 2-3% of these flies bristles are observed forming near the distal tip (asterisk). Anterior-like bristles are often formed in these wings mostly in the proximal blade region or within the costal structures (arrow). E) A full wing revertant, vg^{WRK1}/+, is indistinguishable from wild type. The specific TR, DR and PR margin bristle patterns are all present indicating that both the dominant loss of wing and homeotic phenotype associated with vg^{W} have been eliminated. F) Heterozygous vg^{U}/+ flies also show an almost complete loss of wing tissue. Margin structures are never observed within these wings and the entire wing blade appears to be deleted leaving only portions of the ventral wing hinge (Figure I-5). G) vg^{URK13} represents were the weak revertant class of vg^{U}. These wings are only slightly larger (Class IX) than those produced by vg^{U} (Class X). Some wing blade is formed in this class often including the occasional wing vein (arrow). H) In vg^{URK5} strap wing revertant flies a larger amount of the interior wing blade is formed. The vII, vIII and vIV veins are seen and the pcv (arrow), is clearly seen forming within the wing blade. The occasional presence of margin specific bristles can be detected at the proximal tip of these wings (asterisks). I) vg^{URK6} a full wing revertant of vg^{U}, shows an almost complete restoration of wing with the exception of small nicks in distal regions (arrowhead). J) A wing from a $vg^{W}/+$ fly shown at higher magnification. The margin specific bristles are labeled by an asterisk, while the open arrow indicates missing hinge structures where the wing joins the notum. K) A similarly enlarged view of a $vg^{U}/+$ wing has no margin bristles (asterisk) but the hinge is more fully formed than in $vg^{W}/+$ flies (open arrowhead). L) Df(2R)$vg^{B}/+$. When only one copy of vg^{+} is present, nicks are often present in the distal portion of the wing (arrowhead).

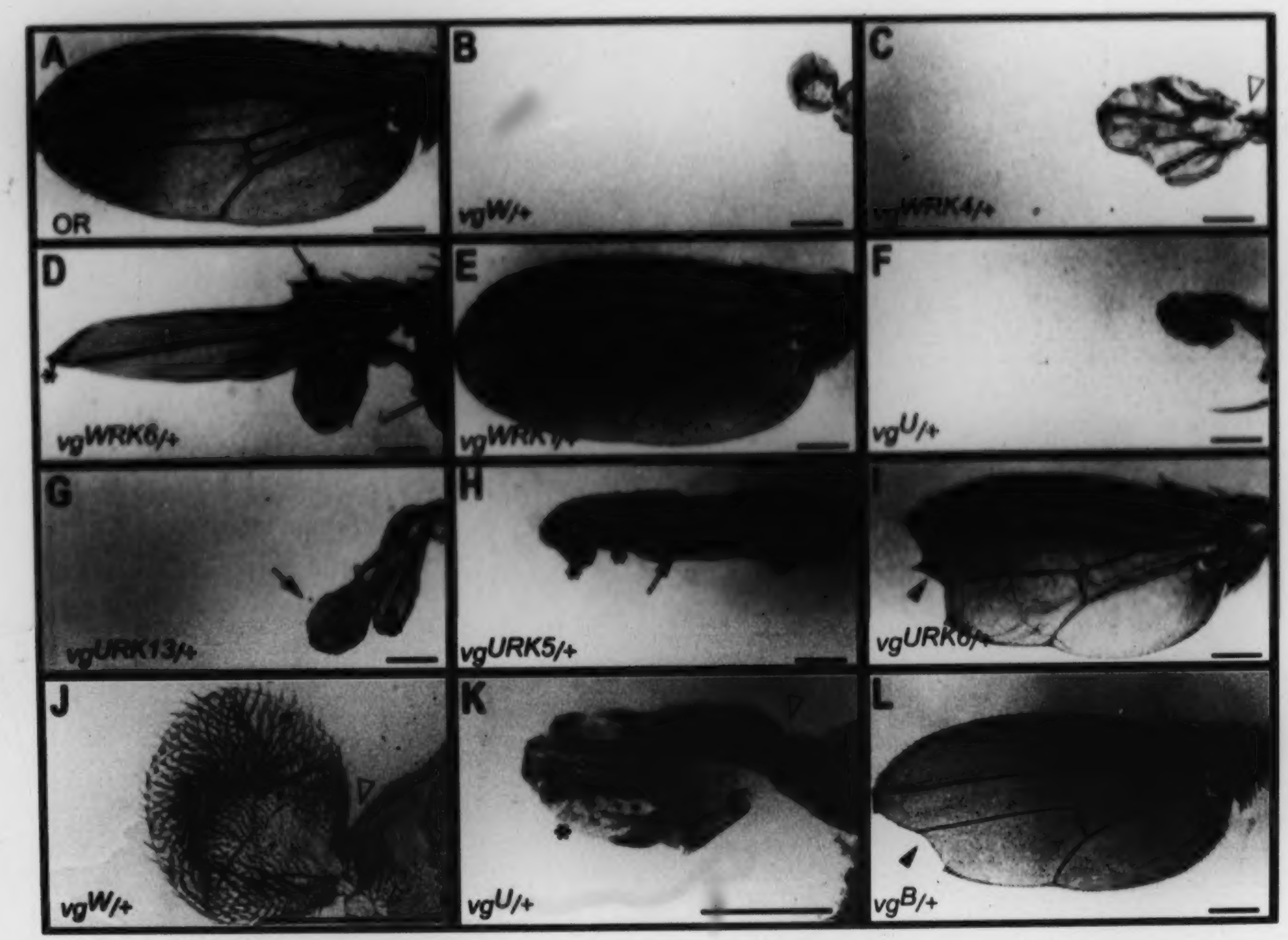
A
OR
B
vgW/+
C
WRK4/+
D
vgWRK6/+
E
vgWRK
F
vgU/+
G
vgURK13/+
H
vgURK5/+
I
vgURK6/+
J
vgW/+
K
vgU/+
L
vgB/+

with the null *vg* allele, Df(vg^B) (Figure II-2I). This suggests that the original dominant *vg* activity has been eliminated, resulting in their conversion to recessive loss of function *vg* alleles. The remaining revertant alleles exhibit some but not all of the original dominant phenotype. These partial revertants were divided into two classes, manifesting either a weak or a strap wing phenotype (Figure II-2). Flies inheriting an allele of the weak revertant class (Figure II-2 C,G) produce wings with less than approximately 20% of normal wing tissue (class IX, Figure I-3). Flies of the strap wing class of revertants produce between 20% and 60% of wing tissue (class VI-VII Figure I-3) compared to wild type (Figure II-2 D, H). In all flies of both partial reversion classes internal wing structures are seen, including veins and a completely formed hinge (Figure II-2 G-I).

The genetic properties of the new vg^W and vg^U revertant alleles were determined by crossing each to a selection of known *vg* mutants. The vg^B allele is a large deficiency covering the entire *vg* locus and is a *vg* expression null (Williams and Bell, 1988). None of the phenotypic revertants, whether full wing or partial, produce any wing specific tissues when heterozygous with vg^B. Further, neither the original dominant alleles nor any of the revertants derived from them show any complementation when heterozygous with the vg^{83b27} allele. This allele can complement many recessive *vg* alleles as it has only a small deletion of the enhancer element located in the second intron (Williams et al., 1994). In each case, it appears that none of the revertants isolated in this screen can supply normal *vg* function. Thus, these revertants represent elimination of some or all of the dominant *vg* effect associated with vg^W and vg^U converting them to either weakly dominant or recessive *vg* alleles. These

Table II-1. Summary of the revertant strains produced from mutagenesis of the vg^{U} and vg^{W} dominant alleles.

	Full Wings[†]	Strap Wings[‡]	Weak Revertant[*]
	$vg^{URK1}/+$	$vg^{URK5}/+$	$vg^{URK13}/+$
	$vg^{URK2}/+$	$vg^{URK16}/+$	$vg^{URK14}/+$
	$vg^{URK3}/+$	$vg^{URK17}/+$	$vg^{URK15}/+$
	$vg^{URK4}/+$	$vg^{WRK5}/+$	$vg^{WRK3}/+$
	$vg^{URK6}/+$	$vg^{WRK6}/+$	$vg^{WRK4}/+$
	$vg^{URK7}/+$		
	$vg^{URK9}/+$		
	$vg^{URK11}/+$		
	$vg^{URK12}/+$		
	$vg^{WRK1}/+$		
	$vg^{WRK2}/+$[§]		
total	11/21	4/21	5/21

[†] Approximately wild type size.

[‡] Between 20% to 60% of wild type.

[*] Greater than the original dominant but less than about 20% of wild type size.

[§] This allele produces wings of wild type size which exhibit a stable anterior to posterior homeotic transformation (Chapter III).

reversions must affect either the sequences within the *vg-mam* or *vg-inv* fusions that cause the dominant *vg* phenotype, or alternatively other sites that act to suppress the dominant *vg* activity.

In normally developing third instar wing discs, *vg* expression straddles the D/V margin which is established by the activity of the *ap* protein (Figure II-3 A). *vg* protein expression is also detected within the peripheral anterior and posterior regions fated to become the wing hinge, portions of the notum, and in the area of the disc fated to become the ventral pleura (Figure I-3) (Bryant, 1975; Williams et al., 1991). Examination of *vg* protein localization in developing wing imaginal discs from vg^{W} and vg^{U} larvae as well as the partial revertant alleles shows that *vg* expression patterns are altered significantly compared to wild type. The change in *vg* expression in the presence of the dominant and partially dominant alleles suggests interference with the establishment of some, but not all, *vg* patterning in the wing disc. The pattern and overall expression level of *vg* protein within the remaining cells of vg^{W} or vg^{U} third instar imaginal wing discs is significantly different from wild type (Figure II-3 A versus B,D), although *vg* expression within the presumptive notum and the discrete scutellar region of the wing disc remains comparable to that of normal wing discs (Figure II-3 A versus B, D). Within vg^{W} imaginal discs, the expression of *vg* is reduced to a narrow stripe along the D/V margin (Figure II-3B). However, this continuous D/V *vg* patterning correlates with the appearance of a continuous band of margin specific bristles in the resulting wing (Figure II-3 B,J). The pattern of *vg* expression appears to bifurcate at or near the centre of the remaining wing pouch along the D/V margin (Figure II-3 B). The lack of *vg* expression at any significant distance from the D/V boundary can be linked to a loss of almost all of the interior wing structures. Loss of specific *vg* expression normally found at the anterior of the wing disc correlates with improper formation of the hinge (Figure

II-3 B). When the vg^{U} allele is present, there is no continuous stripe of D/V expression in larval wing imaginal discs (Figure II-3 D). Correspondingly, no margin is ever formed in the wing of vg^{U} flies (Figure II-3 K). Within vg^{U} imaginal discs a large number cells, expressing *vg* can be detected in the anterior regions of the disc that will form the wing hinge. Imaginal discs isolated from larvae containing partial revertant alleles of vg^{W} or vg^{U} contain proportionally more cells expressing *vg* than discs from larvae possessing the progenitor dominant alleles (Figure II-3 C, E-F). This increase in the total number of *vg* expressing cells within the wing disc correlates with the increase in the relative amount of wing tissue formed in the adult. The discontinuity in the pattern of *vg* expression along the D/V boundary is highly reproducible for each partial revertant allele (Figure II-3 C, E-F). This is best illustrated in Figure II-3 (E) where a small area of *vg* expression appears within the central region of the wing compartment fated to form the distal wing (Figure II-3 E arrows). This leads to the formation of a wing which is deleted along the anterior and posterior margins but is fully formed along the P/D axis (Figure II-3 H).

Further, this discontinuity in the patterning of *vg* associated with partial revertants correlate to mutations within specific regions of *vg*. Southern blot analysis of the various revertant alleles identified those alterations affecting only the *inv* and *mam* fusion genes versus those within *vg* sequences (Figure II-4). Below the map shown in Figure II-5 is a summary of the alterations in the *vg* sequences of vg^{W} and vg^{U} that are associated with partial reversion of the dominant phenotype. Insertions or deletions within the fusion partner genes produced a full wing phenotype although one allele, vg^{URK9}, represents a partial duplication and deletion that extends into the *vg* region. In contrast, mutations

Figure II-3 The localization of *vg* expression within third instar wing discs.

The scale bar at lower left represents 100 μm. The expression of *ap-lacZ* was used to demarcate the position of the D/V compartment border in each case. For each, the single *ap-lacZ* image is on the left (red), the *vg* single image is on the right (green) and a superimposed image is in the middle. A) The normal expression of *vg* within wild type wing discs follows a graded pattern along the D/V margin determined by the limit of *ap* expression. Specific landmarks corresponding to the anterior and posterior wing hinge (h), D/V boundary (arrowheads) and a small area of localized *vg* expression within the presumptive ventral notum (n), are indicated. B) vg^{W}/+ wing imaginal discs show a large size reduction in the area fated to form the wing blade. However, the remaining wing cells expressing *ap* protein within the dorsal compartment express *vg* protein continuously along the D/V boundary (arrow). Each cell along the D/V border appears to be expressing *vg* at an equal level although there appears to be more *vg* expressing cells within the ventral compartment (arrowhead). C) Wing discs from vg^{WRK4}, a weak revertant allele, contain more tissue within the wing pouch than do vg^{W} discs. However, in these discs, expression of *vg* protein along the D/V margin is not continuous. It is strongest within the regions of the wing disc fated to form the hinge and proximal wing structures while fading to below detectable limits in the regions fated to form distal structures (arrowhead). D) Imaginal discs isolated from vg^{U}/+ larvae show some *vg* expression within the hinge, but no elevated *vg* expression can be observed within the extremely reduced region of the disc fated to form the wing (arrow, arrowhead). E) vg^{URK5} wing discs of the strap wing class show discontinuous patches of elevated *vg* expression along the D/V boundary (arrowheads). In these discs, *vg* protein is detected at high levels near the point where proximal wing structures originate.

Gaps in the continuous D/V expression of *vg* appear between the presumptive hinge regions and the center of the wing disc. These correspond to regions of the imaginal disc fate map (Figure I-2) that form the wing margin deleted in the adult (Figure II-2 H). F) Wing imaginal discs isolated from weak revertant vg^{URK13} show the selective removal of *vg* expression from the center of the wing disc along the D/V boundary (arrowheads) although *vg* protein expression within cells of the hinge regions is similar to wild type.

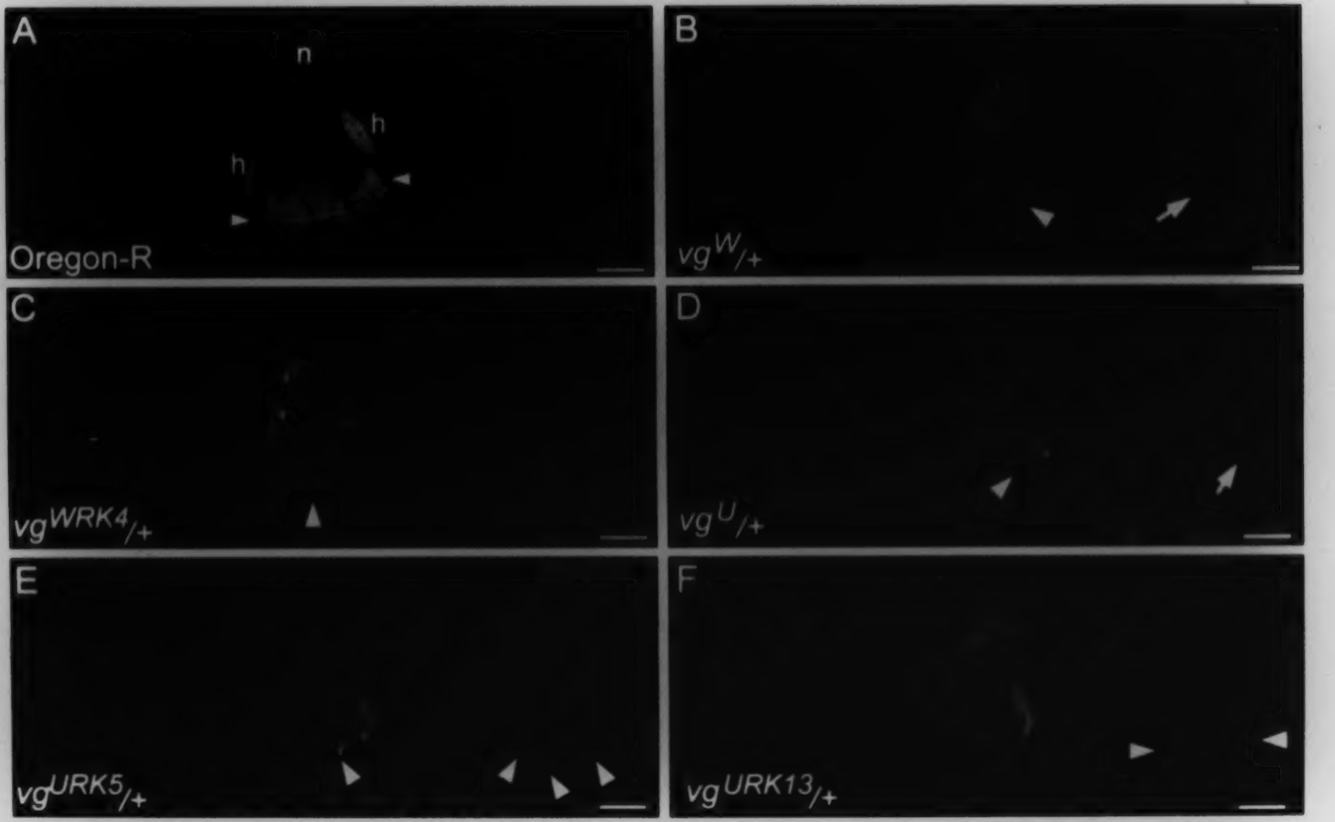
A
n
h
h
Oregon-R
B
vgW/+
C
vgWRK4/+
D
vgU/+
E
vgURK5/+
F
vgURK13/+

that produce a partially reverted phenotype are most often deletions of small regions within the *vg* sequences of the dominant alleles. The alterations within *vg* sequences were further analyzed by PCR to accurately map the extent of the deletions. In all cases, the revertant strap wing phenotype is associated with deletions that cluster between the second and third exon of *vg* near, but not overlapping, the inversion breakpoints. Similarly, deletions associated with the weak revertant class cluster to a region overlapping the fourth *vg* intron. None of the mutations associated with partial reversion of the dominant *vg* phenotype appears to remove exonic sequences 3' to the fourth intron (Figure II-5). A single reversion mutation that affects this region was isolated which causes a complete reversion of the *vg* wing phenotype, but retains a homeotic transformation associated with vg^{W}. This allele removes the 3' end of the *vg* coding region including the majority of the 3' un-translated sequences. This allele is described in detail in Chapter III. One of the weak revertant alleles, vg^{URK3}, showed no alterations within *vg* or *mam* and may involve a second gene that suppresses the dominant phenotype. Alternatively, it may be caused by a mutation too small to be detected with the methods outlined above. However, the mutations associated with the partial revertants define three broad regions within the *vg* portion of the gene fusions that play a role in mediating the dominant *vg* activity.

Since significant amounts of *vg* protein can be detected within larval imaginal discs in the presence of a dominant or partially dominant *vg* allele, quantitative examination of the levels of *vg* protein was undertaken using Western blot analysis (Figure II-6). To establish the relative level of *vg* protein normally present during each developmental stage, a wild type protein expression profile was constructed (Figure II-6 A). This shows that the relative fraction of Vg within total protein extracts is highest during embryonic

Figure II-4 Alterations within the *vg* portion of the revertant alleles of vg^{W} and vg^{U} alleles are associated with a partial revertant phenotype.

A) **Left** - Samples from flies containing each of the revertant alleles were cleaved with *Xho*I or *Sst*I and probed with a fragment (TP) derived from a *Sst*I-*Pst*I region of *vg.* The genotypic designations of each sample are located at the top of each lane. Bands that are different from the progenitor vg^{W} or vg^{U} alleles are indicated by arrows. **Right** -Specific mapping to determine the breakpoints for one allele, vg^{WRK6}. The genotypic designations are shown above each lane and the restriction enzymes used to cleave the samples in each case are indicated at the bottom. The DNA fragment (RR) used as a probe is indicated in the map shown in B. The band corresponding to the *vg* sequences of vg^{W} is reduced in size in the *Bam*HI, *Sal*I, *Sst*I, and *Hin*dIII, lanes. The appearance of a larger band in the *Xho*I, lane indicates that the deletion associated with vg^{WRK6} removes the *Xho*I site located at *vg* position 3.0 (Figure II-5). A summary of the locations where alterations affect the *vg* portion of the remaining dominant alleles is shown in Figure II-5. A map of the *vg* coding sequence associated with the dominant *vg* alleles and the various probes used for southern hybridization of this region is shown above. Also shown is the location of each of the PCR primers used for PCR to further characterize the deletions. C) Probes specific for the *mam* (left) or *inv* (right) portions of the vg^{U} or vg^{W} fusions show no alterations associated with flies possessing the partial revertant phenotype except for vg^{URK9} which extends into both the *vg* and *mam* regions.

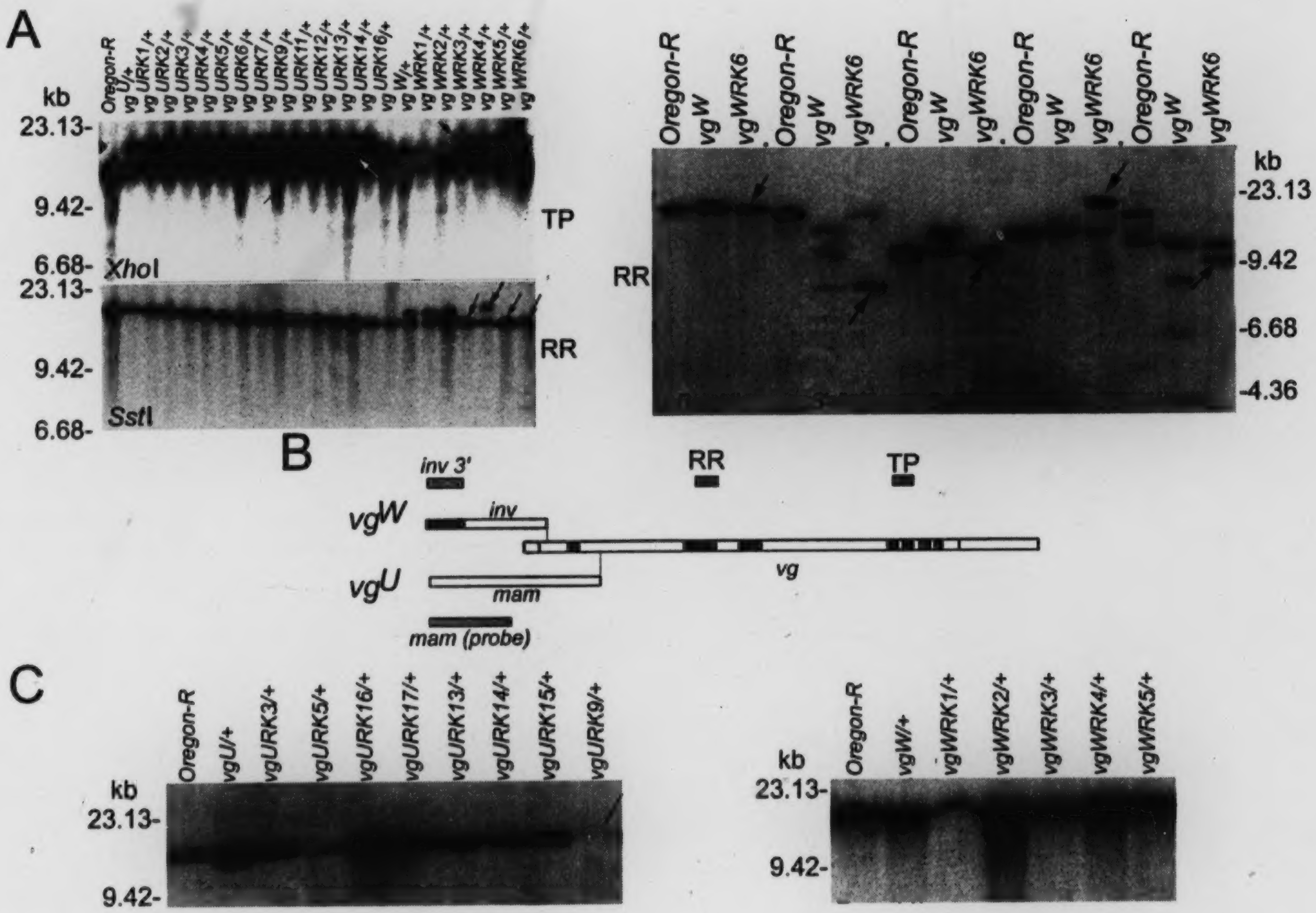
A
kb
23.13-
9.42-
6.68-
23.13-
9.42-
6.68-
Oregon-R
vg U/+
vg URK1/+
vg URK2/+
vg URK3/+
vg URK4/+
vg URK5/+
vg URK6/+
vg URK7/+
vg URK9/+
vg URK11/+
vg URK12/+
vg URK13/+
vg URK14/+
vg URK16/+
vg W/+
vg WRK1/+
vg WRK2/+
vg WRK3/+
vg WRK4/+
vg WRK5/+
vg WRK6/+
TP
XhoI
RR
SstI
Oregon-R
vgW
vgWRK6
Oregon-R
vgW
vgWRK6
Oregon-R
vgW
vgWRK6
Oregon-R
vgW
vgWRK6
Oregon-R
vgW
vgWRK6
RR
kb
-23.13
-9.42
-6.68
-4.36
B
inv 3'
RR
TP
vgW
inv
vg
vgU
mam
mam (probe)
C
Oregon-R
vgU/+
vgURK3/+
vgURK5/+
vgURK16/+
vgURK17/+
vgURK13/+
vgURK14/+
vgURK15/+
vgURK9/+
kb
23.13-
9.42-
Oregon-R
vgW/+
vgWRK1/+
vgWRK2/+
vgWRK3/+
vgWRK4/+
vgWRK5/+
kb
23.13-
9.42-

Figure II-5 A physical map of revertants affecting the *vg* region of the vg^{W} and vg^{U} alleles.

A complete summary of the molecular lesions associated with partial reversions of the dominant *vg* phenotype is shown. The distances, restriction map, and intron/exon boundaries are from Williams et al. (Williams et al., 1991). The *vg* coding region is shown below the restriction map. Exons are indicated as large boxes, with the translated region indicated by shading. Each of the introns are numbered and marked with a line joining each of the exons. The smaller boxes within intron 2 and 4 indicate the approximate location of the intronic *vg* enhancer elements. Most full wing reversion mutations were restriction mapped 5' of the respective fusion breakpoints and the associated lesions are within the *inv* or *mam* sequences (Figure II-4 C). However, one revertant, vg^{URK9}, appears to involve a more complex rearrangement involving both a duplication as well as a deletion that extends from *mam* into the *vg* sequences. All of the partial revertants were associated with deletions that localize within the *vg* coding region. The mutations mapping to the 4.5-8.0 region of *vg* give a strap-wing phenotype. The weak revertant class is associated with mutations that extend up to 13.0 on the *vg* map. None of the partial reversion mutants extends into the exonic sequences located past 13.0 on the *vg* map. The vg^{WRK2} mutation, which does map to this region, forms full wings but retains the homeotic phenotype associated with vg^{W}. The boxes above each genotypic designation represent the approximate extent of the respective deletions. The arrows shown immediately above the third and sixth exon indicate the position of *vg* specific primers used for RT-PCR analysis (Figure II-7).

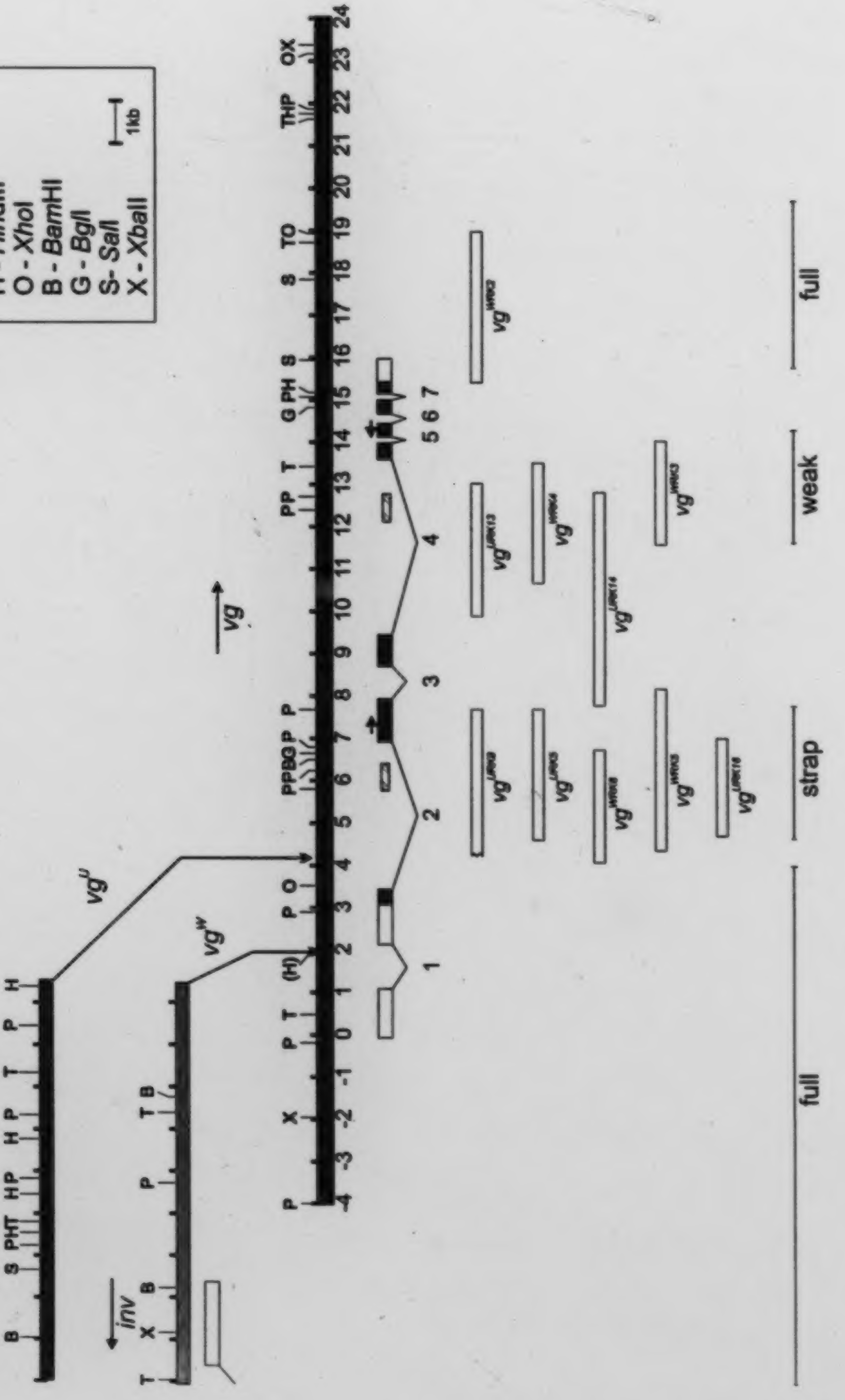
P - PstI
T - SstI
H - HindIII
O - XhoI
B - BamHI
G - BglI
S- SalI
X - XbaII
1kb
mam
inv
vg
vg^U
vg^W
B S PHT HP H P T P H
T X B P T B
P X P T (H) P O PPBGP P PP T GPH S S TO THP OX
-4 -3 -2 -1 0 1 2 3 4 5 6 7 8 9 10 11 12 13 14 15 16 17 18 19 20 21 22 23 24
1 2 3 4 5 6 7
full
strap
weak
full

and early pupal stages (Figure II-6 A). The intensity of the *vg*-specific bands was normalized to a second antibody that recognizes cellular actin. This method appears to give a reliable measure of protein levels, as the relative amount of *vg* protein expressed at each stage is similar to previously determined expression levels of *vg* mRNA (Williams et al., 1990a). This correlation between the levels of *vg* transcription with levels of *vg* protein at each stage suggests that no post-transcriptional control of *vg* is occurring. It is interesting to note that during third larval instar, a critical point at which *vg* is required for wing disc patterning, the levels of *vg* protein are relatively low (Figure II-6 A).

To examine *vg* protein expression in the presence of the vg^{W} and vg^{U} alleles, corresponding Western blots were run using total protein extracts from early and late third instar larvae as well as newly formed pupae (Figure II-6 B-D). Protein extracts from larvae and pupae that were homozygous *vg* null (vg^{32b27R}/vg^{32b27R}), or contained a single copy of *vg* ($vg^{B}/+$) were added for comparison of relative expression levels. Also, extracts from larvae and pupae homozygous for a mutation that removes the wing specific expression of *vg* (vg^{83b27}/vg^{83b27}) were included as this allele eliminates only wing specific *vg* expression (Williams et al., 1991). The genotype $vg^{B}/+$ produced approximately half the wild type amount of *vg* protein (Figure II-6 B-D). It appears that *vg* protein expression from the vg^{+} allele is not suppressed by either vg^{W} or vg^{U} since significant amounts of *vg* protein are detected. However, there appears to be a slightly higher level of expression associated with vg^{W} than vg^{U}. Further, when protein extracts from vg^{W}/vg^{B} larvae were examined, a faint band above background could sometimes be detected on blots exposed for extended periods of time (not shown). This suggests that a low level of expression of a protein recognized by the *vg* antibody can be associated with the vg^{W} allele. No *vg* protein can be detected in protein extracts from larvae where vg^{U} is

Figure II-6 Western blot analysis of *vg* protein expression in the presence of dominant *vg* alleles.

Hybridization with an actin antibody is shown below each blot as a loading control. The bar graph below each lane indicates the relative intensity of each *vg* band compared to the actin control as determined by densitometric scanning. The extraneous bands either above or below the prominent Vg band in each of the lanes may represent cross hybridization with other proteins that have a weak similarity to the C-terminal portion of *vg*. Alternatively, these bands may be modified forms of the *vg* protein. Ectopic bands of a size smaller than Vg that are seen in only a single lane likely represent a degraded form of the *vg* protein. A) A developmental profile shows that in Oregon R flies, the highest amounts of *vg* protein are found during embryonic stages and 60h after the beginning of pupariation. The designations are as follows: Embryo - 12hr embryos, L1- first instar larvae, L2- second instar, L3 - third instar, Pupa - 60hr after pupariation, Adult - newly eclosed adults. During larval stages, where significant differences in *vg* patterning are found, the relative level of *vg* protein is quite low. B) Early third instar vg^{W} and vg^{U} larval protein extracts contain *vg* protein in amounts equal or greater to that present when a single copy of the vg^{+} gene is present. The Oregon R control represents two functional copies of vg^{+}. $vg^{W}/+$ and $vg^{U}/+$ represent the expression found in organisms harboring the dominant alleles in the presence of a vg^{+} chromosome. Df (2R) vg^{B} is a deficiency that fully eliminates the *vg* coding region, thus heterozygous individuals should produce approximately half the wild type *vg* protein seen in wild type larvae. vg^{83b27} is a homozygous recessive mutant that removes an intronic enhancer element and is thought to represent the basal level of *vg* protein expression outside that found at the D/V wing boundary (Williams et al., 1993). The wild type level of *vg* is established as one unit. The level of *vg* protein produced by $vg^{B}/+$ is approximately one half the value of wild type. Comparison of protein extracts from larvae containing *vg*^{W} and *vg*^{U} to that of wild type indicates that the amount of *vg* is reduced it is not lower than produced in *vg*^{B}/+ larvae. C) The levels of *vg* protein in late third instar also show no reduction compared to *vg*^{B}/+. The *vg*^{83b27R} lane is an additional control that corresponds to protein extracts isolated from a *vg* homozygous null strain. D) During early pupal stages, (60h after pupariation) the relative differences between *vg*^{W} and *vg*^{U} are still apparent. The bands immediately above and below the prominent *vg* band represent cross-hybridizing proteins that react to the *vg* antibody. These bands can be suppressed but not eliminated by additional blocking of the membrane and pre-absorption of the *vg* antibody against early embryos.

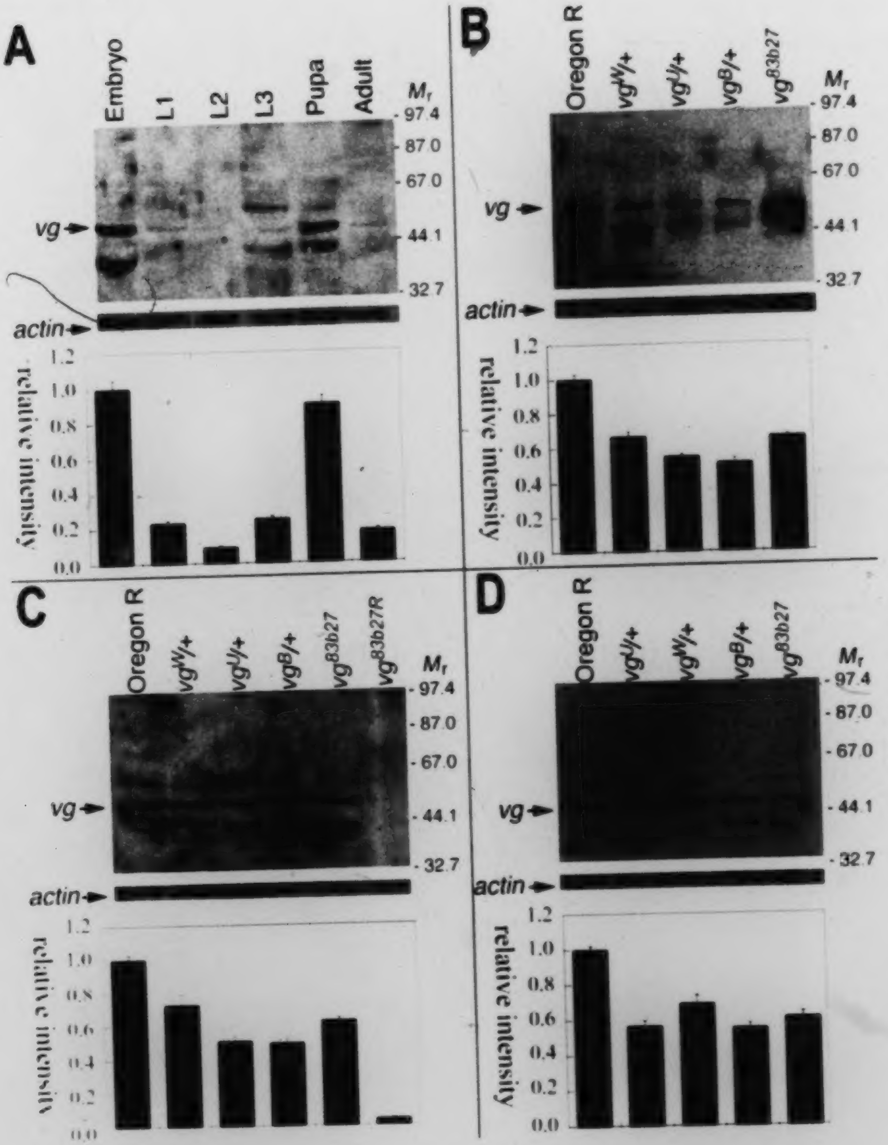
A
Embryo
L1
L2
L3
Pupa
Adult
M_r
97.4
87.0
67.0
44.1
32.7
vg
actin
relative intensity
0.0
0.2
0.4
0.6
0.8
1.0
1.2
B
Oregon R
$vg^{W}/+$
$vg^{U}/+$
$vg^{B}/+$
vg^{83b27}
M_r
97.4
87.0
67.0
44.1
32.7
vg
actin
relative intensity
0.0
0.2
0.4
0.6
0.8
1.0
1.2
C
Oregon R
$vg^{W}/+$
$vg^{U}/+$
$vg^{B}/+$
vg^{83b27}
vg^{83b27R}
M_r
97.4
87.0
67.0
44.1
32.7
vg
actin
relative intensity
0.0
0.2
0.4
0.6
0.8
1.0
1.2
D
Oregon R
$vg^{U}/+$
$vg^{W}/+$
$vg^{B}/+$
vg^{83b27}
M_r
97.4
87.0
67.0
44.1
32.7
vg
actin
relative intensity
0.0
0.2
0.4
0.6
0.8
1.0
1.2

heterozygous with the vg^B deletion. These observations are consistent with the location of the respective breakpoints of vg^W compared to vg^U. The translational start point of *vg* is not affected by the breakpoint associated with the vg^W inversion but it is separated from the greater portion of the *vg* coding region in the vg^U allele. Therefore, the protein recognized by the *vg* antibody in extracts from vg^U/+ individuals can be attributed solely to that contributed by the heterozygous vg^+ allele. In vg^W/+ individuals it appears that a portion of the measured *vg* protein may be contributed by vg^W. In either case, expression from the vg^+ allele heterozygous to vg^W and vg^U is not suppressed by the presence of the dominant alleles, since the amount of *vg* protein is equivalent to or higher than that produced by vg^B/+ individuals. The relative amounts of *vg* protein are consistent throughout early third instar, (Figure II-6 B), late third instar (Figure II-6 C), and 60 hour pupae (Figure II-6 D). Parallel Western blots performed with a second *vg*-antibody against the amino terminal domain of the *vg* protein displayed identical results to those shown in Figure II-6. The smaller bands occasionally seen in only some of the lanes likely represent degradation products. The weakly staining bands located above the predominant *vg* band could be reduced but not eliminated by a more extensive blocking step or by pre-absorbing the antibody against unfixed early embryos. This suggests that these bands likely represent other proteins cross-reacting to the *vg* antibody or a less abundant modified form of *vg* protein. No consistent band of any size other than that predicted for *vg* was ever strongly bound by the *vg* antibody. This suggests that the majority of the protein product produced by vg in a wild type background or in the presence of the dominant alleles is of the predicted size.

Since a *vg*-like protein appears to be produced by the interrupted *vg* sequences of vg^W, the expression of *vg* mRNA in the presence of the dominant alleles was examined. Total RNA was isolated from the head region of third instar larvae heterozygous for a dominant or partially dominant allele and a null *vg* allele. A reverse transcriptase coupled polymerase chain reaction (RT-PCR) was then performed, using primers that amplify a 1.6kb fragment representing the 3' portion of the *vg* transcript (Figure II-7). No transcript could be detected from RNA isolated from vg^{U}/vg^{83b27R} larvae. However, a band of similar size to wild type can be detected from vg^{W}/vg^{83b27R} larvae suggesting that the *vg* sequences associated with vg^{W} are being transcribed.

Since the presence of dominant *vg* alleles causes both the expression of *vg* and the imaginal disc morphology to be severely aberrant during the late third larval instar, *vg* patterning was examined during developmental stages prior to this point. Analysis of vg^{U} and vg^{W} embryos before stage 11 shows that *vg* induction does not occur before that of wild type (Figure II-8 A). From stage 12 onwards, the *vg* protein is normally found within discrete regions of the thoracic segments that will ultimately form the wing imaginal discs (Figure II-8 B arrows, arrowheads) (Cohen et al., 1993; Williams et al., 1991). The spatial pattern of cells expressing *vg* protein within the wing and haltere imaginal disc primordia of vg^{W} or vg^{U} embryos is comparable to wild type embryos of the same stage (Figure II-8 B arrows, arrowheads). The expression pattern of *vg* remains identical to wild type until at least 3 hours prior to hatching (stage 16). An example of embryos at stage 16 is shown in Figure II-8 (C arrows, arrowheads).

The expression of *vg* at this point within the T1 segment (Figure II-8 arrow) is limited to a few cells in wild type and vg^{W} and vg^{U} embryos. Following hatching of the embryo, normal levels of *vg* protein remain detectable in the wing and haltere imaginal discs of second and early third instar larvae. However, small alterations within the pattern of *vg* appear to be associated with the presence of dominant alleles during mid third instar (Figure II-8 D-E).

Figure II-7 RNA transcripts containing *vg* sequences can be detected from the vg^W dominant allele and its derivatives.

RT-PCR, performed on RNA isolated from wing discs detects *vg* transcripts in these tissues. The primers used amplified a region extending across the 3' region of *vg* representing 1.6 kb of the *vg* coding region. The positions of these primers are indicated above the map shown in (Figure II-5). From left to right: λ-*Hind III* - DNA size marker. *vg* cDNA - The cloned *vg* cDNA used as a positive control. Oregon R - Wild type. A brightly staining band representing the wild type *vg* transcript is indicated by the arrow on the right. vg^{83b27R}/vg^{83b27R}- A homozygous *vg* null strain (Williams et al., 1993). vg^{83b27R} produces no detectable expression of *vg*. vg^W/vg^{83b27R} - The presence of a band approximately the same size as vg^+ from vg^W suggests that the *vg* portion of the gene fusion is transcribed. A weakly staining, 450 bp band is occasionally seen and may represent an artifact of the PCR reaction as it could not be consistently reproduced in all reactions. vg^W/vg^+-When vg^W is heterozygous to wild type only the wild type band is seen. vg^U/vg^{83b27R} - No band is detected from vg^U. This is expected, as the inversion breakpoint associated with vg^U is beyond the *vg* translational start site. vg^U/vg^+ - When vg^U is heterozygous to vg^+ a normal *vg* transcript is detected.

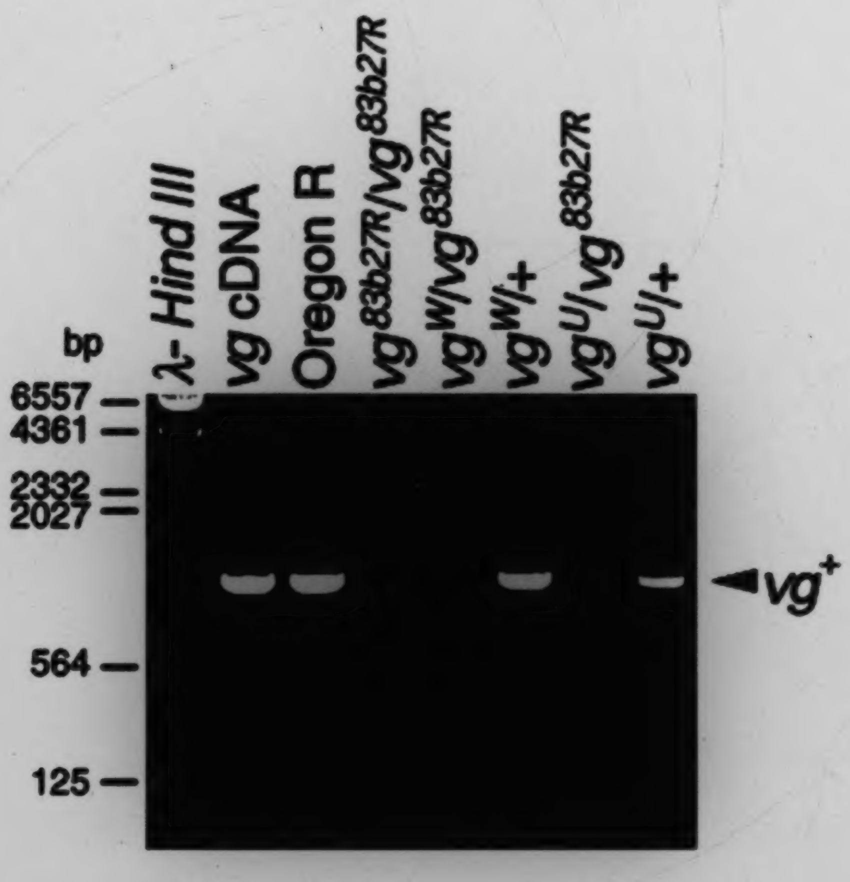
bp
6557
4361
2332
2027
564
125
λ- *Hind III*
vg cDNA
Oregon R
vg^{83b27R}/vg^{83b27R}
vg^{W}/vg^{83b27R}
$vg^{W}/+$
vg^{U}/vg^{83b27R}
$vg^{U}/+$
vg^{+}

Figure II-8 The presence of dominant *vg* alleles does not affect early *vg* expression.

Stage 10 embryos were examined for *vg* expression and shown as: A) Oregon R (left), vg^{W}/+ (middle), and vg^{U}/+ (right). Early embryos show no *vg* protein expression within the thoracic segments detected by a *vg* antibody. B) Stage 12 embryos all show similar timing and localized appearance of the wing and haltere disc primordia as evidenced by the activation of *vg* in the T2, and T3 segments (arrowheads). Transient activation of *vg* in the T1 segment is also seen (arrow). Wild type embryos have the same number and grouping of cells expressing *vg* as does either vg^{W}/+ or vg^{U}/+. C) Later stage embryos (stage sixteen) retain a similar pattern of *vg* expression suggesting that embryonic patterning of *vg* is not affected by the presence of dominant *vg* alleles. D) Late second instar imaginal discs show a pattern of elevated *vg* expression forming along the D/V margin. This initial D/V *vg* patterning appears not to be suppressed by the presence of the dominant alleles. E) Early third instar wing imaginal discs also show the presence of a D/V *vg* pattern although there may be fewer cells expressing *vg* in the hinge of vg^{W} wing discs (arrow) or in the middle of the discs from vg^{U} larvae (arrow). F) Mid-third instar wing discs show a significant suppression of *vg* expression in the middle of the wing disc associated with vg^{U} and vg^{W} (arrows) compared to wild type (Oregon-R).

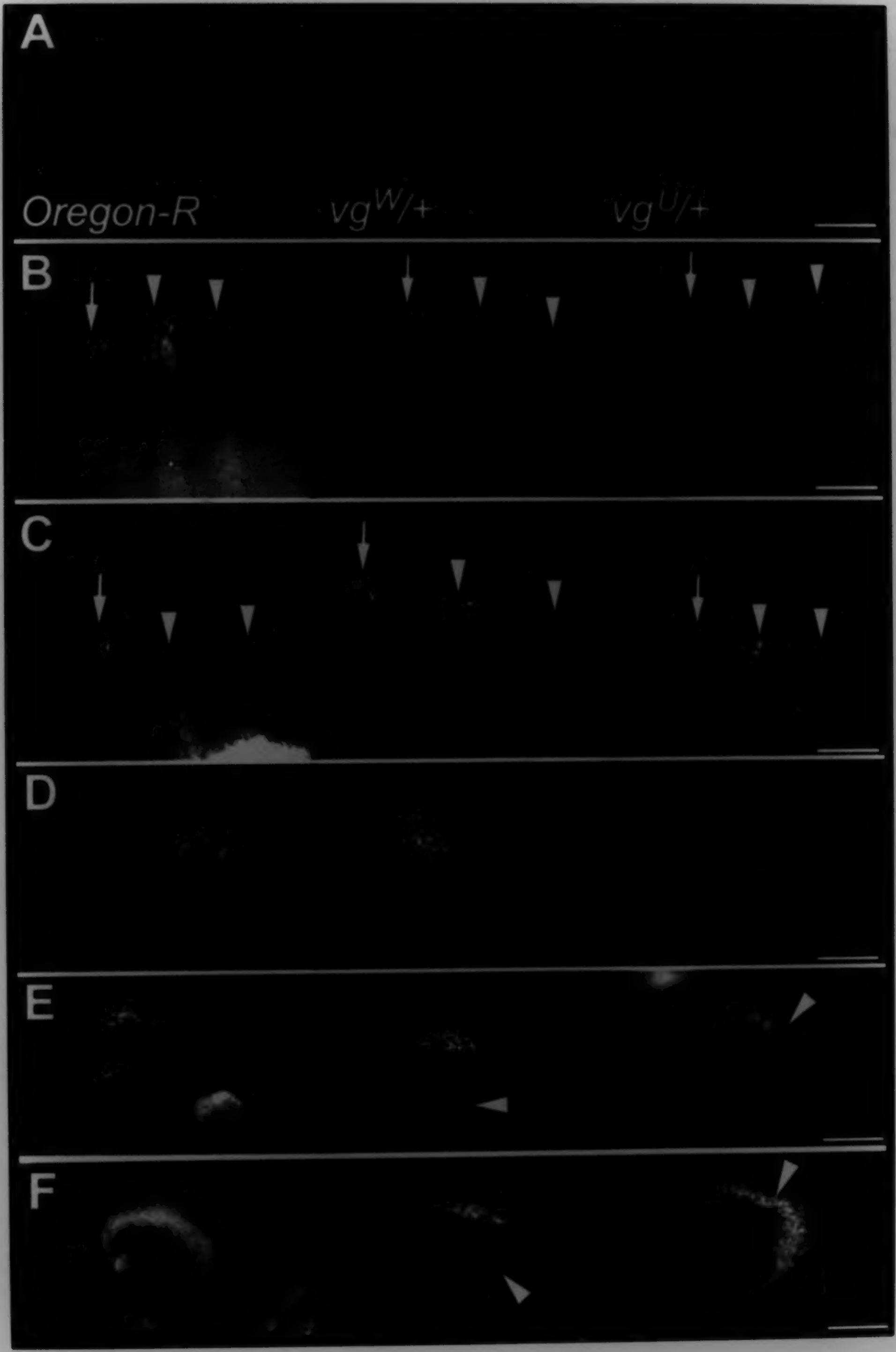
A
Oregon-R
vg^W/+
vg^U/+
B
C
D
E
F

These differences include a loss of *vg* expression in the posterior hinge region (*vg*^{W}) and from along the D/V boundary in the presence of *vg*^{U} during early and mid third instar (Figure II-8 E-F arrowheads)

The morphology of the wing discs associated with the dominant and partially dominant alleles indicated that the alteration in *vg* patterning was causing either a lack of cell proliferation or cell death. Acridine orange staining was employed to examine cell death, as it has been shown to be a reliable indicator of apoptosis within embryos and imaginal discs (Abrams et al., 1993; Massucci et al., 1990). In wild type wing imaginal discs, there is a normal pattern of programmed cell death scattered throughout the wing blade during late third instar (O'Brochta and Bryant, 1983) (Figure II-9 A). Within the wing disc of recessive *vg* homozygotes of the same stage, areas containing more dying cells are observed (Figure II-9 E). A large number of apoptotic cells can be seen within the wing compartment and this is typical of the level associated with recessive *vg* mutants (Fristrom, 1968). Within late third instar *vg*^{W} imaginal discs, the total amount of cell death is relatively low, presumably as most cells have died earlier (Bownes and Roberts, 1981a) (Figure II-9 D). However, within second and early third instar imaginal discs from *vg*^{W}/+ larvae, a large number of apoptotic cells can be seen scattered throughout the region fated to form the wing blade (Figure II-9 B-C). The pattern of cell death in second and early third *vg*^{U} wing discs is similar to *vg*^{W}, although a few apoptotic cells may still be detected during the late third instar (Figure II-9 F-H) (O'Brochta and Bryant, 1983). Early third instar discs from the weak revertant class still contain large groups of apoptotic cells in the regions of the wing discs fated to form the anterior and posterior wing margin (Figure II-9 J). However, in contrast to what is observed in second and third instar wing imaginal discs of the progenitor dominant alleles, a large number of apoptotic cells appear during the late third instar (Figure II-9 J). The relative amount of apoptotic cells within the wing imaginal discs of the weak revertants remains lower at this stage than the number exhibited by classical *vg* recessive mutants (Compare Figure II-9 E to J). Discs isolated from larvae possessing revertant alleles of the strap-like wing class contained an elevated number of apoptotic cells relative to wild type, but showed less clustering of these apoptotic cells into discrete regions (Figure II-9 K). In discs from the strap wing class, the majority of apoptotic cell death is delayed until later in the third instar; similar to recessive *vg* alleles (Compare Figure II-9 E and L).

The effect of the dominant *vg* alleles upon D/V patterning was examined by observing alterations in the expression of *wg* within the wing disc. Wg protein is necessary for activation of *vg* and *sd* and may act in concert with *vg* to pattern the wing disc along the D/V border (Ng et al., 1996). The early expression of *wg* in the second larval instar outlines the wing primordia in the wing imaginal disc (Ng et al., 1996). By late third instar, wild type *wg* expression as detected by a *wg-lacZ* enhancer trap outlines two compartments in the wing pouch (Figure II-10 A). The outer concentric circle of *wg* expression defines the region of the wing fated to form hinge structures while the inner circle defines the region fated to form the wing blade (Figure II-10 A D/V). The D/V specific expression of *wg*, which appears in mid third instar, bisects both these circles and plays a critical role in patterning *vg* (Cohen, 1993; Williams et al., 1993). The *wg* expression in the presumptive notum (Figure II-10 A notum) can be used as a marker for the size and orientation of the remaining wing disc as it is uninvolved in wing patterning (Williams et al., 1993). To determine the effect of the dominant *vg* alleles upon the expression of the heterozygous *vg*$^{+}$ allele, the *vg* intron-2 and *vg* intron-4 *lac-Z* reporters were crossed to each dominant allele and to the strap wing revertant *vg*^{URK5}.

Figure II-9 Altered patterns of apoptotic cell death associated with the dominant *vg* activity.

Each scale bar represents 80 µm. A) In vg^+/vg^+ late third instar wing imaginal discs little apoptotic cell death is seen as evidenced by the appearance of few brightly staining nuclei within the wing pouch region (arrowhead). An arrow in any panel indicates brightly staining cells that are associated with tracheal tissue and not the imaginal disc. B) Late second instar or C) early third instar wing discs isolated from $vg^W/+$ show a large number of apoptotic cells compared with that seen in D) Late third instar. By late third instar there is an absence of apoptotic cells within the wing pouch region (arrowhead). E) Late third instar wing discs isolated from larvae homozygous for the recessive vg^{83b27} allele show high levels of apoptotic cell death in the wing pouch (arrowhead). A pattern of early cell death similar to $vg^W/+$ is seen with $vg^U/+$ (F) second instar (arrow), (G) early third instar, and the wing pouch (arrowhead) and hinge (arrow) of (H) late third instar imaginal discs. I) Within imaginal discs isolated from a weak revertant, (vg^{URK15}), some cell death is detected during the early third instar. J) Unlike what is observed with the original dominant alleles, discs from weak revertants show a persistence of apoptosis into late third instar within the wing pouch (arrowhead) and hinge (arrow). K) Strap wing revertant alleles (vg^{URK5}) have fewer apoptotic cells during early third instar. L) Late third instar vg^{URK5} discs show a significant amount of cell death in the wing pouch (arrowhead) and hinge (arrow) similar to that seen with recessive *vg* mutations (E).

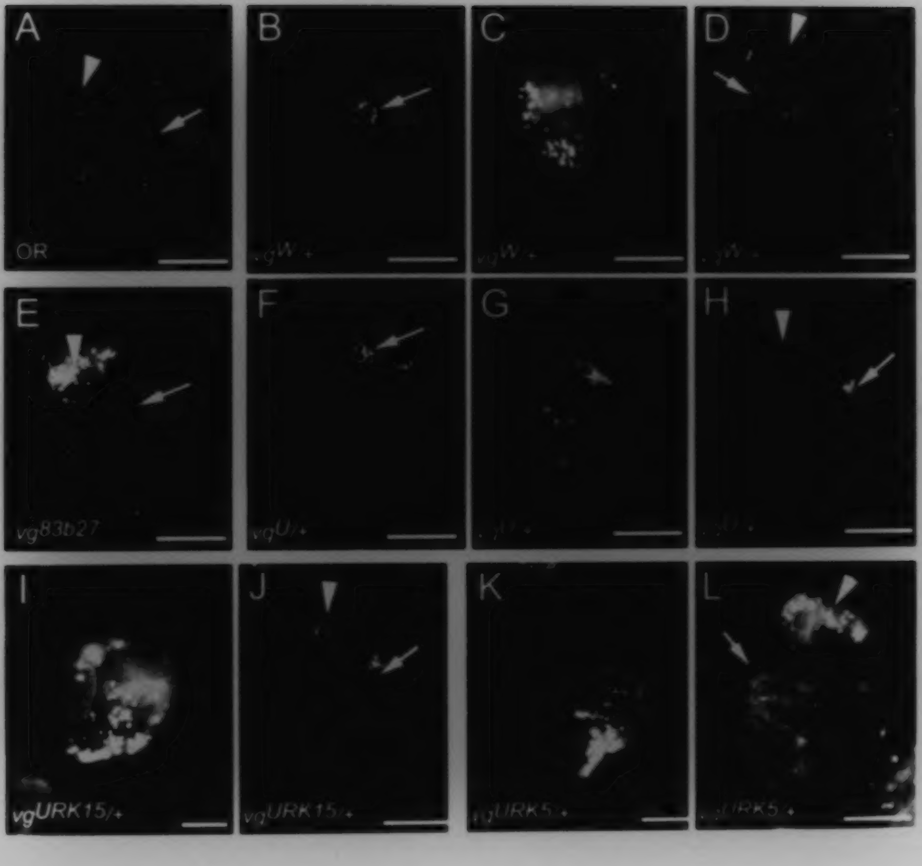
A
OR
B
vgW/+
C
vgW/+
D
vgW/+
E
vg83b27
F
vgU/+
G
vgU/+
H
vgU/+
I
vgURK15/+
J
vgURK15/+
K
vgURK5/+
L
vgURK5/+

The activation of the *vg* intron-2 enhancer is controlled by the action of the D/V patterning pathway, which is mediated in part by the activity of *wg* (Kim et al., 1996). In wild type wing discs the pattern of the *vg* intron-2 enhancer reporter expression extends immediately along the D/V margin with a small amount of notum-specific seen as well. *wg-lacZ* staining remains similar to that of wild type while *wg* expression in the wing primordia is significantly altered (Figure II-10 B-C). With vg^{W} there is only a single circle of *wg*-lacZ staining observed within the wing pouch. Remnants of the D/V *wg* expression also appear within this area (Figure II-10 B). As very little of the hinge structure is formed in vg^{W} adults, it is assumed that the remaining circle of *wg* expression in these discs represents that which defines the wing (Neumann and Cohen, 1996a). The D/V *wg* expression associated with vg^{W} also correlates with the appearance of a well-defined and complete margin of the residual wing formed in vg^{W} adults Figure II-2 B,J). The pattern of the *wg-lacZ* expression in the presence vg^{U} is quite different from that observed with vg^{W}. In vg^{U} wing discs two concentric circles of *wg* expression can still be seen (Figure II-10 C). In these discs the apparent distance between these circles of *lac-Z* staining appears greater than wild type (Figure II-10 A). This may be a factor of the severe reduction of the wing blade region to a small circle outlined by *wg* within the interior of the wing disc (Figure II-10 C). In the wing discs that have a large enough interior circle of *wg*-lacZ expression to allow for observation of interior structures, the D/V specific *wg* pattern is not seen. This again correlates with the absence of wing margin in the residual wing structures formed in vg^{U} adults (Figure II-2 F,K). The correlation between *vg* and *wg* protein localization can be better seen in Figure II-11. The detection of both *wg* and *vg* protein in the presence of vg^{U} clearly illustrates that *vg* expression is limited to the hinge and notum. In vg^{W}

Figure II-10 The expression of *wg*, *sd* the *vg* intron-2, and the intron-4 enhancer elements in the presence of dominant *vg* alleles.

A) The expression of *wg* in wild type is seen as two concentric circles of *wg* expression, which outline the presumptive wing and hinge of the wing disc and a stripe demarcating the presumptive D/V boundary of the wing blade. B) In the presence of vg^{W}, the expression of *wg* is reduced to a single circle outlining the wing compartment. In addition, the stripe that demarcates the D/V margin in the wing pouch is reduced to a small zone within the wing pouch of these discs. C) The action of vg^{U} greatly reduces the wing compartment as outlined by *wg*. Unlike what is seen with vg^{W} however the outside circle of *wg* expression remains. The D/V expression of *wg* is eliminated in these imaginal discs. D) The expression of *wg* in the presence of vg^{URK5} roughly approximates that seen in wild type although the D/V expression of *wg* is weak and often incomplete. E) The expression of *sd* mirrors that of *vg* in wild type wing discs extending from the wing compartment into the anterior and posterior hinge regions. F) In the presence of the vg^{W} allele, the expression of *sd* in the remaining wing pouch is reduced to a stripe along the presumptive D/V margin. A break in the expression of *sd* is seen in the centre of the wing disc (arrowhead). G) The expression of *sd* is almost totally absent in the presence of vg^{U} although weak staining is seen in the centre of the wing disc (arrow) and residual expression is seen in the ventral surface. H) There is a patchy expression of *sd* in the presence the strap wing vg^{URK5} allele. Breaks in the expression of *sd* (arrowheads) are seen in the pattern of *sd*-lacZ staining along the D/V margin (arrows). I) *vg* intron-2 expression in a wild type wing disc. J) In the presence of vg^{W} the intron-2 enhancer element is activated along the D/V margin in a pattern that mirrors that of *sd*. K). In vg^{U} wing discs there is no activation of the intron-2 enhancer in the wing disc although residual expression is seen outside the presumptive wing pouch. L) The presence of the *vg*^{URK5} allele leads to interrupted activation of *vg* along the D/V margin mirroring that of *sd*. M) The pattern of expression of the *vg* intron-4 enhancer in wild type wing discs. N-O) There is no detectable action of *vg*-intron 4 in either *vg*^{W} or *vg*^{U}. P) The *vg*-intron4 enhancer is weakly activated in the *vg*^{URK5} wing disc.

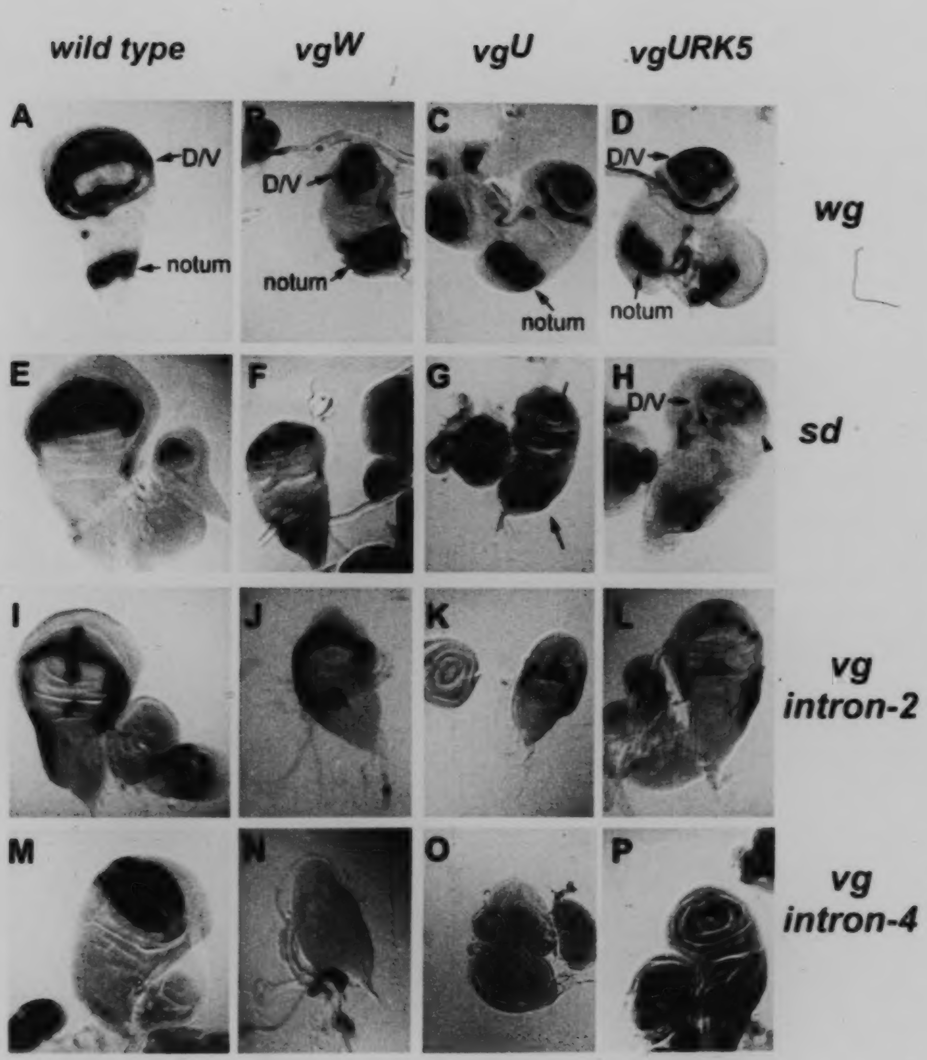
wild type
vgW
vgU
vgURK5
A
D/V
notum
B
D/V
notum
C
notum
D
D/V
notum
wg
E
F
G
H
D/V
sd
I
J
K
L
vg
intron-2
M
N
O
P
vg
intron-4

imaginal discs *vg* and wg expressing cells are not symmetric along the D/V margin and there are significantly cells more dorsal cells expressing *vg* than within the ventral compartment. The lack of one circle of wg expression can be correlated with an absence of hinge structures in vg^{W} adults (Figure II-2). An example of the strap-wing revertant class (vg^{URK5}) shows a pattern of *wg*-lacZ staining intermediate between that of vg^{U} and wild type. In these discs, the wing compartment defined by *wg* is larger than that seen with vg^{U}, although abnormal interruptions in the outer circles of *wg* expression are occasionally seen (Figure II-10 D arrow). However, these interruptions may be due to the altered morphology of the wing discs harbouring the vg^{URK5} allele. The *wg-lacZ* staining seen in these discs is incomplete along the D/V margin with significant gaps seen at either the anterior or the posterior limits. (Figure II-10 D D/V). This can be correlated to the lack of continuous *vg* expression in vg^{URK5} imaginal discs Figure II-2 E) and subsequently to the discontinuous formation of margin in the resulting wing (Figure II-2 H). The establishment of *sd* expression within the wing compartment is partially dependent upon *vg*, and *sd*-lacZ staining approximately mirrors that of *vg* throughout normal wing disc development (Figure II-10 E) (Williams et al., 1993). This expression of *sd* remains localized to the D/V margin of wing discs isolated from vg^{W} larvae (Figure II-10 F). Within this D/V stripe of *sd* expression there is a bifurcation within the region that will form the wing similar to that seen with *vg* protein (Figure II-10 F arrowhead). In vg^{U} wing discs the residual *sd* expression is confined to a small circle in the wing compartment and to the hinge region (Figure II-10 G). The patterning of *sd* in vg^{URK5} wing discs shows a number of significant gaps and other alterations along the D/V margin (Figure II-10 H). This again is coincident with the pattern of *vg* expression in these discs (Figure II-3 E) with staining extending dorsally and

Figure II-11 Dual antibody detection of *vg* and *wg* protein in *vg*^{W} and *vg*^{U}.

The expression of *vg* protein in the presence of *vg*^{U} is limited to the hinge and notum region. The two concentric circles of *wg* as detected by *wg* antibody are seen surrounding the remaining cells of the wing pouch. The double image shows that while *vg* protein is found within cells between the two *wg* circles of expression, it does not extend into the wing pouch. This can be correlated with the presence of wing hinge structures in *vg*^{U} adults.

A residual stripe of *vg* expression is seen along the D/V margin in *vg*^{W} wing discs. Staining the same disc with *wg* antibody detects only a single circle of *wg* expressing cells surrounding the wing pouch but unlike *vg*^{U}, the D/V *wg* expression pattern remains. Note however, that *vg* and wg expressing cells are not symmetric along the D/V margin and there are significantly cells expressing vg in the dorsal compartment (below the D/V margin) than in the ventral compartment. The lack of the second circle of wg expression can be correlated with the absence of any hinge structures in *vg*^{W} wings (Figure II-2)

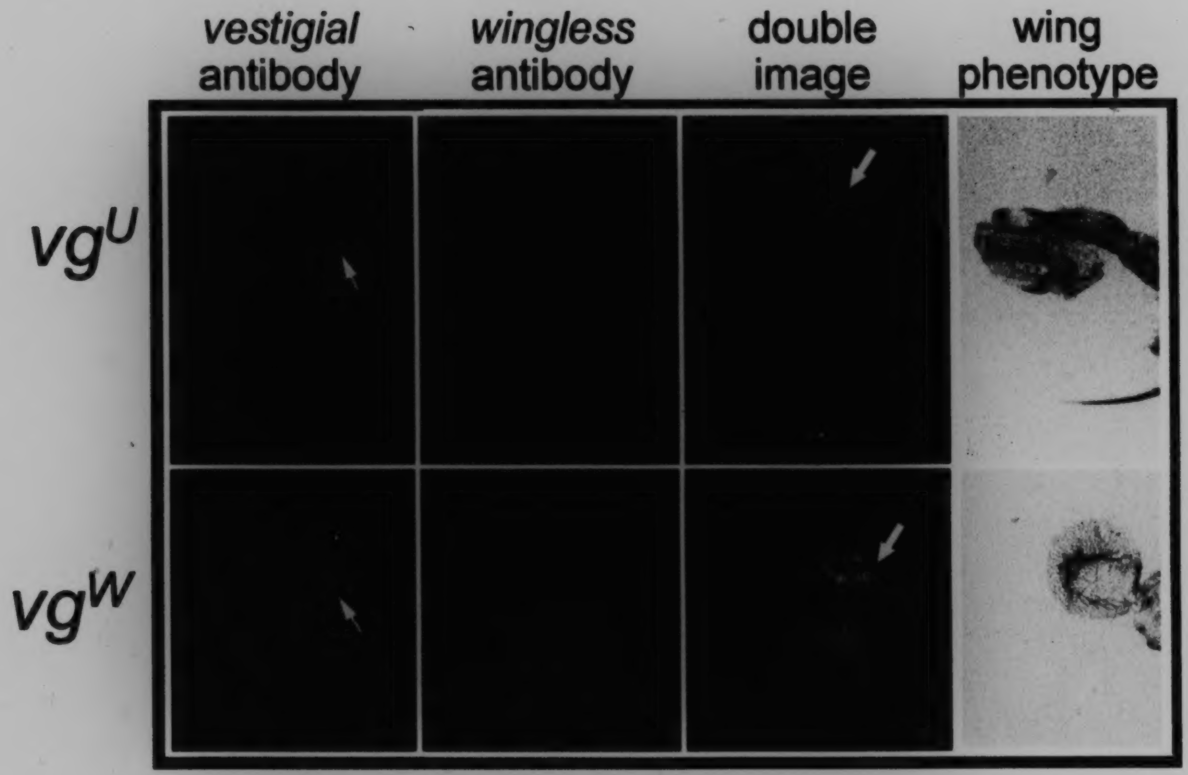
vestigial antibody
wingless antibody
double image
wing phenotype
vg^U
vg^W

ventrally along the A/P axis (Figure II-10 I). The activation of *vg* expression from the *vg* intron-2 enhancer element in turn controls the *vg* intron-4 enhancer which drives *vg* expression in the dorsal and ventral cells of the wing pouch (Figure II-10 M). The pattern of *vg* intron-2 *lac-Z* staining associated with any of the dominant alleles is approximately identical to wild type alleles for areas outside the wing pouch (Figure II-10 I-L). However, within the wing compartment the activation of this enhancer appears to be abnormal. Within vg^{W} imaginal discs there is a bifurcated pattern of staining on either side of the D/V margin at the approximate point where it meets the A/P compartment boundary (Figure II-10 J). This pattern is completely mirrored by the expression of *sd*-lacZ (Figure II-10 F). This likely represents the activation of *vg* in the presence of vg^{W} as no staining is observed with the *vg* intron-4 enhancer *lac-Z* reporter (Figure II-10 N). In vg^{U} imaginal discs there is no activity of the *vg* intron-2 or *vg* intron-4 enhancer element in the wing pouch region (Figure II-10K, O). However, this does not correlate with *sd* expression which remains present in the wing pouch region of vg^{U} wing discs (Figure II-10 G). The patterning of the *vg* intron-2 *lac-Z* reporter in the strap wing revertant vg^{URK5} shows the basic wild type pattern of this enhancer element but in a discontinuous fashion. Gaps in the expression of this element along the D/V margin appear just anterior and posterior to the A/P boundary (Figure II-10 L). These breaks in the pattern of *vg* intron-2 *lacZ* reporter expression correspond to similar gaps seen in the localization of *vg* protein (Figure II-3 D). After extensive incubation in X-gal weak staining from the *vg* intron-4 enhancer *lac-Z* reporter in seen is a small central region of the wing disc in the presence of vg^{URK5} (Figure II-10 P).

Discussion

It was previously determined that the fusion partner genes play an important role in causing the dominant *vg* phenotype (Williams et al., 1990b). The newly created series of partial phenotypic revertant alleles of vg^W and vg^U described herein show that *vg* sequences are also critical for the creation of the dominant phenotype. Specifically, the reversion mutations with physical lesions within the *vg* portion of the dominant alleles are notable in that they reduce but do not eliminate the dominant phenotype. The physical lesions associated with these mutations map to two broad domains within *vg* which correlate with the classes of resulting wing phenotypes, each class associated with characteristic restorations of various amounts of wing tissue in the adult. Conversely, alterations in the fusion partner genes (Chapter-II, Williams et al., 1990b) or in the extreme 3' portion of *vg* (Chapter III) produce full wing revertants. While the detailed molecular mechanisms that mediate the effect of dominant *vg* phenotype remains elusive, it has become clear that the dominant effect is a consequence of altered *vg* protein expression during larval development. In all cases, the copy of vg^+ heterozygous to the dominant alleles or their derivatives appears to be expressing normal levels of *vg* protein within the whole organism. In addition, the expression of *vg* protein in the presence of the dominant alleles does not appear to be altered temporally, as there is no alteration of early *vg* expression in embryos prior to hatching. Therefore, any changes in *vg* patterning caused by dominant alleles occur just prior to the third larval instar when significant developmental decisions are occurring within the imaginal disc.

Early temperature shift and disc transplantation experiments defined a critical time requirement for proper *vg* expression during second and third larval instar (Bownes and Roberts, 1981b; James and Bryant, 1981). No alterations in *vg* protein localization are seen during embryogenesis, but by late third instar, patterning is significantly altered in the partial revertant alleles isolated in this study. This indicates that the dominant effect of vg^W and vg^U occurs during larval development during this time, when the wing compartment is being defined (Bryant, 1975; Couso et al., 1995; Ng et al., 1996). The number and relative pattern of apoptotic cells within these imaginal discs also changes when the dominant phenotype is reverted. This suggests that the additional apoptotic cells that are associated with the dominant and revertant *vg* alleles are a result of this altered *vg* patterning. Paradoxically, alterations in the pattern of apoptosis associated with vg^W and vg^U occur during second instar, when the apparent expression of *vg* as detected by *vg* antibody shows no differences to wild type. This suggests that the effect of the dominant alleles may be happening as early as second instar, just as the pattern of *vg* expression is being established. However, since the basic pattern of *vg* expressing cells does not change compared to wild type, this suggests that the dominant effect is occurring in only few cells at this stage. These cells might then become apoptotic and are removed from the wing disc. One critical element of *vg* patterning during second instar is the suppression of *vg* in dorsal cells of the wing disc (Williams et al, 1993). If the dominant alleles interfere with early restriction of *vg* to the ventral portion of the disc, subsequent patterning of *vg* may not be established properly leading to the alterations in *vg* protein expression seen at later stages.

The requirement for *vg* sequences in mediating the effect of the dominant alleles suggests that some transcription is occurring from the dominant *vg* alleles. The protein produced from vg^W is recognized by *vg* antibody, indicating that the transcript that encodes this protein contains the majority of the *vg* coding region. The inversion breakpoint associated with *vg*^{W} only removes the first untranslated exon leaving the normal *vg* translational start site intact. Therefore, any transcription of these sequences can not be using the normal *vg* start site. While no transcript or protein was detected associated with *vg*^{U}, there is a possibility that low levels of a novel transcript containing *vg* sequences produce very low levels of other proteins that are undetectable by Western blot or PCR analysis. Alternatively, the *vg*^{U} sequences could be acting upon *mam* to disrupt *vg* establishment through ectopic *mam* expression. An additional possibility as to the cause of the dominant effect is that the remaining *vg* sequences are being acted upon by the associated *mam* or *inv* genes to remove factors required for normal *vg* establishment from the cell. These factors could include elements needed for activation of the intron-2 and intron-4 enhancers that serve to establish elevated *vg* expression along the D/V wing boundary. However, until the mechanism of activation of these enhancers is better established, it would be difficult to test this hypothesis.

The loss of wing phenotype observed in the *vg*^{W} and *vg*^{U} mutations is not simply due to a haplo-insufficiency of *vg* expression, since Df (*vg*^{B})/+ produces a wild type wing. Thus, other explanations must be considered. Hodgkin (1993) suggests that genes involved in regulatory processes may be more liable to mutate to a dominant allele than is normally expected. Hyper-activation, hypo-activation, ectopic expression and altered temporal expression could each produce an easily observed dominant phenotype. An example of a gene involved in wing patterning that has this kind of mutation is *Ser*. The *Ser*^{Dominant} (*Ser*^{D}) mutation is associated with constitutive activation of the *Ser* protein (Thomas et al., 1995). *Ser*^{D} heterozygotes have an easily observed dominant wing-nicking phenotype (Thomas et al., 1995). However, this hyper-mutability appears not to be the case with *vg*, as extensive mutagenesis experiments have produced mutations which are for the most part fully recessive (Lindsley and Zimm, 1992). The wing phenotype associated with *vg*^{B}/+ suggests that the amount of *vg* is in limiting quantities within the cells of the wing pouch. Thus, small disruptions in the establishment of this wing-specific *vg* expression, especially during earlier development where few cells are present would have significant effects later. One model that could account for the dominant effect of *vg*^{W} and *vg*^{U} is based upon the observation that *vg* is expressed at a low level throughout the wing disc during early development (Kim et al., 1996; Williams et al., 1994). In *vg*^{W}, a cryptic transcriptional start site either within *vg* or the adjacent *inv* sequences is producing a hybrid *vg* transcript. However, the protein putatively attributed to translation of a transcript from the *vg*^{W} allele is still recognizable by antibodies directed to normal *vg* protein. It is not easy to envision how such a protein expressed at low levels would suppress the function of wild type *vg* product. The inversions that create the dominant alleles place ectopic sequences near the *vg* enhancer elements within the *vg* coding region, including those in the second and fourth *vg* intron (Williams et al., 1994).

The intron-2 element is thought to respond to D/V signaling through binding of Su(*H*) protein (Kim et al., 1996). Thus, the gene fusions create a situation where internal *vg* enhancer sequences are present but disconnected from 5' *vg* controls. These sequences could titrate out necessary factors in establishing *vg* expression such as *Su*(*H*) or *sd* that would remove some but not all of the subsequent *vg* patterning. Since recessive *vg* mutations would also bind these putative factors in a similar manner but do not produce a dominant phenotype, this model would assume that the proximity of the *inv* and *mam* sequences somehow alters the activity of these *vg* enhancer elements. The correlation of each class of revertants to mutations that remove either of the intronic enhancer elements strongly suggests that this might be the case. The case for the dominant *vg* alleles interfering with *vg* establishment is supported by the patterning of *wg* in the presence of *vg*^{U}. This allele, where the inversion removes the start site normally used during wild type *vg* translation, does not show any D/V patterning of *wg* and correspondingly forms wing tissue lacking any D/V margin. One model that might explain this is the removal of *wg* expression from cells along the D/V margin is the lack of maintenance of *vg* expression in these cells. However, this does not preclude the possibility of transcription from the *vg*^{U} allele since a novel transcript was seen with a previous revertant of *vg*^{U} (Williams et al., 1990b).

A strong correlation can be made between the classes of partial revertants and the specific loss of patterns of *vg* protein localization along the D/V boundary in wing imaginal discs. This supports a model in which the *vg* sequences of the dominant alleles are acting together with the fused *inv* and *mam* genes in mediating the dominant effect. The dominant activity of *vg*^{W} and *vg*^{U} appears to disturb the activation and patterning of *vg* expression in the wing disc (Figure II-3, Figure II-10). This property of *vg*^{W} and *vg*^{U} provides an opportunity to observe the results of restricted spatial expression of *vg* at specific time points while otherwise retaining significant levels of *vg* expression. The selective repression of wild type *vg* expression specifically within the wing disc could not be accomplished easily with a synthetic system such as that devised by Brand and Perrimon (1993). The patterning seen in *vg*^{W} imaginal discs (Figure II-3 B) shows that when *vg* expression is limited to a thin stripe along the D/V border wing margin structures form normally. However without expansion of *vg* expression dorsally and ventrally the wing blade is reduced almost to nonexistence by extensive cell death (Figure II-9 J). Even though a large portion of the cells within the wing compartment have been lost, the remaining cells retain the ability to pattern a complete margin and wing blade given the presence of *vg* protein. Alternatively, if *vg* expression is limited to the peripheral regions of the wing disc (Figure II-3 C, D-J) the remaining cells of the wing compartment will form hinge but not wing blade or margin (Figure II-2C-D, F-J,I-K). However, if there is any restoration of *vg* expression at the center of these wing discs (Figure II-3 E) there will be a corresponding reappearance of wing blade tissue (Figure II-2 D, H). The relationship between patterning of *vg* protein in imaginal discs and the resulting wing structure suggests that *vg* protein acts as a potent specification element in the development of wing structure. This role appears to be one of a general definition of wing since the requirement of *vg* can be correlated with the appearance of a number of different tissue types including wing margin, blade and hinge.

From this study, it appears that there is a strong requirement for not only the spatial localization of high levels of *vg* protein but that this localization must occur during critical early developmental stages for proper wing development to occur. In the presence of massive amounts of cell death, the remaining wild type *vg* expression remains localized along a re-specified D/V boundary, as determined by the extent of *ap* expression. Therefore, it appears that the dominant effect of vg^W and vg^U interferes with establishment of *wg* and *vg* mediated patterning along the D/V margin. However, as evidenced by the patchy expression of *vg* in wing discs from the partial revertants, this interference does not occur equally in all regions of the wing compartment. This may indicate that the establishment of *vg* in some regions of the wing disc is more susceptible to interference by the dominant effect than others. Other genes including *Notch*

(*N*), *fringe (fng)*, *Ser*, and *wg* have been shown to be critical elements in establishment of localized *vg* expression within the wing disc (Couso et al., 1995; Doherty et al., 1996; Irvine and Wieschaus, 1994; Kim et al., 1995; Rabinow and Birchler, 1990; Williams et al., 1993). If the requirement for these elements in the patterning of *vg* differs in one region of the disc to another, then the dominant alleles might remove some but not all *vg* expression from the developing disc. In the case of vg^{W}, it appears that while altered *vg* expression within the wing disc removes a large number of cells through cell death. However, the remaining cells still express *vg* in a reduced pattern that is continuous along the D/V border. This indicates that the remaining tissue in the wing compartment patterns *vg* normally. Therefore, there appears to be a primary role for *vg* during the rapid proliferation of cells that occurs between early and late third instar, and a second role in defining the wing margin identity during later development. The *vg* gene is activated comparatively early during imaginal disc development and is one of the first genes expressed within the wing imaginal disc primordia during embryogenesis (Cohen et al., 1993). The correlation between the presence of *vg* protein and successful proliferation of cells within larval imaginal discs to form adult wing provides evidence for the action of *vg* in normal wing development. The nuclear localization of *vg* protein (Williams et al., 1991) suggests a role in controlling transcription. This transcriptional control may occur cooperatively with the *sd* protein which is a LIM transcription factor that is expressed in an identical pattern to *vg* in the wing imaginal disc (Campbell et al., 1992; Williams et al., 1993). The primary role of *vg* appears to be that of a wing determinant that marks the cells within the imaginal disc thus promoting rapid proliferation during formation of the wing blade and hinge.

The additional reversion mutations of *vg*^{W} and *vg*^{U} that were isolated in this study extend our understanding of these types of dominant mutations and the functioning of *vg* in the development of the wing. Expression of *vg* in other imaginal discs has been shown to induce a wing cell identity (Kim et al., 1996). Therefore, the cell death associated with the dominant *vg* alleles may be attributed to loss of identity caused by the loss of *vg* expression. Furthermore, some mechanisms associated with dominant alleles of other genes have been discounted as a cause of *vg* dominance. These include mechanisms whereby the expression of the *vg*$^{+}$ allele is suppressed in dominant heterozygotes or the possibility of temporal or spatial ectopic *vg* expression within the cells of the wing primordia. Rather, it appears that the establishment of *vg* protein expression along the D/V margin in developing larval imaginal wing and haltere discs is suppressed in a region specific manner. This suppression of the normal *vg* expression patterns in the wing discs leads to an elimination of corresponding regions within the wing via apoptotic cell death. These results are complementary with a model suggesting that *vg* protein is necessary for the growth of the wing from the imaginal disc. Correspondingly, when *vg* expression is suppressed in the wing imaginal disc, cells become apoptotic instead of forming the appropriate wing tissue. Further experiments, in which transgenes of factors such as *wg* or *sd* are expressed at higher than normal levels, would determine if the dominant alleles are titrating out these factors or otherwise making them unavailable to the heterozygous *vg*$^{+}$ sequences. However, this can not be a simply due to the presence of extra copies of the intron-2 or intron-4 enhancer elements. Transgenic flies containing up to eight copies of the intron-2 element show no dominant *vg* phenotypes. The effect of the adjacent *inv* and *mam* sequences in *vg*^{W} and *vg*^{U} respectively upon the establishment of *vg* patterning is critical to the dominant phenotype as alterations to these regions can also eliminate the dominant effect (Williams et al., 1990b). Further examination of additional reversion mutations of *vg*^{W} and *vg*^{U} that map to these regions should establish which specific sequences are working in tandem with the *vg* portion of the *vg*^{W} and *vg*^{U} alleles to create a dominant phenotype.

Chapter III - Distinguishable functions for the *engrailed* and *invected* genes of *Drosophila*[1]

Introduction

One of the earliest patterning decisions in *Drosophila* imaginal disc development is the formation of the A/P compartment boundary. Each appendage derived from the imaginal discs exhibits morphological differences between its anterior and posterior. Either this A/P compartmentalization occurs during or immediately after the definition of the imaginal disc precursor cells. The imaginal disc primordia are derived from adjacent cell populations that lie across the embryonic parasegmental border (Garcia Bellido et al., 1973). Cells along the border between the anterior and posterior compartments are believed to take on a special role in the organizing and patterning of the remaining cells in the imaginal disc (Meinhardt, 1983). The molecular mechanism responsible for establishment of the A/P compartment border is thought be initiated by the posterior-specific expression of the selector gene, *engrailed* (*en*) (Garcia Bellido et al., 1973; Kornberg, 1981a; Lawrence and Morata, 1976). A selector gene shows expression within a subset of cells in a field, thus specifying the identity of these cells as being different from their neighbouring cells outside the compartment (Garcia Bellido, 1975). In the cells of the wing imaginal disc, the expression of *en* is required for correct determination of a posterior fate (Morata and Lawrence, 1975). Loss of function *en* mutations that allow survival to adults produce defects restricted to the posterior compartment including the ectopic formation of anterior structures (Garcia Bellido and Santamaria, 1972). When alleles that produce a complete loss of *en* activity are examined in mitotic clones within the wing imaginal disc, the A/P compartment boundary is lost (Morata and Lawrence, 1975). Cells derived from *en*⁻ clones no longer respect the compartmental boundary and develop into anterior specific structures (Kornberg, 1981b; Lawrence and Morata, 1976; Lawrence and Struhl, 1982; Morata and Lawrence, 1975). Thus, it has been known for a relatively long time that the *en* gene has a determinative role in defining the A/P compartment boundary in the wing imaginal disc and also in the establishment of identity within the cells of the posterior compartment.

---

[1] Portions of this chapter have been published previously as Simmonds, A.J., Brook, W.J., Cohen, S.M. and Bell, J.B. (1995) *Nature* **376:** 424-427

Within cells of the wing imaginal disc, the action of *en* is mediated by the activity of several other genes. While the *en* protein is restricted to the nucleus of cells within the posterior compartment, the *hh* protein is actively secreted by cells expressing *en* (Lee et al., 1992; Tabata et al., 1992). The *hh* product functions as a short-range diffusible morphogen acting upon the anterior compartment cells immediately across the A/P border (Heemskerk and DiNardo, 1994; Tabata et al., 1992). Cells that react to the *hh* signal begin to express the *patched* (*ptc*) protein (Phillips et al., 1990). Within the anterior compartment, *ptc* shows graded expression, peaking in cells along the A/P border (Capdevila et al., 1994). *ptc* and *hh* ultimately activate the expression of *dpp* in anterior cells along the A/P border (Capdevila et al., 1994; Zecca et al., 1995). The *dpp* gene is a *transforming growth factor* β (*TGF*β)-homologue acting as a long range diffusible signaling molecule patterning A/P polarity within the wing and other imaginal discs (Blackman et al., 1991; Lecuit et al., 1996). The restriction of *dpp* expression to a narrow stripe of cells along the A/P border of the anterior compartment is also controlled by other genes. Within the anterior compartment, the expression of the intercellular signaling molecule *Protein kinase A* (*Pka*) can block *dpp* transcription (Jiang and Struhl, 1995). It is the activity of *hh* protein, diffusing from the posterior compartment, that removes this block allowing the expression of *dpp* within a few cell diameters inside the A/P border (Pan and Rubin, 1995). One gene that has been shown to have ubiquitous anterior compartment expression is *cubitus interruptus* (*ci*) (Orenic et al., 1990). The *ci* gene codes for a DNA binding protein that contains putative zinc finger domains and can act to suppress *hh* expression within cells of the anterior compartment (Dominguez et al., 1996; Orenic et al., 1990). Coincident with the role *ci* plays in suppressing *hh* expression, *ci* is suppressed in the posterior compartment by the activity of *en* (Eaton and Kornberg, 1990). The presence of a tightly controlled cascade of gene expression controlling *dpp* activity illustrates the importance of *en*-mediated expression of the *dpp* along the A/P border. Due to this importance in A/P patterning, the majority of recent investigation into *en* function has focused upon this role. Far less scrutiny has been applied to the other role of *en* in establishing the posterior compartment identity of cells within the imaginal discs.

Observations that *en* mutations produce defects limited largely to posterior structures has led to the proposal that *en* also acts to define posterior compartment identity (Lawrence and Morata, 1976; Morata and Lawrence, 1975). Similar to the pathway of gene expression mediated by *en* to establish the A/P boundary, it would be expected that other regulatory genes play important roles in defining posterior compartment identity. This is best illustrated by the observation that mitotic clones containing *en* null mutations are unable to fully transform tissue within the posterior compartment into anterior structures (Gubb, 1985; Lawrence and Struhl, 1982). Further doubt can be cast upon a model where *en* solely specifies posterior compartment identity. Blair (1992) showed that *en* expression extends a small distance into the anterior wing blade during the late third larval instar. However, the expression of an *en*-related gene, *inv*, remained localized to the posterior compartment (Blair, 1992). Therefore, it was proposed that *inv* may function to specify posterior compartment identity either dependently or in conjunction with *en*. The *inv* locus, although located immediately adjacent to *en*, was isolated via sequence similarity to the *en* homeobox rather then by identification of an *inv* mutant phenotype (Poole and Kornberg, 1988). The *inv* and *en* proteins are predicted to contain an identical homeodomain and a further similarity extending across 117 additional amino acids (Poole and Kornberg, 1988). *inv* and *en* mRNAs co-localize within the embryo and the larval imaginal discs, and it has been suggested that these genes might perform similar developmental roles (Coleman et al., 1987). However, no phenotype has been unequivocally associated with a mutation at the *inv* locus (Coleman et al., 1987). A phenotype where the wings are held out and down has been suggested to be associated with *inv* loss of function (Williams et al., 1990, Tabata et al., 1995). The proximity of the *inv* and *en* sequences has made it difficult to isolate deletions remove one gene specifically (Tabata et al., 1995). Recently, the availability of mutations that specifically eliminate *inv*, or both *en* and *inv*, has provided evidence that both genes may have a role in conferring posterior identity (Tabata et al., 1995). Within the wing, clones containing homozygous *en* and *inv* mutant cells show a complete transformation of posterior into anterior structures not seen with *en* mutant clones alone (Hidalgo, 1994). Gúillen et al. (1995) propose a model in which *en* has a dual role. In this model, the primary role of *en* in the wing disc is the creation of the A/P compartment border from which further patterning of the wing is accomplished through the activation of the secreted proteins *hh* and *dpp*. A secondary, and possibly later, role for *en* is the determination of posterior identity within the posterior wing compartment. This later patterning activity has been suggested to be mediated by *inv* (Gúillen et al., 1995).

The inversion associated with vg^{W} has been shown to be intimately involved with both the *inv* and *en* genes (Williams et al., 1990b). Initial characterization of the vg^{W} allele indicated that the mutation is caused by an inversion between regions 48A to 49D on chromosome 2R (Bownes and Roberts, 1981a). Consequently, the entire coding region and 5kb of the upstream region of *inv* is brought into the vicinity of a large portion of the *vg* coding region (Chapter-II; Williams et al., 1990b). However, the *vg* and *inv* coding sequences are juxtaposed in such a manner that they would be transcribed divergently from the inversion breakpoint if the promoter were still present (Williams et al., 1990b). While the phenotype of vg^{W} includes an almost total loss of all wing and haltere structures, another phenotype associated with this allele is the suspected homeotic transformation observed within the remaining wing tissue (Bownes and Roberts, 1981a). The presence of a vg^{W} allele also causes a partial duplication of the notum (Bownes and Roberts, 1981a; Williams et al., 1990b). However, the notum duplication phenotype associated with *vg* alleles other than vg^{W} is likely a function of the dominant *vg* effect rather than the homeotic transformation associated with the remaining wing tissues (Girton and Bryant, 1980; Mglinetz and Balakireva, 1982). Thus, the vg^{W} mutation can be seen to cause two distinct phenotypes; the loss of wing tissue and a dominant homeotic effect causing the transformation of anterior to posterior wing. During a screen for reversion of the vg^{W} loss of wing phenotype, a dominant mutation of *inv* was identified based upon a transformation of the anterior compartment of the wing into a posterior compartment phenotype. This line was initially named $vg^{Wingless\text{-}Revertant\text{-}K2}$ (vg^{WRK2}) as it did not show the dominant wing loss phenotype associated with vg^{W}. However, this reversion mutation appeared to retain the dominant homeotic transformation. Subsequent characterization of this allele has shown that the homeosis observed is caused by a mis-expression of the *inv* gene in a highly restricted pattern corresponding to that of *vg* in the anterior wing compartment. Based upon the observation that the homeotic transformation phenotype is primarily caused by mis-expression of *inv* protein, this allele was subsequently re-named $inv^{Dominant}$ (inv^{D}). In the presence of the inv^{D} allele, a mirror image duplication of posterior wing structures is observed (Simmonds et al., 1995).

Since the margin and interior structures of inv^{D}/+ flies are patterned normally, it appears that the re-specification of anterior cells to a posterior fate does not affect establishment of either the A/P or D/V compartment borders. Ectopic *inv* expression does not cause significant changes in the expression of any genes associated with the establishment of the A/P and D/V compartment borders. Thus, the functions of the *inv* and *en* genes appear to be distinguishable by their ability to specify the A/P compartment boundary, and therefore show redundant function only for the ability to define posterior identity. When these observations are compared with the genetic evidence provided by *inv* and *en* mutant clones, it appears that *inv* may have a specific role in the maintenance of posterior compartment identity within the wing imaginal disc.

Results

During a mutagenesis screen for phenotypic revertants of vg^{W}, a unique line was isolated that had completely formed wings with an anterior to posterior transformation. This transformation includes a symmetric duplication of the posterior wing across the A/P boundary (Figure III-1 A). The surface of the wing that would have normally formed the anterior compartment appears larger and the triple row of wild type anterior bristles is replaced with the single row of fine bristles characteristic of the posterior wing (Figure III-1 E). The interior of the anterior wing compartment also appears to take on a posterior fate including the characteristic pattern of wing veins. Within wings from inv^P /+ flies, the second anterior vein is replaced by two veins connected by a cross vein in the same relative location as the posterior cross vein (Figure III-1 A). The patterning of the veins within the wing itself suggests a mirror image duplication of the posterior wing blade and the corresponding loss of all anterior-specific structures (Figure III-1). No transformation of the wing hinge, notum, or pleural thoracic tissues occurs indicating that the re-specification of anterior to posterior fate is specific for the wing blade itself (Figure III-1 B-E). The transformation phenotype is induced by a single copy of inv^P as homozygotes of this allele are lethal during embryogenesis. The progenitor allele of inv^P is also homozygous lethal and therefore it appears that the lethality associated with vg^W is not alleviated by genetic separation of the dominant *vg* from the dominant homeotic phenotype. A weak transformation of haltere to wing is also observed in inv^P/+ flies, although this was reported previously as being associated with vg^W (Bownes and Roberts, 1981a).

As the *en* and *inv* genes are closely associated with the vg^W inversion, the expression pattern of both genes was examined in wing imaginal discs. The 4D9 antibody recognizes a conserved epitope between the *inv* and *en* proteins and as such will simultaneously detect both protein products (Patel et al., 1989). The gross morphology of wing imaginal discs isolated from inv^P/+ larvae appears to be similar to wild type (Bryant, 1975). However, these wing discs appear to be slightly wider than wild type within the region fated to form the wing blade (Figure III-2 A). Within the anterior compartment of inv^P/+ wing discs, the 4D9 antibody detects weak ectopic expression in the wing compartment (Figure III-2 A). This expression is detected most strongly along the D/V compartment border

Figure III-1. Wings from inv^P flies show a homeotic transformation of anterior to posterior wing.

A) Adult flies possessing the dominant inv^P allele heterozygous with a wild type balancer chromosome have wings with a mirror image homeotic transformation of anterior wing to posterior wing. This transformation replaces all anterior wing blade structures with a mirror image of the posterior including a posterior cross vein joining the two characteristic longitudinal veins (arrowhead). B) A magnified view of the wing hinge of an inv^P wing corresponding to the boxed region in A. Note the presence of normal anterior costal structures (Co) and humeral plates (HP) (See Figure I-5 for a diagram of the wild type wing hinge). C) The inv^P mutant does not affect either the notum or pleura derived from the wing imaginal disc. The pattern of notum bristles is identical to wild type. Areas of the notum often duplicated in vg^W flies appear wild type in inv^P (arrows) D) A wild type wing shown for comparison. Wild type wings possess a characteristic row of macrocheate (m) along the anterior edge and the single anterior wing vein (vII) and the posterior cross vein, (pcv). The anterior costa in these wings (arrowhead) is identical to that shown in B) indicating that the transformation of inv^P affects only the wing blade. E) The anterior edge of inv^P/+ wings shows a single row of margin bristles that is characteristic of those found in the posterior wing. F) A wild type anterior margin with the triple row of bristles shown for comparison.

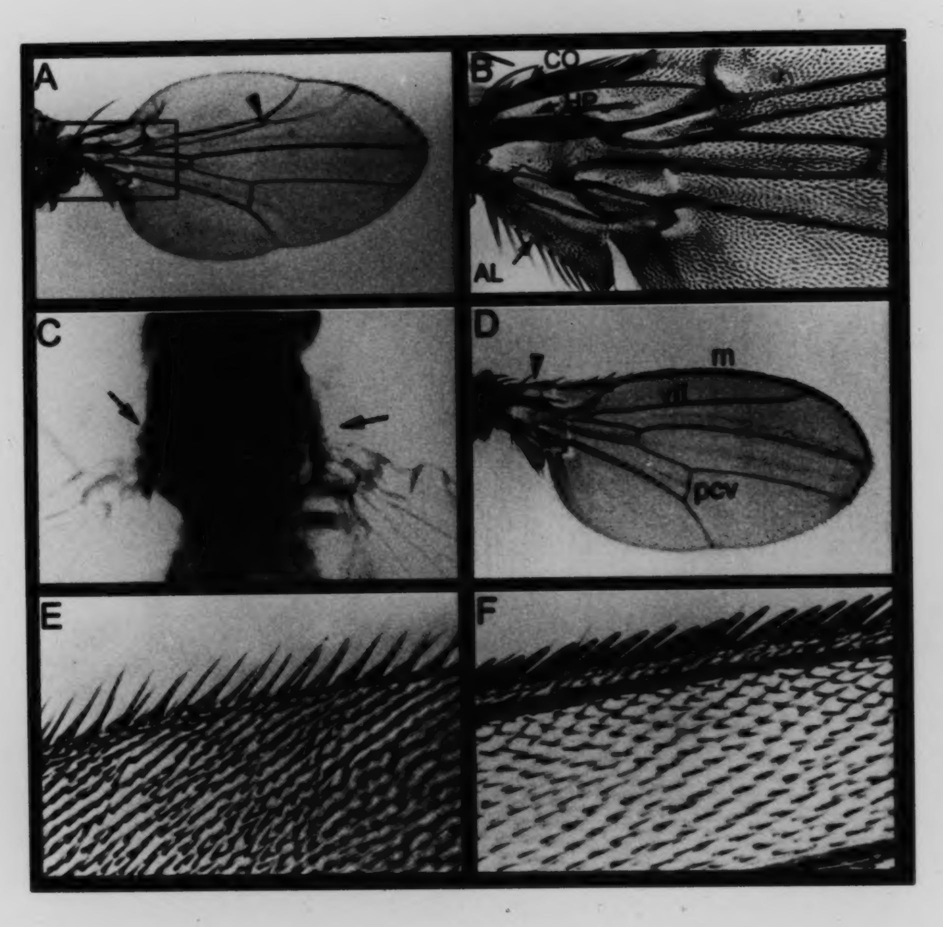
A
B
CO
HP
AL
C
D
m
vii
pcv
E
F

(Figure III-2 B arrowhead) and mirrors the expression of *vg* (Figure III-2 F). When observed at high magnification, the amount of staining in the anterior wing compartment is relatively weak compared to that observed in the posterior compartment (Figure III-2 B). The expression of either *inv* or *en* in the anterior compartment is consistent with the ectopic expression being driven by a single gene copy, compared to each of two copies of *inv* and *en* expressed in the posterior region. This ectopic protein expression is associated only with inv^P, as the 4D9 antibody does not recognize any proteins in the anterior compartment of wild type discs stained under identical conditions (Figure III-2 C). The reversion mutation that creates inv^P from vg^W eliminates repression of *vg* protein along the D/V margin. However intense sub-regions of *vg* are often detected in duplicated patterns mirrored along the A/P border in these discs (Figure III-2 D-E). Therefore, it appears that restoration of any amount of *vg* expression in the wing compartment of the wing disc is sufficient for complete formation of the wing as evidenced by inv^P. However, the anterior compartment of this wing is being transformed to a posterior identity by the presence of either *en* or *inv* ectopic expression that fills the region of the imaginal disc fated to form the wing.

To determine if *inv*, *en*, or both were ectopically expressed in the anterior compartment of inv^P/+ wing discs, anti-sense RNA probes specific to each gene were hybridized to wing discs isolated from late third instar inv^P/+ larvae. Each of these probes is derived from the 5' sequences of either *en* or *inv* that are unique to each gene. The *inv*-specific probe hybridizes strongly within cells along the D/V margin in the anterior compartment of inv^P/+ wing imaginal discs (Figure III-3 A). A similar pattern of ectopic *inv* is seen within the haltere disc, while the mesothoracic leg disc shows *inv* expression limited to the posterior

Figure III-2 Alterations are seen in the localization of *vg* and *inv* / *en* protein in late third instar wing imaginal discs derived from *inv*^{P}/+ larvae.

A) The pattern of *inv*/*en* 4D9 antibody staining observed in *inv*^{P}/+ imaginal discs shows a specific anterior mis-expression of *inv*, *en* or both extending into the anterior compartment. B) When viewed at a higher magnification, the pattern of mis-expression of *inv* or *en* (arrowhead) appears limited to a gradient along the dorsal/ventral boundary. The relative intensity of staining in anterior cells adjacent to the A/P border appears to be approximately one quarter that of the posterior. C) Wild type wing discs stained with the 4D9 antibody that detects both *en* and *inv* protein. The expression of these two proteins is limited to the posterior of the region fated to form adult wing and does not cross the A/P border. D-E) Imaginal discs derived from *inv*^{P} larvae express *vg* protein in a pattern similar to that seen in wild type discs. However, variable patterns of intense *vg* staining mirrored across the A/P margin appear within the normal *vg* pattern (arrows). F) The pattern of *vg* expression in wild type wing discs stained under identical conditions extends in a gradient from the D/V margin and does not show the darker patches of staining like those observed in the presence of *inv*^{P}.

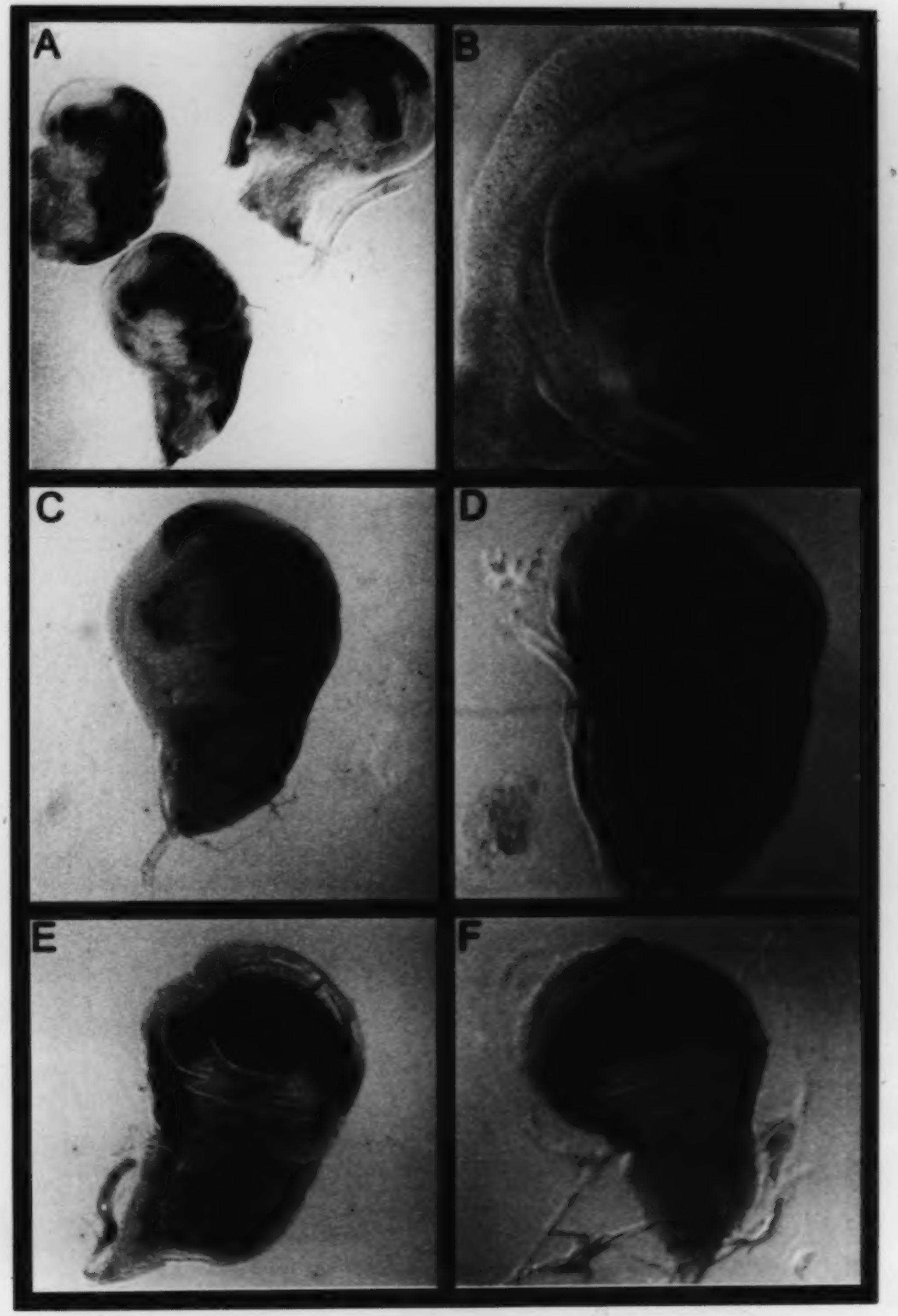
A
B
C
D
E
F

compartment (Figure III-3 A). In wing discs isolated from wild type larvae, the *inv* probe hybridizes only within the posterior compartment (Figure III-3 B). When probes specific for *en* mRNA are employed, no corresponding ectopic *en* expression is detected in the anterior of *inv*^{P}/+ wing discs, (Figure III-3 C). Similarly, the *en*-specific probe shows the same posterior hybridization in wild type wing discs as seen with the *inv*-specific probe (Figure III-3 D). Therefore, it is ectopic *inv* expression being detected by the 4D9 antibody in the anterior compartment and subsequently re-specifying the anterior wing to a posterior identity.

To identify the specific molecular event that led to reversion of the wing loss phenotype associated with *vg*^{W}, both the *inv* and *vg* sequences of the *inv*^{P} allele were examined by restriction mapping. The *vg* sequences fused upstream of *inv* in *vg*^{W} contains at least two intronic enhancer elements that direct the high level of *vg* expression along the presumptive D/V margin within the wing pouch in late third instar wing discs (Kim et al., 1996; Williams et al., 1994). Both restriction mapping and PCR analysis indicated that these elements are completely intact within the *inv*^{P} chromosome (Figure II-4 A). However, restriction mapping detected alterations within sequences at the extreme 3' end of the *vg* coding region (Figure III-4 B). The alterations represent a deletion adjacent to the *Bgl*II restriction site located within the last *vg* exon. This deletion covers approximately a 4kb region including the 3' untranslated region (UTR) of *vg* (Figure III-4 B). Cloning of the *Bam*HI fragment representing the 3' *vg* portion of *inv*^{P} indicated that the sequences immediately after the breakpoint are derived from a region distal to *vg*. A probe derived from sequences that include the deletion breakpoint hybridized to portions of a wild type λ clone of *vg*

Figure III-3 In situ analysis with specific *inv* or *en* probes indicates that only *inv* is ectopically expressed in the anterior compartment.

A) In *inv*^{D} wing discs (wing), the *inv*-specific anti-sense probe produces staining which extends into the anterior compartment of the disc along the dorsal ventral boundary (arrowhead). This anterior mis-expression of *inv* (arrowhead) is mirrored in the haltere disc (haltere) while the leg disc (leg) shows only posterior specific staining. The border between the anterior (a) and posterior (p) compartment is shown by a dotted line in each disc. The difference in intensity of the ectopic *inv* staining in the anterior compartment compared to that in the posterior compartment appears much less than that observed with the *inv/en* antibody. This is a factor of using a specific RNA probe with recognizes the differences between the anterior and posterior expression of *inv* alone. B) A wild type wing disc stained with the same *inv* specific probe shows only posterior compartment staining. These wild type wing discs are highly over-stained and no *inv* expression can be detected in the anterior compartment. C) In *inv*^{D} wing discs, *en* mRNA expression remains limited to the posterior compartment. D) A wild type wing disc stained with the same *en* specific probe used in C).

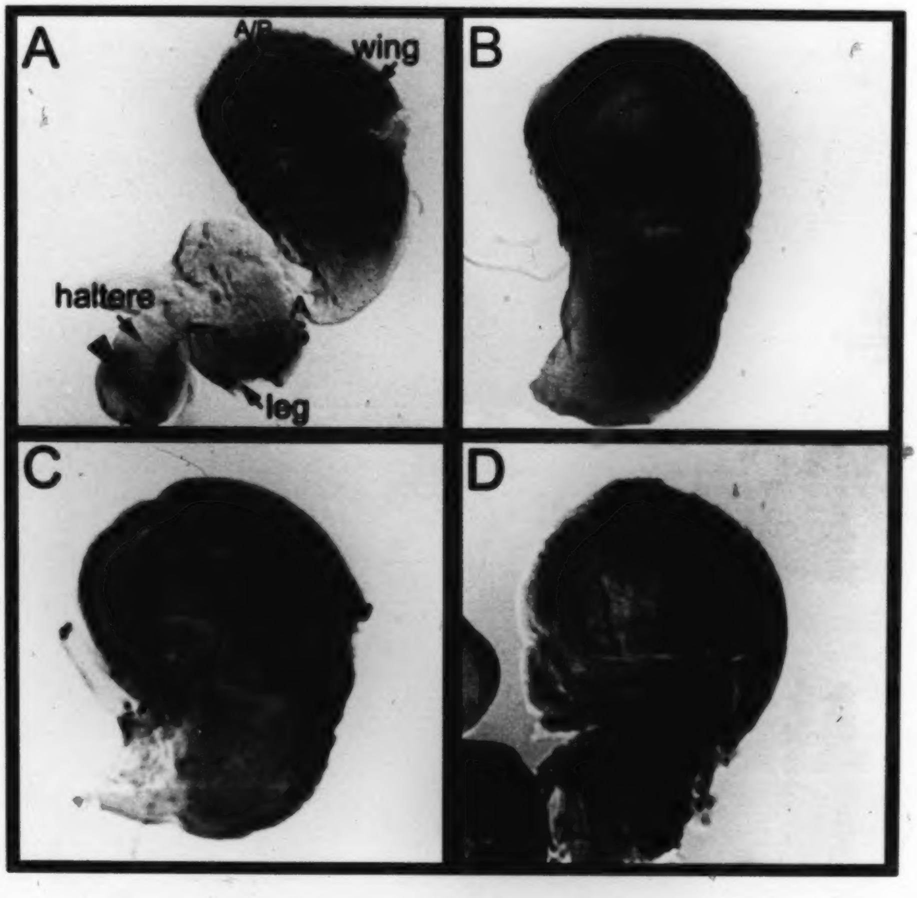
A
A/P
wing
haltere
leg
B
C
D

Figure III-4 A deletion in the 3' end of the *vg* coding region of *vg*^{W} causes the *inv*^{P} phenotype.

A map showing the organization of the *vg* and *inv* sequences juxtaposed across the inversion breakpoint associated with *vg*^{W} (from (Williams et al., 1993). The hatched bars indicate regions that correspond to the intronic enhancers that control wild type *vg* expression (Kim et al., 1996; Williams et al., 1994). PCR analysis with the primers shown above the exon map indicates that these elements are intact in *inv*^{P}. B-E) The *inv*^{P} allele is associated with a large, (approximately 4kb), deletion of the *vg* coding sequence within *vg*^{W}. Southern hybridizations show the differences in *inv*^{P} compared with both *vg*^{W} and *vg* wild type restriction maps when probed with *vg*-specific probes. B) The appearance of a smaller band in the *Xho*I lanes indicates that the deletion is approximately 4kb in size. No alteration is seen within the remaining lanes indicating that the breakpoint is distal to the *Hin*dIII site located at 15.0 of the *vg* map. C) When probed with sequences near the inversion breakpoint, no alterations can be detected in *inv*^{P} as compared to *vg*^{W}. D) A 5' *vg* exon probe shows the disappearance of the sequences distal to the *Bgl*II site at position 15 on the *vg* map. This suggests the deletion associated with *inv*^{P} removes a 4 kb sequence distal to this region. E) A southern blot probed with the *inv* cDNA showing that the coding region of *inv*^{P} shows no alterations compared to that of either *vg*^{W} or wild type.

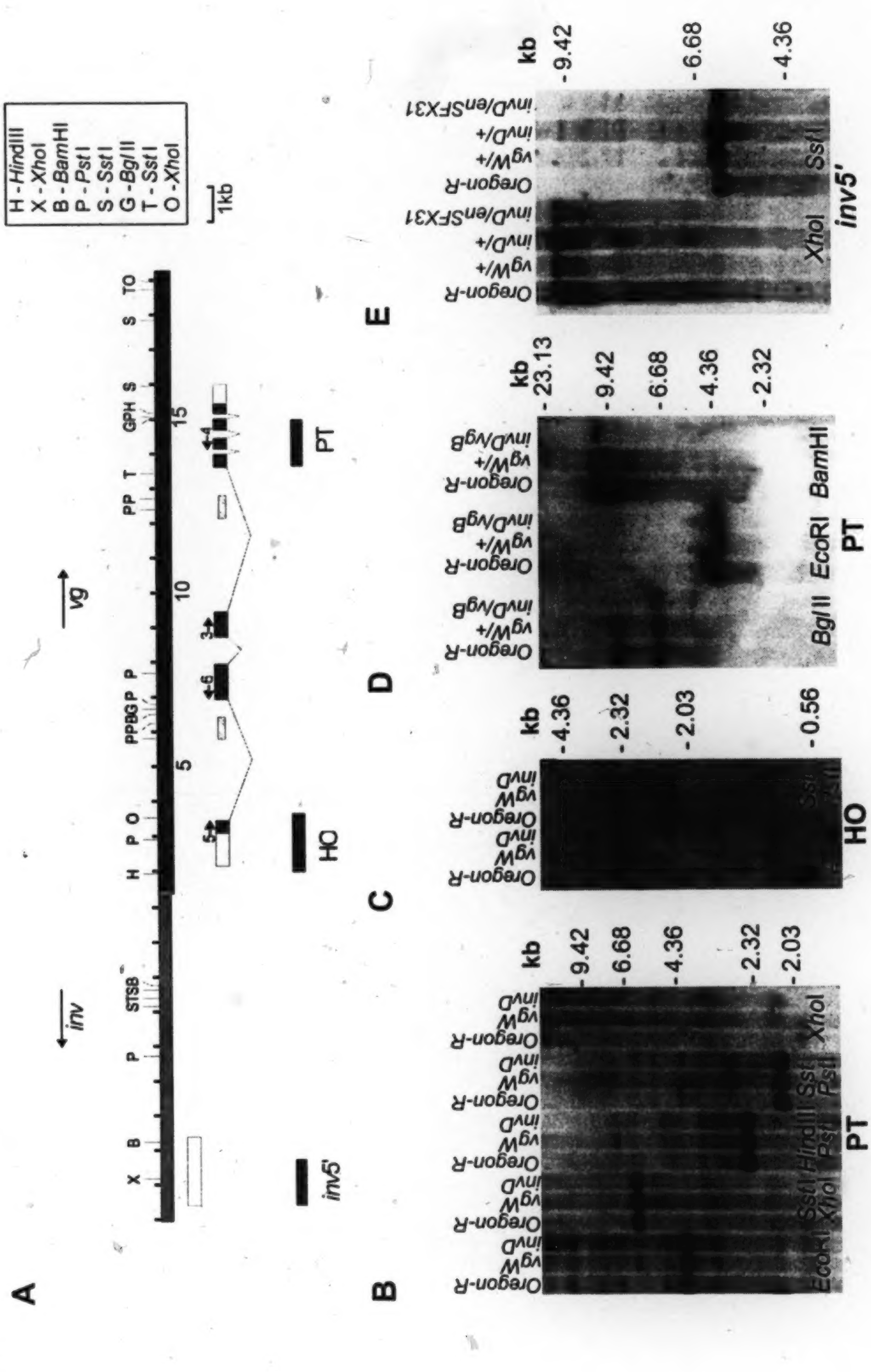
A
inv
vg
H - HindIII
X - XhoI
B - BamHI
P - PstI
S - SstI
G - BglII
T - SstI
O - XhoI
1kb
X B P STSB H P O PPBGP P PP T GPH S S TO
5
10
15
inv5'
HO
PT
B
Oregon-R
vgW
invD
EcoRI
SstI XhoI
HindIII PstI
SstI PstI
XhoI
PT
kb
-9.42
-6.68
-4.36
-2.32
-2.03
C
SstI
HO
-4.36
-2.32
-2.03
-0.56
D
vgW/+
invD/vgB
BglII
EcoRI
BamHI
PT
-23.13
-9.42
-6.68
-4.36
-2.32
E
invD/+
invD/enSFX31
XhoI
SstI
inv5'
-9.42
-6.68
-4.36

approximately 4-5kp distal to the *Bgl*II site. A restriction map of *inv* sequences from inv^{P} show no alterations compared to that of vg^{W} (Figure III-4 E). Thus, the alteration of *vg* sequences is sufficient to eliminate the dominant wing loss associated with vg^{W}, separating this phenotype from the homeotic transformation mediated by ectopic *inv*. The remaining homeotic phenotype is the basis for naming the inv^{P} allele. Double labeling experiments with the *inv/en* 4D9 antibody and anti-*vg* confirmed the co-localization of *vg* and *inv* expression within cells in the anterior inv^{P}/+ wing imaginal disc (Figure III-5 A). To confirm that the small alterations in *vg* patterning associated with inv^{P} do not interfere with its wing specific function, the expression of *sd* was examined in the presence of inv^{P}. The *sd* product is required for wing and wing border formation and is initially specified by the activity of *vg* (Williams et al., 1993). The expression pattern of *sd* in the wing imaginal disc mirrors that of *vg* both spatially and temporally (Campbell et al., 1992). Since no corresponding alteration in the pattern of *sd*-lacZ are detected like those seen using the anti-*vg* antibody in inv^{P}/+ wing discs, it appears that the variations observed in *vg* patterning do not affect subsequent *vg* function associated with *sd*. (Figure III-5 B). The co-localization of ectopic *inv* with *vg* and *sd* expression suggests that *inv* is being mis-expressed in the anterior compartment under the control of the *vg* intronic enhancers (Figure III-4). These enhancers normally act to drive the expression of *vg* to high levels along the D/V compartment boundary. The expression of *vg* in the wing pouch driven by these enhancers shows a weak temperature sensitivity that can suppress or enhance the wing loss phenotype (Nakashima-Tanaka, 1968). The phenotype of inv^{P} within the anterior compartment also shows parallel temperature sensitivity. Figure III-6 shows the wing phenotype inv^{P} /+ flies raised at 18°C, 25°C and 28°C. The transformation phenotype associated with both the wings and halteres of inv^{P} is weakest at lower temperatures. Thus, in addition to the spatial similarities between ectopic *inv* and *vg* both the anterior *inv* expression and *vg* share similar temperature sensitivity in their expression. This further suggests that the mechanism driving *inv* in the anterior compartment is the presence of the *vg* enhancer elements now in a region 5' to the *inv* start site on the *inv^P* chromosome.

While the ectopic expression of *inv* is able to provide posterior compartment identity to cells in the anterior wing, patterning of these transformed anterior wings by signals from the A/P compartment border appears to remain unaffected. This is suggested by the formation of a completely duplicated posterior interior wing vein structure and margin in the re-specified anterior compartment. To observe the effect of *inv^P* upon formation of the A/P compartment border, the wing imaginal disc expression patterns of *hh*, *dpp*, *ptc*, and *ci* were examined in the presence of *inv^P*. These genes were chosen because the expression of *hh* and *ptc* are required for *en*-mediated induction of *dpp* along the A/P border (Basler and Struhl, 1994; Campbell et al., 1993; Capdevila et al., 1994; Sanicola et al., 1995). Additionally, the expression of *ci* is limited to the anterior compartment and is repressed by *en* expression in the posterior compartment (Lee et al., 1992). In wild type wing imaginal discs the expression of *hh*-lacZ is limited to the subset of cells in the posterior compartment that also express *en* (Figure III-5 C). In the presence of *inv^P* the expression of the *hh-lacZ* reporter remains posteriorly localized within the wing disc. The β-galactosidase is highly stable and would persist in cells for a significant time even if activation of *hh* was removed (Dominguez et al., 1996; Schwartz et al., 1995). This would allow the detection of even transient activation of *hh*. However, in every imaginal disc examined, the presence of the

Figure III-5 Dual confocal immunofluorescent images showing expression of A/P and D/V patterning genes in larval wing discs from *inv*^{P} third instar larvae. Each disc was stained with the 4D9 *inv/en* monoclonal antibody that recognizes both *inv* and *en* expression (red). The expression of the second gene was examined either by using a specific antibody or by the expression of an enhancer trap inserted into that gene and detected by an anti β-galactosidase antibody (green). A) The expression of *vg* and ectopic *inv* in the anterior compartment are coincident. A yellow colour is formed when the red and green signals overlap. B) The expression of a *sd*-lacZ reporter does not show any alterations in the normal D/V localization in wing imaginal discs isolated from larvae containing the *inv*^{P} allele. C) The localization of *hh*-lacZ staining in wild type wing discs is found within the posterior compartment cells expressing *en*. D) The ectopic expression of *inv* within the anterior wing disc does not induce *hh*-lacZ expression. E) The expression pattern detected by the *hh*-lacZ reporter is identical to that observed when discs are stained with a *hh* antibody, indicating that *hh* is not induced even transiently in the anterior compartment by the presence of *inv*. F) Wild type *ptc* expression appears strongest in the anterior compartment cells along the A/P boundary and diminishes in a gradient fashion in cells anterior. G) The expression of *ptc* is unchanged in the presence of ectopic inv. The strong A/P specific pattern of *ptc* expression does not follow the border of cells ectopicly expressing *inv* (arrow). The lower levels of *ptc* in more anterior structures are also unaffected. H) The expression of *dpp* in wild type imaginal discs is seen within the anterior compartment in a narrow band of cells along the A/P border. I) A/P expression of *dpp* remains unchanged in the presence of cells expressing *inv* protein in the anterior compartment. However, it appears that there is some suppression of *dpp* in the center of the wing disc (arrow). J) The suppression of *dpp* in the presence of *inv*^{P} is confirmed by *in-situ* hybridization with a *dpp*

specific probe. K) The anterior specific expression of *ci* protein in wild type wing discs as detected by the *ci-lacZ* reporter. L) The expression of the ci-*lac-Z* reporter is unchanged in the anterior compartment in the presence of *inv* protein. M) To ensure the persistence of the highly stable β-galactosidase protein did not mask subtle reductions in *ci* protein a ci-specific antibody was also used and no reduction of *ci* protein could be detected. N) The expression of *wg* in wild type imaginal discs shows two concentric circles which outline the wing compartment (w) and a D/V specific pattern that is partially responsible for establishing *vg* expression (d/v). O) The expression of *wg* is unaffected by the anterior to posterior transformation caused by the presence of the *inv*^{P} allele.

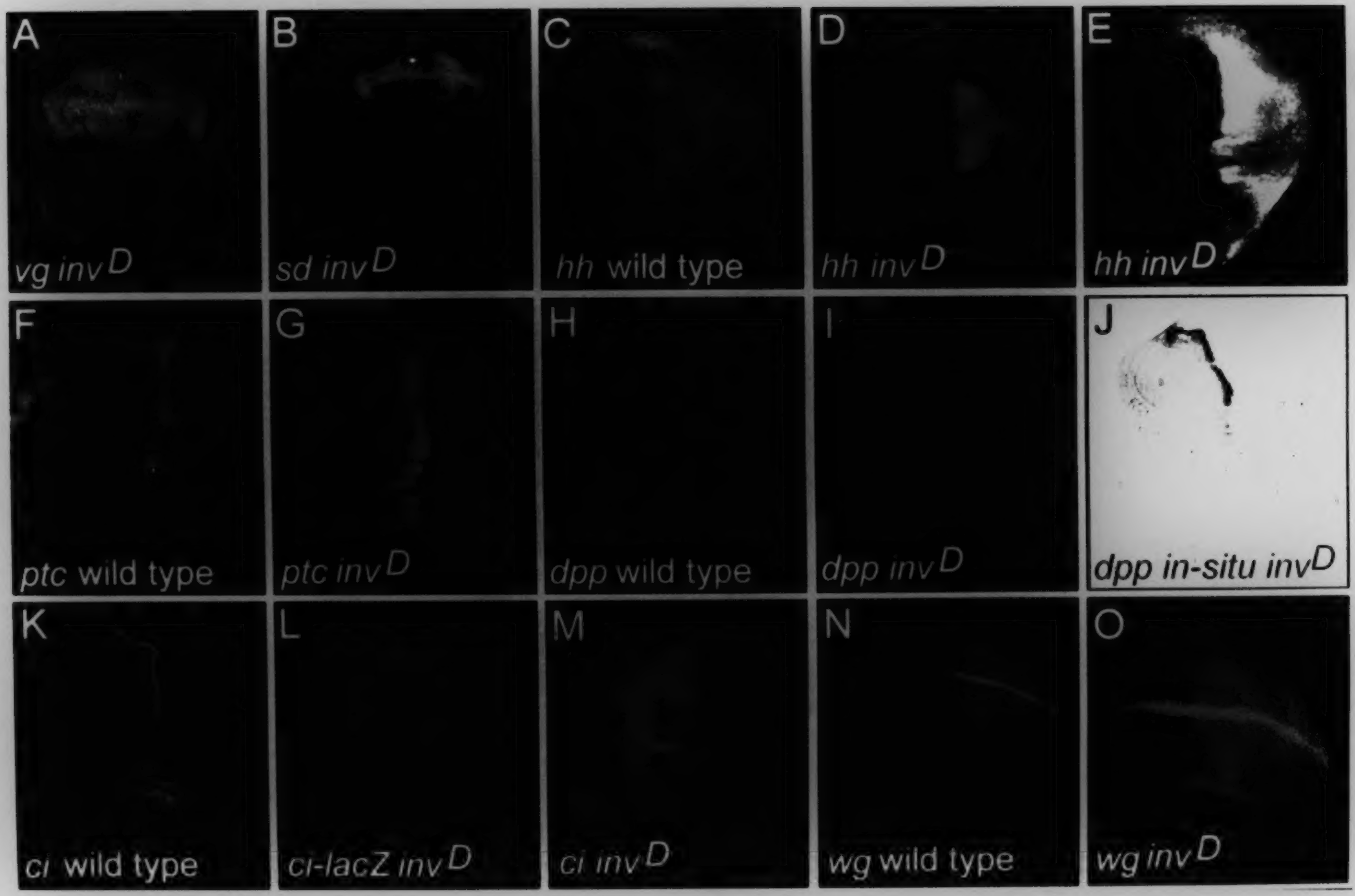
A
vg inv^D
B
sd inv^D
C
hh wild type
D
hh inv^D
E
hh inv^D
F
ptc wild type
G
ptc inv^D
H
dpp wild type
I
dpp inv^D
J
dpp in-situ inv^D
K
ci wild type
L
ci-lacZ inv^D
M
ci inv^D
N
wg wild type
O
wg inv^D

inv^P allele did not induce the expression of *hh* in the anterior compartment (Figure III-5 D). Further, the *hh*-lacZ accurately detects the entire activation of *hh* expression in the *inv*^{P}/+ wing disc as an anti-*hh* antibody detects only posterior localization of *hh* protein (Figure III-5 E). Note that there is a stripe of intense expression of *en*/*inv* just anterior to the cells expressing *hh* (Figure III-5 D). This is representative of the anterior expression of *en* within the wing disc as reported by Blair (1992) and is not a function of the mis-expression of *inv*.

The expression of *ptc* within the anterior compartment of the wing disc is highest along the A/P compartment border and decreases in a graded fashion anteriorly (Phillips et al., 1990) (Figure III-5 F). Like *hh*, the expression pattern of *ptc* is also unchanged in the presence of the *inv*^{P} allele (Figure III-5 G). The expression of *dpp* is normally found in a thin stripe along the A/P compartment boundary (Figure III-5 H). Since expression of *hh* and *ptc* are not altered by the presence of ectopic *inv*, it is anticipated that *dpp* would remain localized along the A/P margin in imaginal discs isolated from *inv*^{P}/+ larvae (Figure III-5 I arrow). However, some repression of the *dpp*-lacZ expression is seen within the cells located at the junction of the A/P-D/V compartment borders (Figure III-5 I). To examine if this repression was an artifact caused by using a *lacZ* reporter or of an actual repression of *dpp* expression, *in-situ* hybridization using a *dpp* probe was performed on *inv*^{P}/+ wing discs. The *in-situ* analysis confirmed that there is a small number of cells that have lowered *dpp* expression where the A/P and D/V borders intersect (Figure III-5 J). Whether this repression is a property of the presence of the *inv* protein directly, or a secondary effect of the homeotic transformation in these wing discs, is unknown. A useful marker for anterior compartment cells in normal wing imaginal discs is the expression of *ci* (Orenic et al., 1990). During normal wing development the expression of *ci* is limited to the anterior compartment as it is repressed in cells expressing *en* (Figure III-5 K)

(Schwartz et al., 1995). In *inv*^{P}/+ wing imaginal discs the expression of *ci-lacZ* and correspondingly that of *ci* as detected by anti-*ci* antibody is unchanged (Figure III-5 L-M). This indicates that ectopic *inv* alone does not actively repress *ci* activation in the anterior compartment. Additionally, since these cells have a posterior identity, ci expression does not need to be repressed to allow for posterior cell identity. To determine if *ci* expression was affected during earlier stages within the cells ectopically expressing *inv*, expression of *ci* was detected by a *lacZ* reporter. The reporter produces a highly stable β-galactosidase protein that would persist even after suppression of the endogenous *ci* expression as detected by the *ci* antibody. The concordance of normal *ci*-lacZ and *ci* antibody expression within anterior cells ectopically expressing *inv* suggests that *ci* is not suppressed by *inv* (Figure III-5 L-M). To examine the formation of the D/V organizer in the presence of *inv*^{P}, the expression of *wg* was examined. *wg* signaling is involved in the establishment of the A/P border, later patterning of the D/V border, and the subsequent expression of *vg*. The pattern of *wg* expression in *inv*^{P} imaginal discs (Figure III-5 O) also shows no significant alterations compared to that seen in wild type discs (Figure III-5 N). This suggests that the D/V compartment border is being established normally within the cells ectopically expressing *inv* in the anterior compartment. Thus, the altered patterning of *vg* detected in *inv*^{P}/+ wing discs is a function of the re-specification of the anterior compartment. The lack of any alteration in the specification of *hh, ptc, dpp, ci* or *wg* patterning associated with *inv*^{P} suggests that *inv* can specify a posterior compartment identity without altering the specification of the A/P compartment border by *en*. Further, the re-specification of the anterior compartment to a posterior fate does not affect the activity of the D/V border, including the establishment and activity of *vg*. Therefore, the *inv*^{P}

Figure III-6 The inv^D allele shows a temperature dependent phenotype. A) The transformation phenotype of inv^D is weakest when flies are grown at 18°C. The ectopic posterior cross vein (asterisk) is often missing from the re-specified anterior compartment of these wings and anterior-specific bristles are seen in the distal most portion of the anterior margin (arrow). B) At 25°C, mirror image symmetry is seen between the normal and ectopic posterior compartment. The slight size difference is a due to fewer cells being located within the anterior compartment (Bryant, 1975). C) When raised at 28°C the interior wing vein pattern of inv^D/+ wing discs becomes more disorganized.

A
B
25°C
C
28°C

phenotype illustrates that the wing loss phenotype associated with *vg*^{W} can be selectively eliminated by mutations within the *vg* sequences. Such mutations indicate that regions located in the extreme 3' portion of the *vg* coding sequence, or alternatively within the 3' UTR of *vg*, are important for mediating the dominant *vg* activity. This further illustrates that both *inv* and *vg* sequences are important in causing the original dominant *vg*^{W} wing loss phenotype (Chapter II).

Genetic analysis of the *inv*^{P} chromosome provides evidence that the elements causing the ectopic expression of *inv* in a pattern corresponding to the D/V pattern of *vg* appear to be operating in a *cis*-dependent manner. The transformation of anterior to posterior wing margin in the *inv*^{P}/+ heterozygote is occasionally incomplete with anterior bristles seen at the P/D extremes. When *inv*^{P} is crossed to a deletion that affects only *en* and *inv*, (*en*^{E}), the resulting flies show no significant alteration in the amount of transformation of anterior wing (Table III-1). Therefore, the ability to confer posterior identity upon the anterior wing compartment is inherent within the *inv* sequences of *inv*^{P}. The presence or absence of a wild type copy of *inv* does not alter the transformation phenotype significantly. When *inv*^{P} is crossed to a smaller deletion that affects only *inv*, the anterior compartment remains transformed although the ectopic posterior cross vein seen in *inv*^{P} /+ heterozygotes is often not present (Figure III-7 A). Similarly, when *inv*^{P} is made heterozygous with various *en* alleles, only few *en* mutations appear to affect the severity of the *inv*^{P} phenotype (Table III-1). Therefore, the homeotic activity associated with the *inv*^{P} allele does not affect any required elements of *en* expression. When *inv*^{P} is crossed to a large number of embryonic and larval lethal *en* mutations, the resulting flies are fully viable (Table III-1). Therefore, the *en* gene located adjacent to the fused *vg-inv* sequences of *inv*^{P} appears to be functioning normally during embryonic

Table III-1 The phenotypes of inv^D heterozygous to alleles of *en*, *inv* and *vg*.

Allele	Description	Viability	Wing phenotype
vg^B	large deletion covering *vg*	+	extreme *vg* [a]
vg^{83b27R}	*vg* null	+	extreme *vg* [a]
vg^{83b27}	deletion of *vg* intron-2 D/V enhancer	+	*vg*
vg^W	inversion	-	*N/A*
vg^{WR1}	deletion (derived from vg^W)	-	*N/A*
vg^1	recessive *vg* allele	+	weak *vg* [b]
en^{SFX31}	large deletion covering both *en* and *inv*	+	inv^D [c]
en^E	deletion of *en* and *inv* only	+	inv^D
en^1	insertion upstream of *en* (viable)	+	inv^D
$en^{28\text{-}11\text{-}1}$	*en* point mutation	+	inv^D
en^2	inversion (lethal)	+	inv^D
en^7	*en* point mutation (lethal)	+	inv^D
en^{10}	larval lethal allele of *en*	+	inv^D

[a] Deletes all adult structures derived from wing disc, including notum.

[b] Adult flies have significantly more wing then flies homozygous for vg^1.

[c] A wings held out and down phenotype has been attributed to *inv* mutants. (Williams et al., 1990b)

Figure III-7 The inv^P phenotype is enhanced by alleles of *en* and *ph* but not by *inv*.

Anterior specific margin bristles are occasionally seen when the inv^P allele is heterozygous to the *Roi* (inv^+) balancer. A) Mutations affecting only *inv* (inv^{30}) eliminate any appearance of anterior specific bristles in the presence of inv^P. However, the wing veins appear not to extend to the P/D extremities of the wing. B) The wing phenotype associated with the genotype inv^P/ph. A strong suppression of wing vein formation is seen when only a single functional copy of *ph* is present in an inv^P background. C) Wings from flies when the inv^P allele is heterozygous to the large deletion en^{SFX31}, the wings are fully transformed and the interior wing vein structure is strongly disorganized. D) A second phenotype associated with inv^P/en^{SFX31} flies is wings held out and down. This has been suggested to be associated with recessive *inv* mutations (Williams et al., 1990b). E) The phenotype of inv^P/vg^B shows a complete loss of all dorsal thoracic structures. The inv^P allele is complete null for *vg* as evidenced by the elimination of the entire wing and part of the thorax similar to that is seen with *vg* null homozygotes (Williams et al., 1993).

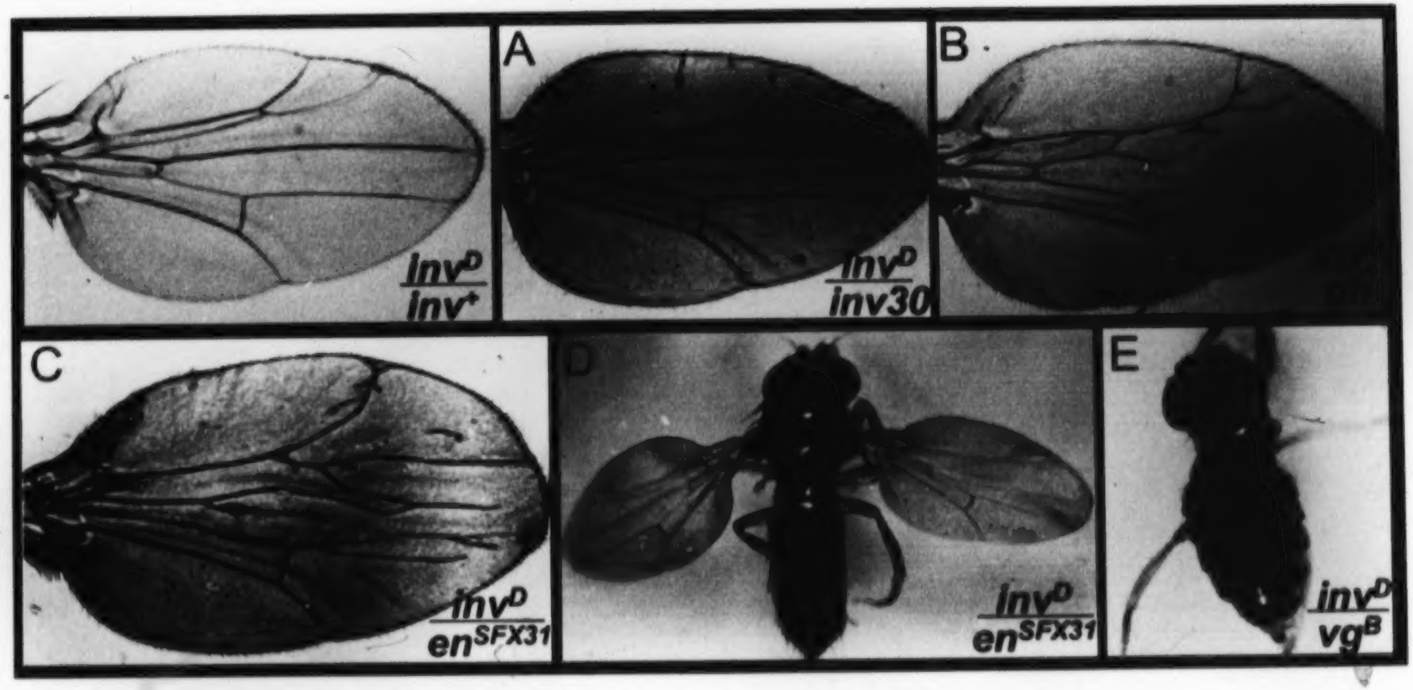
$\frac{inv^{D}}{inv^{+}}$
A
$\frac{inv^{D}}{inv30}$
B
C
$\frac{inv^{D}}{en^{SFX31}}$
D
$\frac{inv^{D}}{en^{SFX31}}$
E
$\frac{inv^{D}}{vg^{B}}$

development. When heterozygous to a weak allele of *ph*, *inv^P* flies show a loss of vein formation within both the normal and transformed posterior wing structures (Figure III-7 B). When *inv^P* is heterozygous to a large deletion affecting *inv*, *en* and *ph* (*en*^{SFX31}), a similar phenotype of disorganized wing veins is seen. This combination also causes the transformed anterior compartment to be larger than the posterior compartment. One additional phenotype of *inv^P/en^{SFX31}* flies is wings held out and down which has been associated with homozygous *inv* mutations (Williams et al., 1990b). However, the *vg* sequences associated with *inv^P* appear to be non-functional a deletion of the extreme 3' end of *vg* is associated with loss of the dominant loss of wing phenotype. An extreme *vg* phenotype is produced when *inv^P* is heterozygous to either the *vg^B* or *vg^{83b27R}* null alleles (Figure III-7 E), but the *vg* wing phenotype is less severe in the presence of the recessive *vg^1* allele (Table III-1). Therefore, *inv^P* represents an recessive expression null allele of *vg* as well as a gain of function *inv* allele.

Discussion

Although the *inv* gene was originally isolated due to its homology with *en*, it appears that these two related genes are not functionally redundant during wing disc development in *Drosophila*. Like *en*, the *inv* protein can induce cells of the anterior wing imaginal disc to adopt a posterior identity but, unlike *en*, mis-expression of *inv* in the anterior compartment does not induce an ectopic A/P compartment boundary. Genetic analysis of mutations for *en*, *inv*, or both suggests that the function of *inv* and *en* are partially overlapping. However, *en* can partially compensate for the loss of *inv* protein in an *inv* null mutant (Tabata et al., 1995). Furthermore, both genes appear to define the posterior wing development as the complete transformation of posterior to anterior fate in the wing can only occur when both *en* and *inv* are removed (Hidalgo, 1994; Sanicola et al., 1995). The differences associated with inv^- clones compared to inv^-/en^- clones in the wing suggests that, unlike *en*, *inv* is only necessary during the later development of the wing, specifically when the posterior structures are patterned (Tabata et al., 1995). A model where *inv* is only required during later development is further supported by the observation that *inv*-null alleles produce no mutant phenotype during embryogenesis and are completely viable (Tabata et al., 1995). However, it is interesting to note that homozygotes of the en^E mutant, which deletes both *en* and *inv*, produce more extreme abnormalities in the developing embryo than do mutants lacking only *en* (Tabata et al., 1995). It is not known how ectopic *inv* would affect embryogenesis and it is possible that this may be contributing to the embryonic lethality associated with both vg^W and inv^D homozygotes. However, it is unlikely that ectopic *inv* could be solely responsible for embryonic lethality. While ectopic *inv* may be deleterious to the embryo in vg^W, reversion mutants that eliminate the homeotic phenotype and presumably no longer mis-express *inv* are still embryonic lethal (Chapter-II; Williams et al., 1990b).

The timing of ectopic *inv* expression induction in the wing imaginal disc via the *vg* intron enhancers might also play a role in producing the inv^D phenotype. The division of the wing disc into specific anterior and posterior compartments, through the action of *en*, occurs early in development during the period at which embryonic segmentation occurs (Cohen, 1993). Expression of *vg* also occurs within the wing disc primordia during early embryonic development as well, (stage 10) (Williams et al., 1991). However, in terms of embryogenesis this is long after the initial segmentation of the embryo by *en*. Although the exact timing of the activation of the *vg* remains unknown, it is likely that the mis-expression of *inv* in the wing imaginal disc primordia mediated by *vg* would occur after initial determination of the anterior-posterior compartment boundary. However, the *vg* intron-2 enhancer is active in the wing imaginal discs at least as early as the second larval instar (Williams et al., 1994). Clones of en^{E} induced during the second instar via FLP-mediated recombination produced abnormal third instar wing discs that showed corresponding mis-expression of *ci*, *ptc*, *dpp*, and *hh* (Sanicola et al., 1995; Tabata et al., 1995). Adult wings that contain large en^{-} and inv^{-} mitotic clones induced during the second instar show extensive re-patterning when the clone is located in the posterior compartment (Hidalgo, 1994; Tabata et al., 1995). However, when the same *en* mutants used to create the double en^{-} and inv^{-} mutant clones described above are used separately in clonal analysis different results are seen. Also, clones of en^{-} cells alone cause pattern abnormalities throughout the posterior compartment without causing extensive transformation of posterior to anterior cell fate. This is similar to the results that have been obtained on multiple occasions with *en* mutants in the wing, and confirms that the *inv* gene is playing some role during normal specification of the posterior wing compartment (Brower, 1984; Garcia Bellido and Santamaria, 1972; Gubb, 1985; Hidalgo, 1994; Kornberg, 1981a; Lawrence and Morata, 1976).

The anterior to posterior transformation phenotype associated with inv^{D} wings is diametrically opposed to the posterior to anterior wing transformation seen with homozygotes of the en^{1} mutation (Morata and Lawrence, 1975). However, en^{1} appears to be an unusual allele of *en*. Mitotic clones of the genotype en^{1}/en^{1} in an en^{1}/en^{+} background can cross the A/P compartment border but manifest a phenotype only in the posterior wing (Lawrence and Morata, 1976). This initially suggested that the requirement for *en* function is limited to specification of the posterior wing compartment. However, when an *en* antibody was used to detect *en* expression in homozygous en^{1} mutant wing imaginal discs it was found that *en* protein is suppressed but not completely eliminated in the region of the wing disc that forms the wing blade (Brower, 1986). Thus, the presence of *en* in the posterior compartment cells of wing imaginal discs is required to initiate the formation of the A/P compartment border as well as the initial definition of posterior identity. (Morata and Lawrence, 1975; Tabata et al., 1992). The phenotype of the *en*^{1} mutation can be reconciled with the observations of the homeotic transformation associated with clones of cells mutant for both *en* and *inv*, if relatively low expression of *en* is sufficient to establish the A/P compartment border while higher levels of *en* are needed for the maintenance of *inv* within the cells of the posterior compartment. Additionally, when mitotic *en*^{1}/*en*^{1} clones are induced during early development, the frequency of transformations of wing drops significantly 40 hours before pupariation (Garcia Bellido and Santamaria, 1972). This is compatible with a model in which activation of *inv* begins to control posterior compartment identity at this stage.

The *inv*^{D} phenotype suggests that *inv*-mediated transformation of anterior to posterior cell fate within the wing does not involve alterations in the expression of *en*-effector genes that establish the A/P compartment border. Thus, the establishment of the A/P compartment border is distinct from the designation of anterior or posterior specific developmental fate within the cells of that compartment. When *en* is mis-expressed along the D/V margin in the anterior compartment, a phenotype vastly different from *inv*^{D} is observed. The presence of elevated ectopic *en* expression within the wing hinge leads to duplications within the anterior compartment and formation of ectopic wings. When *en* is expressed at a high level along the D/V border in the wing disc, a transformation of anterior to posterior fates occurs within the wing hinge, but the wing margin exhibits a paradoxical transformation of posterior to anterior (Simmonds et al., 1995). Thus, although *en* is expressed at quite high levels along the wing margin, the cells adopt a posterior identity at a lower frequency than is induced by the relatively low levels of ectopic *inv* associated with *inv*^{D}. Lower levels of ectopic *en* expression within the anterior wing can induce the expression of *hh* and *dpp* and the repression of *ci* expression (Simmonds et al., 1995; Tabata et al., 1995). The apparent difference between ectopic *en* and *inv* expression along the D/V border can be explained by the observation that ectopic *en* can cause repression of the endogenous *en* and *inv* genes in the posterior compartment (Simmonds et al., 1995; Tabata et al., 1995). This expression of *en* is mediated by autoregulatory interactions with members of the *Polycomb* group (*Pc*-G) of genes including *polyhomeotic* (*ph*). The expression of *ph* may be activated by the *en* protein while the *Pc*-G genes have been shown to repress *en* and *inv* in the anterior compartment (Busturia and Morata, 1988; Serrano et al., 1995). This would also account for the alteration of the *inv*^{D} phenotype observed in the presence of strong *ph* alleles and large deficiencies of *en* (Figure III-7). The reduction of *ph* protein levels associated with *ph* hypomorphs may remove an element of repression in the anterior compartment of *inv*^{D} alleles leading to enhancement of the transformation phenotype (Figure III-7).

The phenotype associated with *inv*^{D} indicates that *inv* may act as a patterning gene that maintains compartmental identity in imaginal discs rather than acting as a border patterning element like *en* (Garcia Bellido, 1975). In this manner, *inv* is more similar to the activity of *vg* in specifying wing-specific identity in a compartment that has its borders defined by the activity of *wg*. In developing *Drosophila* an embryo it has been shown that en is not clonally inherited and must be maintained through an interaction with *wg* within the posterior compartment (Vincent and O'Farrell, 1992). Since ectopic expression of *inv* associated with *inv*^{D} only causes a re-specification of anterior compartment identity and does not affect P/D or D/V patterning. Thus, it is possible that during

Drosophila larval development the role of *inv* is to preserve posterior identity within imaginal discs while *en* continues to interact with *wg* and other patterning genes such as *Distal-less* (*Dll*) (Cohen and Jürgens, 1989).

The partial redundancy of the *inv* and *en* genes suggests that these genes have diverged recently in evolution. Both an *en* and an *inv*-like gene can be found in other insects such as the silkworm *Bombyx mori* and the honeybee *Apis melifera* (Hui et al., 1992; Waldorf et al., 1989). In vertebrates there are up to four copies of *en*-like genes in *Xenopus*, zebrafish, hagfish and chicken (Ekker et al., 1992; Fjose et al., 1992; Hemmati-Brivanlou et al., 1991; Holland and Williams, 1990; Logan et al., 1992). The mammalian genome also contains two *en*-like genes, *En-1* and *En-2*, found in both mice and man (Joyner et al., 1985; Joyner and Martin, 1987; Logan et al., 1992). In mice, *En-1* expression begins earlier (one somite stage) than that of *En-2* (5 somite stage) (Joyner et al., 1985). Similar to the situation illustrated by the *en* and *inv* genes in Drosophila, En-2 mutations appear to be far more mild than those associated with *En-1* (Wurst et al., 1994). Furthermore, as with *Drosophila inv* and *en*, *En-1* and *En-2* mutants affect either the mid or hind-brain of the mouse, indicating that despite having coincident expression patterns and sharing a homeobox motif they do not have identical developmental roles. The conservation of multiple *en*-like genes from insects to vertebrates suggests that while being partially redundant in function, the diverged en-like sequences are dissimilar enough to be evolutionarily conserved. In Drosophila, *inv* and *en* share a large region of homology within their 3' regions but differ at their 5' ends. These differences may represent the sequences that have diverged in order to allow the acquisition of distinguishable functions (Coleman et al., 1987). Support for recent divergence of *inv* and *en* function in *Drosophila* is found in the observation that the leech, sea urchin and the brine shrimp *Artemia franciscana* have only one *en* class gene (Dolecki and Humphreys, 1988; Manzanares et al., 1993; Wedeen et al., 1991). The single *en*-like gene of *Artemia* has sequences that are similar to the unique portions of both *en* and *inv* from *Drosophila* and *Bombyx* (Manzanares et al., 1993). This may represent a larger precursor en-like gene that is the progenitor of *en* and *inv* in *Drosophila*. Therefore, it appears that the *en* and *inv* genes either diverged from a common ancestor, or alternatively they have re-combined in other species like *Artemia* to perform both functions in a single gene. In either case, the pattern of evolutionary conservation of *en*-like genes suggests that the multiple roles that *en*-like genes perform are partitioned into several active genes in more complex organisms. The *en* and *inv* genes of *Drosophila* may represent a situation where this partitioning remains incomplete with only a far subtler role in development played by *inv* compared to that of *en*.

Chapter IV - *In vitro* interactions between the *vg* and *sd* protein

Introduction

While mutations within a large number of genes affect *Drosophila* wing development, only a few appear to be required globally for formation of these tissues (Lindsley and Zimm, 1992). A wing specific gene would be one that performs functions needed during wing formation but is not required for the development of other *Drosophila* appendages. Formation of wing structures appears to be induced by signals emanating primarily from the D/V boundary, a unique property as compared to other limb development where patterning occurs via the A/P or P/D axis (Cohen, 1993). Therefore, it is reasonable to assume that specialized gene products would be needed during patterning of the wing and haltere. This link between D/V compartmentalization and subsequent wing formation distinguishes the dorsally located wing and haltere from ventral appendages such as the legs, which appear to be primarily patterned along the A/P and P/D axis. Along the D/V border of the developing wing disc, interactions between the dorsal *ap*-expressing and ventral *fng*-expressing cells induce *vg* expression via *wg* through tightly controlled and evolutionarily conserved enhancer elements (Kim et al., 1996; Williams et al., 1994). During normal wing imaginal disc development, *vg* and *sd* are co-expressed throughout the wing compartment and show peak expression along the D/V margin in the later stages of the third instar (Williams et al., 1988). Thus, not only are the temporal and spatial expression patterns of *vg* and *sd* identical within the wing disc but expression of one is dependent upon the other and loss of function in one gene causes the loss of the normal D/V expression in the other.

While a link between *vg* and *sd* during wing development is suggested by their co-expression, the cell death associated with loss of either *vg* or *sd* makes it very difficult to test this interdependence within the wing imaginal disc. Flies homozygous for the mutations *sd*^{UC1} or *vg*^{1} have extremely reduced wings including a complete deletion of margin, wing blade, and alar lobe(James and Bryant, 1981). Wing imaginal discs isolated from larvae of the these genotypes show identical patterns of cell death in the regions fated to form the structures that are deleted in the wings. This cell death associated with *vg* and *sd* hypomorphic alleles occurs primarily in the third instar (James and Bryant, 1981). Further, ultrastructural analysis of these discs indicated the presence of elevated cell death concentrated in the presumptive wing blade region (James and Bryant, 1981). The levels of cell death associated with *vg* or *sd* mutations increase with developmental time and by 96 hours AEL the average number of dead or dying cells is twice that of the remaining cells (James and Bryant, 1981). Thus, the timing and localization of abnormal cell death in the third instar wing imaginal discs of *vg* and *sd* mutants suggests that these gene products are both required in the same cells. In the absence of one or both of these gene products, cells in the wing disc enter the apoptotic pathway and a corresponding deletion in the portion of the wing normally formed by those cells is the result.

The mechanism of *vg* and *sd* activation in cells along the D/V compartment border can be examined by the creation of ectopic wing margin structures within the wing imaginal disc. One mechanism that will produce ectopic wing margin within the wing blade is the creation of clones that lack expression of *shaggy (sgg)*, also known as *zeste white-3 (zw3)*. *sgg/zw3* appears to be responsible for determining the identity of specialized bristle-producing cells along the D/V margin of the wing (Simpson et al., 1981). During wing development, *sgg/zw3* is thought to act downstream of *wg* in the specification of wing margin cell fate (Blair, 1994). Ectopic expression of a *sd-lacZ* reporter construct occurs in the cells immediately surrounding *sgg/zw3*⁻ mutant clones generated during the first or second instar away from the D/V compartment border but still within the wing compartment (Blair, 1994). Further, this activation of *sd*-lacZ expression on the border of *sgg/zw3* expressing and non-expressing cells is coupled with an activation of *vg* to similarly high levels (Blair, 1994). However, this ectopic co-activation of *vg* and *sd* is limited to cells surrounding the *sgg/zw3*⁻ clones within the wing compartment. When similar clones were examined within the regions of the wing imaginal disc outside this region, no activation of *vg* or *sd* was observed (Blair, 1994). Thus, the interdependent activation of *vg* and *sd* along the D/V margin appears to be limited to cells within the wing compartment of the wing imaginal disc. This activation of *vg* in the wing compartment occurs through the activity of genes expressed along the D/V border including *wg*, *N*, *Ser*, and *Su*(*H*) (Kim et al., 1987; Ng et al., 1996; Williams et al., 1994). While nothing is yet known about the activation of *sd*, it appears that the expression of *vg* is required to maintain *sd* expression within the wing imaginal disc (Williams et al., 1994).

The *sd* gene encodes a 440 amino acid DNA binding protein of the TEA family of transcription factors (Bürglin, 1991; Campbell et al., 1992; Campbell et al., 1991). The TEA domain is an evolutionarily conserved motif that has been described for the *TEC-1* gene of *Saccharomyces cerevisiae*, the *abacus-A* gene of *Aspergillus nidulans* and the *mTEF-1* /*hTEF-1* genes of mice and humans (Blatt and DePamphiliis, 1993; Laloux et al., 1990; Mirabato et al., 1989; Xiao et al., 1991). Based upon homology between these genes the TEA domain is defined as a block of 66-68 amino acids containing three helices with strongly hydrophobic regions that bind distinct sequences in the Ty element enhancer (Bürglin, 1991). The TEA domain of *sd* is most closely related to *hTEF-1*, identical over 70 of 72 amino acids of the region containing the TEA domain (Campbell et al., 1992). Additionally, *hTEF-1* and *sd* share 68% amino acid identity and 81% similarity over the entire aligned sequence (Campbell et al., 1992). In *Drosophila*, expression of *sd* is first detected within embryonic neuroblasts during germ band extension (Stage 9). Later expression is seen in the PNS including the sense organs in the supraesophageal ganglion (Campbell et al., 1992). During early larval development, *sd* remains expressed in the CNS and in many of the imaginal discs including the progenitors of the wing and haltere (Campbell et al., 1991). All of the other larval imaginal discs, except the labial disc, show some *sd-lacZ* reporter gene activity in the larval third instar (Campbell et al., 1992). Specific expression of *sd* is also detected in the larval brain and may be responsible for controlling larval taste behavior (Anand et al., 1990; Inamdar et al., 1993). Mutations of *sd* can produce a number of different phenotypes ranging from wing defects to larval lethality (Campbell et al., 1992; Campbell et al., 1991). The wing scalloping phenotype is similar to that produced by *N*, *Ser* and *cut* (Fleming et al., 1990; Jack and DeLotto, 1992; Xu et al., 1990). However, in addition to wing margin formation, *sd* is also required in a cell autonomous manner in larvae for the development of the entire wing structure (Simpson et al., 1981). This cell autonomy suggests that *sd* protein is involved in the reception and subsequent mediation of developmental signals within the wing. Some alleles of *sd* that show a larval lethal phenotype can complement alleles that produce the wing phenotype, indicating that different regions of *sd* may be required for the sensory and wing development functions (Campbell et al., 1991). The co-activation of *sd* and *vg* within the nuclei of the wing imaginal discs, and the subsequent requirement for each gene to preserve the expression of the other, strongly suggests interactions between these two proteins in the developing wing. However, as loss of either *vg* or *sd* leads to the death of that cell, assaying this interaction within the cells of the wing imaginal disc is not possible. Since clones of both genes are readily available, the ORFs of both *vg* and *sd* were expressed either in bacteria or *in vitro* to produce proteins that could be used to assay for any direct interaction between these two gene products. Both vg and sd exhibit a strong and specific *in vitro* affinity for one another, suggesting that interaction between these two genes occurs via protein binding.

Results

vg cDNA1 cloned into the pET16b vector produces a protein of similar size to the endogenous *vg* protein and is recognized by a *vg* antibody. The highest level of *vg* protein expression from *vg*/pET16b in *E. coli* BL21 (DE3) cells is approximately 90 minutes after induction with IPTG (Figure IV-1 A). At longer times post induction, the levels of *vg* protein within the cells diminish suggesting that the *vg* product is toxic to *E. coli*. The *vg* protein produced from *vg*/pET16b is recognized by the anti-*vg* antibody but is slightly smaller than the predominant band recognized in pupal protein extracts (Figure IV-1 B). The significance of this size difference is unknown since sequencing of the *vg*/pET16b construct indicates that no base changes have occurred compared to the published *vg* sequence (Williams et al., 1991). The size difference may be due to post-translational modifications that are occurring within the *Drosophila* cells. The *vg* protein contains a number of sites for phosphorylation by *Protein kinase C* (*PkC*) and two potential N-linked glycosylation sites. These post-translational modifications would retard the mobility of the endogenous *vg* protein (Williams et al., 1991). Since a *sd* antibody is not available, the bacterially translated *sd* product can not be tested by Western blot analysis. However, *in vitro* translation of the *sd*/pET16b construct produces a protein of identical size to the *sd* product

(Figure IV-1 C) (Campbell et al., 1992). This size of the bacterially expressed putative *sd* protein also matches the protein produced by in vitro translation of the *sd*/pET16b construct. Therefore, it appears that the *sd* and *vg* pET16b expression constructs are able to produce the complete *sd* and *vg* proteins at high levels in *E. coli* BL21(DE3) cells.

To determine if the *vg* and *sd* proteins interact *in vitro*, induced and un-induced samples of protein isolated from *E. coli* cells containing the *vg*/pET16b and *sd*/pET16b constructs were tested by Far-Western analysis. ^{35}S-labeled *in vitro* translated *vg* protein binds specifically with high affinity to the bacterially expressed *sd* protein. To ensure that the protein being recognized is that produced by the *sd*/pET16b construct, samples from both un-induced and induced cells were included. A stronger signal is seen with the induced *sd* expression versus the lane containing the same cells before induction of *sd*/pET16b. Non-specific binding of *vg* to bacterial protein extracts from cells containing the *vg*/pET16b construct or in vitro translated protein from the same construct is not detected (Figure IV-2 A). Protein isolated from cells transformed with an expression construct for a *Drosophila* gene not expressed in wing discs, *β-Ftz* F1/pET16b, was included as a control for non-specific binding and it also does not bind to *vg*. The protein bound by the *vg* protein has a molecular weight of approximately 56 kD, which is the predicted size of the *sd* protein (Campbell et al., 1992).

When ^{35}S labeled *sd* protein is used to probe a parallel blot of the same protein extracts, the *sd* protein is seen to specifically bind both the bacterially expressed and the in vitro translated *vg* protein (Figure IV-2 B). As was seen with the *vg* probe, there is much stronger binding of *sd* protein seen in the lane containing protein from the induced cells containing the *vg*/pET16b construct as

Figure IV-1 The *vg* and *sd* ORFs cloned into the pET16b expression vector allows the production of full length *vg* and *sd* proteins.

A) A Coomassie blue-stained SDS-PAGE gel showing extracts of BL21 (DE3) cells containing the *vg*/pET16b construct at various times post induction. Lanes 1-5 represent 0, 30, 60,90 and 120 minutes after IPTG induction of cells grown to an initial OD_{600} of 0.8. Note that the amount of the 46 kD *vg* protein (arrow) is highest compared to the other bands representing normal bacterial proteins at 90 minutes after induction and reduced at 120 minutes. The relative molecular weights as determined by protein standards are indicated at the right of each gel. B) A Western blot showing that the *vg* antibody recognizes the protein produced by either bacterial expression (*vg*/pET16b) or linked *in vitro* transcription and translation (IVT) of the *vg*/pET16b construct. These bands migrate faster than the band recognized by *vg* antibody within pupal protein extracts (30h pupa). C) *In vitro* transcribed and translated *sd*/pET16b produces a protein of 56 kD. The *in vitro* reaction was carried out using ^{35}S labeled methionine and the resulting protein was run out on a SDS-PAGE gel and exposed to X-ray film for 24 hours.

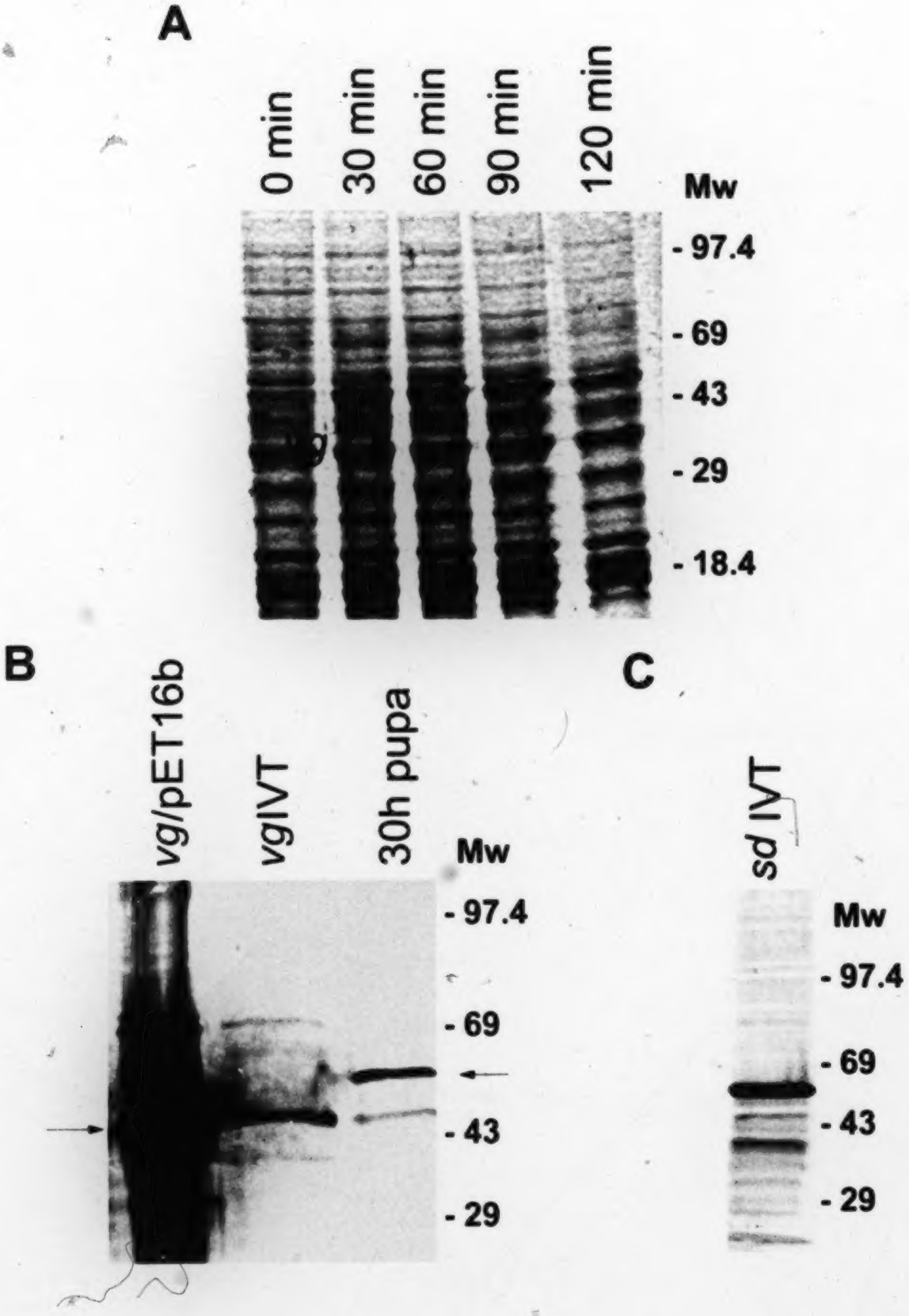
A
0 min
30 min
60 min
90 min
120 min
Mw
- 97.4
- 69
- 43
- 29
- 18.4
B
vg/pET16b
vgIVT
30h pupa
Mw
- 97.4
- 69
- 43
- 29
C
sd IVT
Mw
- 97.4
- 69
- 43
- 29

compared to un-induced samples. The labeled *sd* protein binds to a protein of approximately 46 kD in size which matches that predicted for *vg* (Williams et al., 1991). The *sd* protein does not bind to either itself or to β-*Ftz* F1. Some weak binding of the *sd* protein to bands of larger size than *vg* is seen within lanes containing the bacterial *vg* protein extract (Figure IV-2 B). It is unlikely that this represents *sd* binding to bacterial proteins as no weak staining is seen in the lanes containing *sd* or β-*Ftz* F1 constructs within identical cells. The significance of these bands is unknown, however they may be ascribed to additional modifications of *vg* protein occurring within bacterial cells.

To determine the region of the *vg* protein that is binding to sd, in frame deletions were made within the *vg*/pET16b construct. Three of constructs *vg*-vgΔ1-2, vgΔ7-8 and vgΔ3-6 all retain a strong affinity for *sd*. Since these deletions of the *vg* ORF all retain binding to *sd*, this indicates that the binding region is not within the deleted regions (Figure IV-3 B). To ensure that the deleted *vg* constructs were still able to produce functional *vg* protein, each was *in vitro* translated Figure IV-3 A). The vgΔ3-6 construct deletes the N-terminal half of the *vg* protein localizing the *sd* binding region to the C-terminal portion of *vg*. The vgΔ1-2 plasmid represents a deletion for a basic region containing 28 amino acids composed mostly of repeated histidine and alanine residues near the C-terminal end of *vg*. The binding region for *sd* lies between the vgΔ1-2 deletion and the Δ7-8 deletion, which also binds *sd* (Figure IV-3). Three deletions that are located at the C-terminal end of *vg*, vgΔ2-10, vgΔ8-9 and vgΔ2-8, all the eliminate *sd* binding affinity of *vg* (Figure IV-3). Correlating this data with the proteins that still bind *sd* a region of 78 amino acids is defined that is critical for the protein-protein interaction between *vg* and *sd*. This region is rich in serine residues and contains 3 putative phosphorylation sites (Williams et al., 1991)

Figure IV-2 A strong *in vitro* interaction is detected between full-length *vg* and *sd* proteins.

A) A Far-Western blot showing that labeled, in vitro translated *vg* protein binds only to protein extracts from bacterial cells containing a construct that expresses *sd*. The labeled *vg* protein does not bind to protein extracts containing either vg or β-Ftz F1. The size of the protein bound by *vg* probe is approximately 56 kD. B) When labeled *sd* protein is used to probe a parallel blot, it binds to discrete bands within extracts containing either bacterially expressed or *in vitro* translated *vg* protein. The *sd* protein does not appear to bind either to itself or to the β-Ftz F1 control. The size of the protein bound by Sd is approximately 46 kD.

Each blot contains equal amounts of protein in each lane as determined by Coomassie staining and identical aliquots from the same protein samples were loaded in parallel for each. The samples in each lane are identified by the labels at the top. *sd*/pET16b (un-induced and induced) refers to protein isolated from *E. coli* cells transformed with the *sd*/pET16b construct before (un-induced) or after (induced) induction with IPTG. Samples were also collected from cells containing *vg*/pET16b and these are labeled *vg*/pET16b-induced or *vg*/pET16b-uninduced. *vg* IVT refers to the protein produced via *in vitro* transcription and translation of the *vg*/pET16b construct. *β-Ftz* F1 represents a *Drosophila* protein that is not expressed in wing imaginal discs, which was used as a control. The relative sizes at the right of each blot correspond to that of protein standards run on each gel.

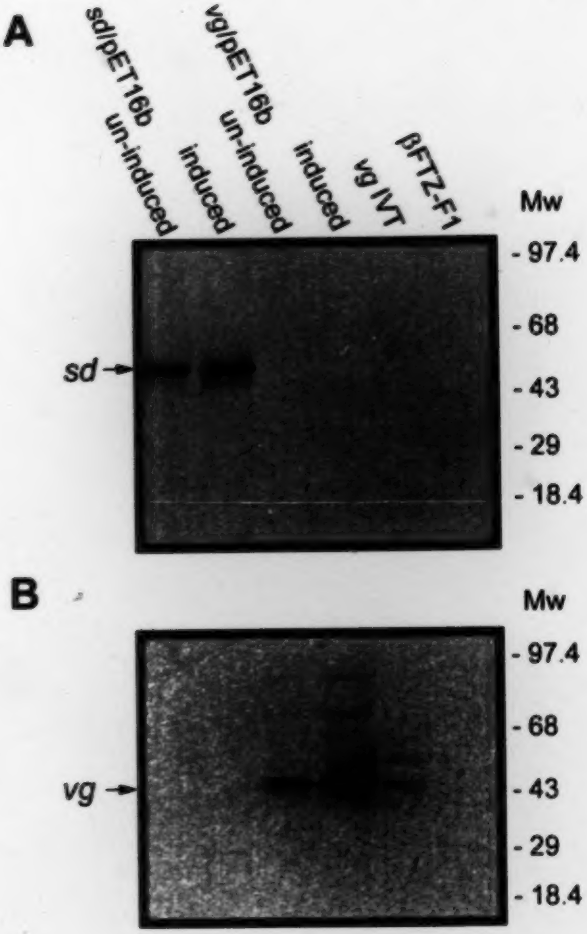
A
sd/pET16b
un-induced
induced
vg/pET16b
un-induced
induced
vg IVT
βFTZ-F1
Mw
- 97.4
- 68
sd
- 43
- 29
- 18.4
B
Mw
- 97.4
- 68
vg
- 43
- 29
- 18.4

Figure IV-3 A 78 amino acid region within the *vg* protein is necessary for binding Sd.

A)Far Western blots probed with radio-labeled Sd show that the portion of *vg* remaining in the vgΔ3-6 and the vgΔ7-8 deletion constructs retain affinity for *sd* protein. These constructs cover the N-terminal half of Vg and indicate that the *sd* binding region is located in the C-terminal portion of the *vg* protein. Constructs that remove amino acids in the C-terminal portion of *vg*, (vgΔ2-10, vgΔ8-9 and vgΔ2-8) eliminate the *vg-sd* protein binding. Below each lane is an *in vitro* translated sample from the same construct to ensure each was being translated properly. Also included is a lucerifase (luc) control that does not bind sd and the full-length *vg* protein (*vg*) which binds *sd* with high affinity.
B) A summary of the *vg* deletions and their effect upon the binding to Sd. The bars shown in gray represent truncated *vg* proteins that retain affinity for Sd. The open areas within each represent the deleted portion of the protein in each case. The black bars represent the locations of the specific primers used to generate the deletions (Table VI-4). The black box above the protein map represents the 78 amino acid region that contains an element required for *vg-sd* protein interaction. The predicted amino acid sequence of this region is shown above. The underlined portions represent the location of putative phosphorylation sites (Williams et al., 1991)

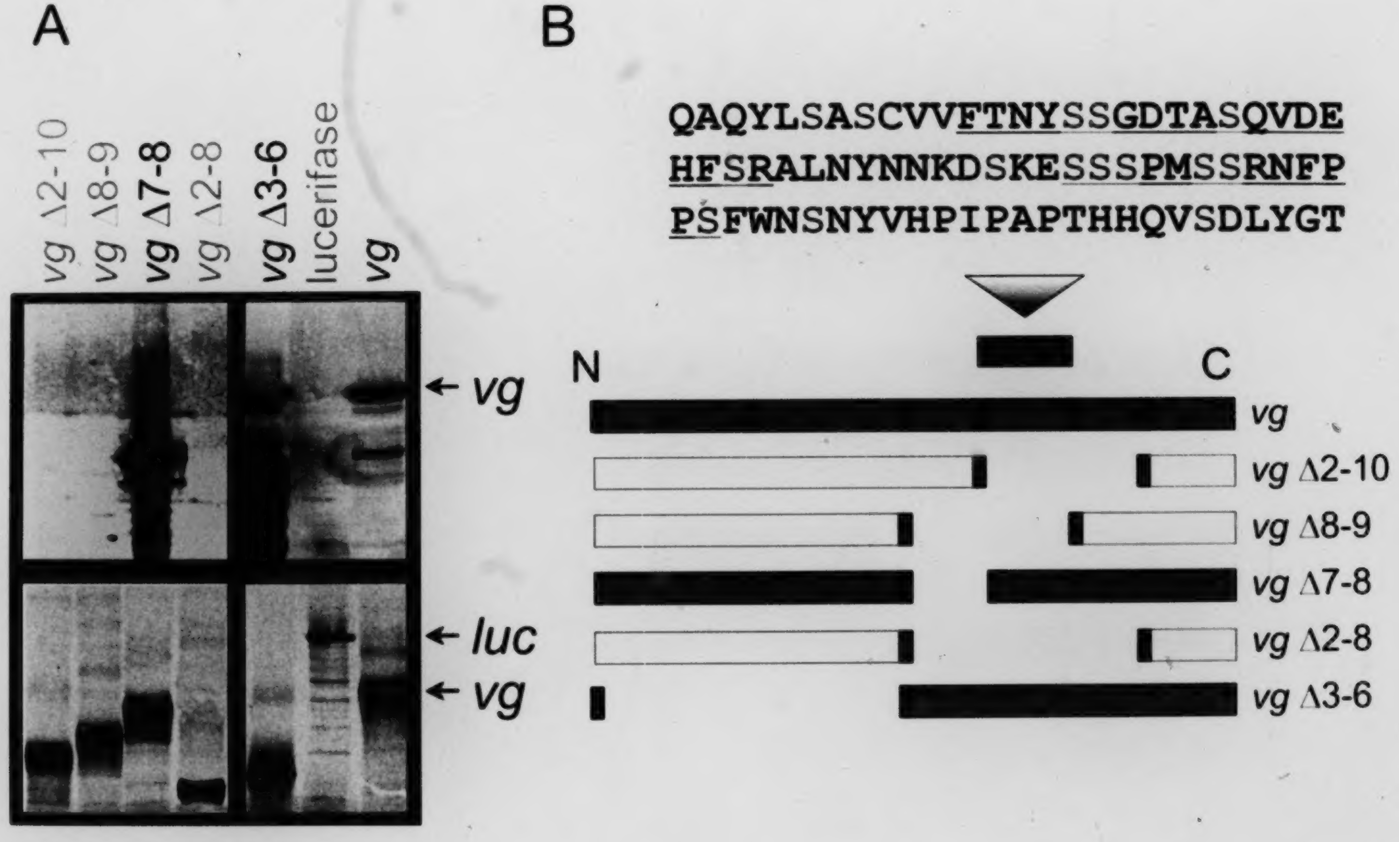
A
vg Δ2-10
vg Δ8-9
vg Δ7-8
vg Δ2-8
vg Δ3-6
lucerifase
vg
← vg
← luc
← vg
B
QAQYLSASCVVFTNYSSGDTASQVDE
HFSRALNYNNKDSKESSSPMSSRNFP
PSFWNSNYVHPIPAPTHHQVSDLYGT
N
C
vg
vg Δ2-10
vg Δ8-9
vg Δ7-8
vg Δ2-8
vg Δ3-6

Discussion

The high-affinity binding of bacterially expressed *sd* and *vg* protein products *in vitro* provides evidence that protein-protein interactions between these two genes are realized *in vivo.* It is unlikely that the bands seen represent artifactual binding of the labeled protein probes to bacterial proteins as the bacterial host for each construct was identical and yet binding of the *vg* or *sd* protein probes is specific to protein extracts containing constructs for either *sd* or *vg* respectively (Figure IV-2). Bacterially expressed hTEF-1 protein shows the same binding capacity to SV40 DNA as either endogenous or cloned hTEF-1 isolated from HeLa cells (Xiao et al., 1991). Thus, expression of *hTEF-1* in a bacterial host does not appear to significantly alter the properties of this protein. This would suggest that the interactions seen with bacterially expressed *vg* and *sd* proteins represent what is occurring within cells of the developing wing imaginal disc. While the histidine-alanine rich region removed in the pET-*VG*Δ1-2 deletion is a good candidate for a region that mediates protein interaction, a *vg* protein lacking this region still binds *sd* with high affinity. Rather, it appears that at least one critical region for *vg-sd* protein binding is located adjacent to this region (Figure IV-3). This 78 amino acid is predicted to form a helix-loop-helix structure with a high concentration of serine amino acids (10/42), within the predicted loop. Further, three putative phosphorylation domains are located within the predicted loop structure, including two overlapping domains between amino acids15-33 (Figure IV-3 B).. The significance of this is as yet un-tested, however it does suggest that protein phosphorylation of Vg, may be playing a role in modifying *vg* activity, including binding of Sd. Further experiments to determine if *vg* is phosphorylated *in vivo* would address this possibility.

The human *sd* homologue, hTEF-1, has been shown to require interactions with limiting, cell specific protein factors to activate transcription from target promoters. The hTEF-1 protein can activate the GT-IIC or Sph enhansons of the SV40 early promoter in HeLa cells but not in MPC11 lymphoid B cells. Transfection of these cells with ordered deletions of hTEF-1 indicated that the C-terminal portion of hTEF-1 appears to contain an activation domain that is activated within HeLa and not MPC11 cells. When the C-terminal domain of hTEF-1 is replaced by the yeast GAL-4 DNA binding domain stimulation of hTEF-1 was observed, while constructs deleted for this region lost the cell specific binding properties associated with wild type hTEF-1 protein (Xiao et al., 1991). The variable activation of SV40 DNA sequences by hTEF-1 in certain cell types suggests that trans-activation of hTEF-1 may require a cell specific transcriptional intermediary factor (TIF) that is present in HeLa cells. The presence of this TIF in HeLa cells was also shown to be limiting by the over-expression of the C-terminal domain of hTEF-1 in these cells. However, a stronger repression effect is seen when the entire protein is used, suggesting that additional sites within hTEF-1 bind the putative cellular TIFs. The site for interaction of hTEF-1 with the TIF is separate from the DNA binding TEA domain.

The high degree of similarity between the *sd* protein and hTEF-1 suggests that *Drosophila* equivalents of TIFs should exist. While no protein corresponding to these predicted TIFs has been isolated from either *Drosophila* or mammalian systems, these proteins would have some predictable properties. TIF proteins would have to be localized within the nucleus to allow for interaction with sd/TEF-1 and would have to be expressed in a cell specific manner. In this context, the *vg* protein is an excellent candidate TIF. The expression of *vg* within the wing imaginal discs is tightly controlled by intron specific enhancers and the protein is found within the nuclei of cells along the D/V compartment border (Kim et al., 1996; Williams et al., 1994). The presence of *vg* protein may be required by *sd* for control of genes that are required for wing development within the imaginal disc. Further, a gradation in the amount of *vg* protein can be detected within the wing disc. Peak levels of vg are detected in cells immediately along the D/V margin while the expression of *vg* is progressively weaker in more dorsal or ventral cells (Williams et al., 1991). This suggests a model in which a limited amount of *vg* protein binding to *sd* would allow the activation of additional genes by the sd/vg complex in cells containing high levels of *vg* protein compared to those expressing *vg* at a lower levels. This would also explain the variable allele specific presence of ectopic margin cell types within the wing blade of some *sd* hypomorphic mutants (Campbell et al., 1992). Viable *sd* mutants that produce the wing loss phenotype cluster to the 3' UTR portion of the *sd* gene and likely impair production of *sd* protein (Campbell et al., 1992; Campbell et al., 1991). Thus, if limited amounts of *sd* were present to interact with equally limited TIFs at a critical period during margin specification, cells that have less than a threshold value of the vg-sd complex would be juxtaposed to those above the threshold, inducing these cells to become margin cells as opposed to wing blade. A model in which *sd* protein is part of a multi-protein transcriptional complex is supported by genetic evidence that *sd* interacts with *Ultrabithorax-like* (*Ubl*) which encodes the large sub-unit of RNA polymerase II (Mortin and Lefevre, 1981). The activity of *vg* in the presence of the *Ubl* mutation is not known at this time.

The ectopic expression of UAS-*vg* via *dpp*-GAL4 can induce wing like tissue transformations in the eye, antenna and head capsule derived from the eye-antennal disc and within structures derived from the leg imaginal discs. No transformation to wing was induced within the labellum, which is derived from the labial disc (Kim et al., 1996). The expression of *dpp* includes all the imaginal discs although *sd* expression is absent from labial disc (Blackman et al., 1991; Campbell et al., 1992). Therefore, the lack of labia to wing transformation by ectopic *vg* expression could be a function of the lack of the *sd* co-factor within these imaginal discs. Targeted expression of UAS-*sd* does not induce wing outgrowths like those seen with UAS-*vg*. However, cells that are induced to express *vg* also begin to express *sd* at higher levels indicating that the presence of *vg* can cause an activation of *sd* (Kim et al., 1996). One possible target for a protein complex containing *vg* and *sd* protein would be the *sd* gene itself. This would also explain the regulatory interaction present in early wing development, where the presence of the *vg* protein is needed for activation of *sd* and subsequently *sd* is required for *vg* function (Williams et al., 1993). The presence of *vg* protein would be required for the activation of *sd* to bind to wing specific genes including *sd* itself. Thus, additional *sd* protein would be produced to bind with *vg* and activate additional genes required for wing development, although the level of *vg* protein would ultimately be the limiting factor. One other role for the putative vg/sd complex in this model would be the suppression of genes that induce apoptosis within developing imaginal disc epithelial cells. Differentiation of wing margin could also be controlled by the graded expression of *vg* if genes involved in the specification of wing margin had a lower affinity for the vg/sd complex than those that determine a wing blade tissue type. Only in the presence of the highest amounts of *vg* would cells acquire a wing margin fate. In this model, *vg* would represent the target of a graded morphogen secreted from the D/V border. One possible candidate for this morphogen is *wg*, a secreted molecule that shows specific D/V expression and is required for activation of *vg* (Williams et al., 1993).

While it appears possible that *vg* may represent a TIF that binds to the *sd* transcription factor and mediates wing development, further analysis is needed to determine the biological significance of this interaction. Additional constructs that remove different portions of the *vg* and *sd* proteins should indicate all of the specific regions of *vg* and *sd* that are required for their interaction. Further, the binding affinity of *vg* for hTEF-1 would also provide evidence for the role of *vg* as a specific TIF that is active in the wing imaginal disc. While the binding of *vg* and *sd* proteins shown by Far-Western blotting is compelling, it represents an *in vitro* interaction that may or may not occur within an eukaryotic cell. Reconstruction of the *vg* and *sd* ORFs within an eukaryotic reporter system such as the two-hybrid system in *Saccharomyces cerevisiae* could establish the binding of these two proteins within an eukaryotic cellular environment. The two hybrid system fuses one protein of interest to a specific DNA binding domain that binds to a region near a reporter gene. A second protein of interest is then fused to a specific activator domain. If the two proteins of interest interact then the activator will be brought into proximity with the reporter gene and allow its expression at high levels (Fields and Song, 1989). Additionally, the over-expression of either *vg* or *sd* via the GAL4/UAS system in wing imaginal discs of hypomorphic *vg* or *sd* mutants would also be informative as to the interdependent role of these proteins. If the relative levels of *vg* versus *sd* protein are important in deciding fate within the wing compartment, then artificially raising the levels of *sd* or *vg* could enhance the mutant phenotype of *vg* or *sd* alleles. However, these models may be overly simplistic and there may be many potential TIFs for *Drosophila sd* that may be active in during wing development. These other factors could be identified by a screen for genes that interact with both *vg* and *sd* via the yeast two-hybrid system.

Chapter V - General Discussion

This analysis of vg^{W} and vg^{U} presented in this thesis represents a basic functional characterization of the activity of these alleles during wing development. Further, the revertants derived from these dominant alleles have provided clues as to the activity of both *vg* and *inv* in the developing wing imaginal disc in *Drosophila*. The dominant suppression of only some the D/V *vg* expression and its subsequent partial alleviation provides a direct correlation between the presence of *vg* protein within regions of the wing disc and subsequent wing development. The characterization of inv^{D} presented in Chapter III provides evidence for a function of the *inv* gene distinguishable from that of *en* during establishment of posterior identity within the cells of the developing wing disc.

The presence of high levels of *vg* is required within a wing primordium, which is defined by *wg* expression for the formation of wing tissue. In the absence of *vg*, apoptotic wing cells are removed from the developing wing imaginal disc. Within late third instar wing imaginal discs, the establishment of *vg* expression appears to be tightly controlled by the gene activity associated with at least two compartment borders. Mutations in *ap*, *wg*, *N*, *Ser*, *fng*, and *Dw* all produce significant loss of wing phenotypes and plays a role upstream of *vg* in the developmental cascade of gene interaction that initially establishes *vg* expression along the D/V border. The activation of *vg* by the *wg* gene suggests that *vg* may act within the nucleus to process the *wg* signal secreted from the D/V margin to exert control over wing specific genes (Cohen, 1996). A phenotype sometimes associated with both *vg* and *wg* mutations is that the remaining cells of the wing compartment that do not become apoptotic instead form a duplicated notum (Williams et al., 1993). If the response of *vg* is dependent upon the relative levels of *wg,* then blocking the *wg* receptor pathway within cells of the wing compartment should correspondingly alter the relative expression of *vg.* The *sgg/zw3* gene has been shown to be a negative repressor in the receptor pathway of the *wg* signal within the wing compartment (Blair, 1994; Blair, 1995; Couso et al., 1994). When *sgg/zw3* mutant clones are induced within the wing pouch but away from the D/V border, *vg* expression takes on a graded appearance that is strongest in the regions furthest from the clonal boundaries (Blair, 1994). It appears that ectopic *wg* expression requires co-expression of *Ser* to induce *vg* expression to high levels within the dorsal or ventral wing compartment (Couso et al., 1995). This is further illustrated by experiments where *wg* and *Ser* are ectopically expressed together in the leg imaginal disc, which transforms the proximal dorsal-posterior regions into cells of a wing identity (Maves and Schubiger, 1995). The limited transformation of this region of leg disc to a wing identity has not been correlated with expression of *sd* that also has a limited expression within a similar region of the leg imaginal disc (Campbell et al., 1992). It would be informative to correlate the localization of *sd* with the ability of ectopic *vg* expression to transform regions of imaginal discs. If *sd* is a required co-factor for *vg* function then the presence of both protein products would be required for transformation of cells outside the wing disc to a wing fate.

Significant alterations of *wg* expression associated with the dominant *vg* mutations (Figure II-10), suggest that the mechanism mediating the dominant effects of vg^{W} and vg^{U} may involve interfering with the response of *vg* to the *wg* signal. Recently, it has been shown that the establishment of *vg* occurs in two steps via *wg* dependent and independent pathways. The induction of *vg* in cells immediately along the D/V border does not require *wg* function (Neumann and Cohen, 1996b). However, long range patterning of cells distant from the D/V border appears to be accomplished by the secreted *wg* protein emanating from this boundary. Further, the activity of *wg* in the dorsal and ventral cells fated to become wing appears to be mediated by the nuclear localized *vg* protein (Neumann and Cohen, 1996b). If *wg* expression is induced in cells within the wing primordia in regions away from the D/V compartment border, this promotes outgrowth of wing structures as well as specifying wing margin fate (Diaz-Benjumea and Cohen, 1995).

The ability of the *mam* and *inv* sequences that are joined to *vg* in vg^U and vg^W to suppress *vg* establishment remains an unknown quantity of the dominant phenotype. Expression of *N* has been shown to be required for the establishment of *vg* expression mediated by the *vg*-intron2 enhancer element immediately along the D/V margin (Kim et al., 1996; Williams et al., 1994). In a screen to recover dominant acting suppressors and enhancers of *N*, a mutation in *mam* can modify the phenotype of a constitutively activated *N* allele. Further, combinations of *mam* and *Su*(*H*) mutations lead to elimination of the wing margin (Verheyen et al., 1996). Additionally, mutations of *mam*, *vg* and *sd* also suppress expression of the *ct* gene mediated by a specific wing margin enhancer. The *sd* TEA domain can bind specifically to this enhancer and thus *ct* represents a gene that is likely controlled by *sd* mediated DNA binding (Morcillo et al., 1996). While it is not known if *mam* represents an additional DNA binding element, staining of polytene chromosomes with anti-*mam* antibody indicates that *mam* protein is binding to several discrete sites including a position close to *ct* (Bettler et al., 1996). The expression pattern of *mam* is ubiquitous within the wing disc although it may be higher within cells immediately along the D/V border (Bettler et al., 1996; Schmid et al., 1996). This suggests a mechanism for the dominant activity of vg^U where the remaining *mam* sequences joined to *vg* somehow interact to suppress *vg* establishment along the D/V border. This is evidenced in the *vg* patterning associated with vg^{U} where no D/V patterning remains within the remaining tissue of the wing discs. Correspondingly, in vg^{U} imaginal discs D/V cells that would normally be expressing *wg* are likely removed by apoptotic cell death caused by the lack of *vg* protein. However, this model would not explain the suppression of wing formation in vg^{W}, as *vg* protein is strongly expressed within cells along the remaining D/V border (Figure II-3 B). The phenotype of the wings produced by vg^{U} and vg^{W} suggests that the mechanism that causes the loss of wing may not be identical in each case. In the presence of vg^{U} no wing blade or margin is ever formed, although the presence of hinge structures is often seen (Figure II-2 K). In contrast, the presence of a vg^{W} allele causes elimination of the wing hinge completely, although a small wing blade including a fully formed margin is produced (Figure II-2 J). Distinct cell fate specification functions have been found for *wg* in the wing blade and hinge regions (Neumann and Cohen, 1996a). The expression of *wg* in a ring around the region of the wing disc fated to form the wing is required for local cell proliferation of the wing hinge but not for the long range patterning (Neumann and Cohen, 1996a). The $spade^{flag}$ (spd^{fg}) mutation produces a phenotype that results in loss of the majority of the wing hinge structures (Neumann and Cohen, 1996a). It has been shown that the spd^{fg} mutation is a specific regulatory allele of *wg* that affects development of the wing hinge (Neumann and Cohen, 1996a; Tiong and Nash, 1990). The concentric circles of *wg* expression in the wing imaginal disc, that surround the wing and hinge primordia, are both associated with cells fated to form specific wing and hinge structures in the adult. The inner circle of *wg* expression is found in cells fated to form the humeral cross-vein, dorsal radius and the base of the alula. The outer ring is associated with the costa and axillary cord (Phillips and Whittle, 1993). One of these rings of *wg* expression is removed in spd^{fg} mutants and is associated with significant loss of hinge structures (Neumann and Cohen, 1996a). This ring is also removed in mutants of *nubbin* and this correlates to the *nubbin* hinge phenotype (Ng et al., 1995).

One ring of the *wg* expression pattern that surrounds the wing pouch, as detected by the *wg-lacZ* reporter, is also removed in vg^W mutants that also remove the hinge structures. However, the vg^W allele does not remove D/V expression of *wg* in the wing disc (Figure II-10B). The strong D/V expression of both *vg* and *wg* in the presence of the vg^W allele suggests that the suppression of *vg* in this case is occurring by a different mechanism than vg^U. The establishment of *vg* expression along the D/V border is not dependent on *wg*, although the patterning activity of *vg* in the remaining wing primordia is partially dependent on *wg* expression (Kim et al., 1996; Neumann and Cohen, 1996b). The establishment of *vg* expression within the remaining wing disc away from the cells of the D/V margin is controlled by the *vg*-intron 4 enhancer element (Kim et al., 1996). This element is partially controlled by elements of both the D/V organizer and the A/P patterning pathway. The *thick veins* (*tkv*) gene is a *Dpp* receptor and is required for activation of *vg* mediated by the *vg*-intron-4 enhancer element (Kim et al., 1996; Nellen et al., 1996). Therefore, establishment of *vg* away from the D/V boundary requires proper specification of the A/P border and subsequent *dpp* expression. It has been previously proposed that the mis-expression of *inv* and possibly *en* associated with vg^W could be responsible for the dominant loss of wing phenotype (Williams et al., 1990b). However, the transformation phenotype associated with inv^D caused by *vg* mediated mis-expression of *inv* indicates that the *inv* product appears to have no role in establishment of the A/P border (Simmonds et al., 1995). Further, simple transformation of anterior to posterior fate within the cells of the wing imaginal disc does not affect the expression of *vg* as inv^D flies have fully formed albeit transformed wings (Chapter-III). Nevertheless, the loss of the hinge and majority of wing blade while preserving the wing margin, coupled with the juxtaposition of *inv* and *vg* associated with *vg*^{W}, suggests an effect on the *vg*-intron-4 enhancer while leaving D/V expression of *vg* intact. It is interesting that by eliminating the intron-2 or intron-4 enhancer regions of the *vg* portion of *vg*^{W} a partial reversion of the dominant phenotype is realized (Figure II-3). A strong correlation between the location of the *vg* enhancers and the deletions that give rise to the partially dominant *vg*^{W} and *vg*^{U} alleles also suggests that an interplay between elements of the fusion partner gene *inv* and the enhancer elements of *vg* is occurring. While the *vg*^{W} allele does not appear to alter the establishment of the D/V border, interactions between the *vg* and *inv* sequences associated with *vg*^{W} may render wing cells unable to activate the *vg*-intron-4 enhancer. This interference could involve a transvection like effect between *vg*^{W} and *vg*$^{+}$, although this is unlikely. However, the inversion that creates *vg*^{W} would also suppress chromosome pairing in this region. Additionally, the phenotype of *vg*^{W} is not significantly altered by the presence of mutants that suppress transvection (Williams et al., 1990b). A second model in which the *vg*^{W} sequences render cells incapable of establishing *vg* expression via the *vg*-intron-4 enhancer element, rendering the same cells incapable of responding to a D/V *wg* signal, is more likely. Alternatively, the *vg*-intron-4 enhancer element may be initially activated within the wing imaginal disc in the presence of *vg*^{W} but the expression of *vg* may not be maintained. This model could be tested by sensitive measurements of the expression of β-galactosidase from the *vg*-intron-4 *lac-Z* reporter element in the presence of the *vg*^{W} allele at specific times during third instar larval development.

While the exact molecular mechanism that causes the dominant phenotype associated with *vg*^{W} and *vg*^{U} is still unknown, it appears that these alleles each cause differing suppression of *vg* establishment during wing development. The presence of a D/V pattern of *vg* associated with *vg*^{W} suggests that the *ap*, *N* and *Ser* mediated establishment of *vg* from the intron-2 enhancer occurs normally. However, the cells of the wing primordia and hinge that respond to a *wg*-mediated signal do not appear to maintain *vg* expression and subsequently undergo apoptotic cell death. It is noteworthy that the strong expression of *vg* along the D/V border associated with *vg*^{W} (Figure II-3 B). This is identical to that produced when *wg* activity is removed from the wing disc during the second instar using the temperature sensitive *wg*^{IL114} allele (Neumann and Cohen, 1996b). Additionally, expression of *wg* is removed from areas of the wing imaginal disc fated to form the wing hinge by homozygous null mutants of *vg* (Neumann and Cohen, 1996b; Williams et al., 1993). Therefore, *vg* and *wg* mediated loss of wing functions appear limited to the hinge and wing blade and not to the D/V margin. This pattern of loss of *vg* activity correlates with the structures that are not formed in the presence of *vg*^{W}. The phenotype of *vg*^{U} can also be explained in these terms if the interactions between *vg*, *wg* and *mam* with the *ct* gene are taken into account. *ct* and *mam* are intimately associated with *N* signaling and interactions between *N*, *Dl* and *Ser* along the D/V boundary are responsible for the activation of the *vg*-intron 2 enhancer by the binding of *Su*(*H*) (Couso et al., 1995; Kim et al., 1995; Morcillo et al., 1996; Verheyen et al., 1996). Interference with the establishment of the D/V expression of *vg* would also suppress activation of the *vg* intron-4 enhancer and would remove all the tissues of the wing blade (Kim et al., 1995). This matches the phenotype of *vg*^{U}, where only the hinge regions are formed. Testing this model will be difficult due to the fact that any loss of *vg* expression is coupled with cell death leading to the loss of the tissue one needs to observe. One experiment that may prove informative is the creation of marked mitotic clones of homozygous *vg*$^{+}$ within a background of *vg*^{W}/+ or *vg*^{U}/+ wing imaginal disc cells. Since *vg* acts in a cell autonomous manner, patterning within these cells should lead to the development of suitably marked wing tissues. By inducing clone formation during different developmental times, the critical period of activity for the dominant allele sequences would be established. Similarly, selective removal of genes like *ct* and *mam* during the second or third instar should produce an extremely reduced pattern of *vg* similar to that observed in *vg*^{U}.

The *inv*^{D} allele provides an interesting and paradoxical addition to the model of posterior compartment specification in the wing. The ability of *inv* to specify a posterior identity to anterior cells but not to induce the formation of an ectopic A/P border defines the potential patterning activity of *inv* as being distinct from *en*. The *inv*^{D} allele will also provide a unique tool to examine the activity and interaction of *en* and *inv* further. Since only *inv* is expressed within the anterior compartment of the *inv*^{D} wing imaginal disc, it becomes possible to screen for genes that are activated by *inv* thus leading to formation of posterior structures. This could be accomplished by screening both alleles of known genes and existing lines containing randomly inserted P-element containing *lac-Z* enhancer trap expressed in wing specific patterns. Putative genes that respond to the presence of *inv* protein would show alterations in expression in the presence of *inv*^{D}. An additional experiment would employ mitotic clones of *inv*$^{+}$/*inv*$^{+}$ cells in the anterior wing compartment in an *inv*^{D}/*inv*+ background. This would allow the determination if any patterning occurs at the border between *inv* expressing and non-expressing cells, similar to *en* mediated establishment of the A/P border. Further mutagenesis of *inv*^{D} would also be informative to establish the critical portions of *inv* that mediate the anterior to posterior transformation phenotype. Recessive mutations of *inv* appear to produce a phenotype so subtle that it is not easily observable (Tabata et al., 1995; Williams et al., 1990b).

Conversely, the *inv^D* mutation provides an easily observable gain of function allele of *inv* that can be employed in a number of experiments to help determine the role of *inv* in controlling posterior cell identity.

The strong protein-protein interaction between *vg* and *sd* shown by the *in vitro* interaction in a Far Western blot, provides evidence for the intercellular role of *vg*. It is possible that the molecular role of *vg* within the wing cells is to bind to one or more transcriptional control factors like *sd* and modify their binding to wing-specific genes. In this model, the role of *vg* would be to integrate the D/V and A/P signals established within the wing and transfer this information within the nucleus to *sd*. The expression of *vg* within the wing disc suggests that it is translating a signal originating at the D/V boundary. This signal is likely mediated via the *wg* protein into a graded response within the nuclei of the cells of the entire wing primordia highest at the D/V margin (Cohen, 1996). While co-expressed within the same cells as *vg*, the expression of *sd* shows a less pronounced gradient within the wing primordia (Campbell et al., 1992). Thus, *vg* likely represents the limiting factor in the activation of other wing specific genes. Enhancer elements of wing specific genes activated by *vg* and *sd* would possess differing affinities for the vg-sd complex. Those genes having relatively low affinity for *sd* would be activated only in the presence of high levels of *vg* while other genes required more ubiquitously for wing development would have high affinity for the *vg-sd* protein complex. One gene known to possess binding affinity for the *sd* protein is *ct*, which is responsible for patterning along the wing margin. The enhancer of this gene has been shown to have an affinity for *sd in vitro*, although whether binding of *sd* to the *ct*-enhancer is modified by the presence of *vg* protein has not been tested (Morcillo et al., 1996). A difference between *vg* and *sd* function within the cells of the wing imaginal disc is also suggested by the temperature sensitivity associated with *vg* but not *sd*. When the level of *vg* protein is reduced by hypomorphic *vg* alleles, the resulting wing phenotype shows greater amounts of tissue loss at higher temperatures. In contrast, corresponding *sd* hypomorphic alleles show no temperature sensitivity (James and Bryant, 1981). Higher temperatures could be altering *vg* protein folding and/or protein-protein interactions within the cells of the wing primordia and thus enhancing the *vg* phenotype. A screen for genes involved in responding to *sd* binding would also provide evidence for a possible role of *vg-sd* protein activity. It is likely that *vg* only represents one protein that interacts with *sd* and a number of other possible TIFs may exist that modify the specificity of the *sd* transcription factor. Further, any possible DNA binding activity of *vg* and *sd* protein either alone or combined needs to be characterized further to establish the sequence motifs that are bound by sd and sd-vg. The area of the *ct*-enhancer that shows highest affinity for *sd* has no similarity to the sequence bound by the *sd* homologue hTEF-1 in human cells (Morcillo et al., 1996). Therefore, it is possible that the interaction of proteins like *vg* with *sd* can alter its DNA binding specificity, or alternatively without the activity of a possible co-factor like *vg*, *sd* non-specifically binds to DNA. It has been shown that *sd* homologues from yeast (TEC-1) bind indiscriminately to DNA without the presence of cellular co-factors that are not yet identified (Laloux et al., 1990). Further characterization of the vg-sd interaction *in vivo* is required to determine if there is any biological significance associated with the *in vitro* interaction described in Chapter IV. The observation of a *vg* and *sd* protein interaction within a eukaryotic cell environment could be easily examined with a yeast two-hybrid system (Fields and Song, 1989). Further characterization is also required to establish the specific domains of both *vg* and *sd* that are involved in mediating the protein-protein interaction. This would be followed by the creation of transgenic flies containing deleted *vg* and *sd* constructs that can be selectively expressed within the imaginal disc tissues to determine the ability of each to specify wing development. By removing the binding of *vg* and *sd,* it becomes possible to determine what functions of each protein require interaction with the other.

Is activity of the *vg* protein and its function in patterning the wing imaginal disc unique to the recent evolutionary development of wings by insects? Alternatively, are there similar proteins that play specific roles in the development of the remaining imaginal discs? The *dachshund* (*dac*) gene encodes a novel nuclear protein that is required for development of the eye and leg imaginal discs (Mardon et al., 1994). Like *vg,* the expression of *dac* appears to be tightly controlled during larval development, and within the leg disc, high levels of *dac* expression are found limited to the areas fated to form the femur, tibia and proximal tarsal segments. Correspondingly, flies that are homozygous for *dac* null mutations are missing these structures, although the remainders of the tissues formed by the leg imaginal disc are formed normally. During eye development, *dac* appears to be required for normal photoreceptor development and reduction of *dac* expression leads to a loss of these structures. Additionally, lack of *dac* expression can be correlated to greatly increased amounts of cell death observed in the late third instar leg and eye imaginal discs (Mardon et al., 1994). Thus, similar to *vg, dac* represents a gene required to promote specific structures via limited expression within the developing larval imaginal discs. Whether *dac* represents another member of a family of nuclear proteins that act via protein-protein interactions with transcription factors like *sd,* or is merely a gene with a similar phenotype to *vg* but acting via a unique mechanism remains untested. The examination of genes other than *sd* whose products bind to *vg* via protein-protein interactions could provide evidence for a multi-protein complex controlling expression of genes required to form the specific structures of the wing.

Chapter VI - Materials and Methods

Origin and Maintenance of Drosophila stocks

All Drosophila stocks were raised at 25°C and maintained upon synthetic agar media, (Nash and Bell, 1968). The origins of the various alleles are listed in Table VI-1. Reversion analysis of the vg^W and vg^U alleles was performed by subjecting heterozygous male flies to 400 Gy of γ radiation from a Cobalt 60 source. Single irradiated males were then mated to virgin females of the respective dominant allele stock (Figure VI-1). Any resulting progeny flies that exhibited larger wings than those possessed by the progenitor vg^W or vg^U stock were retained and made into balanced isogenic lines. Those lines that consistently exhibited a wing size larger than that associated with vg^W or vg^U were retained for further analysis.

Immunohistochemistry

Imaginal discs

Third instar larvae for imaginal disc preparations were grown in uncrowded conditions to ensure optimal growth and the largest disc size (Ashburner, 1989). To ensure growth conditions that precluded crowding, flies were transferred to bottles containing fresh media and allowed to lay eggs for only one to two hours. Bottles were cultured at 25°C for 100-110 hours and late wandering third instar larvae were collected from sides of the bottle and dissected in phosphate buffered saline (PBS). To expose the imaginal discs the head and first third of the larvae were grasped in forceps and separated from the remainder of the body. The interior of the head tissue was then inverted leaving

Figure VI-1 Mutagenesis of vg^W and vg^U to obtain revertant alleles

Flies were subjected to 400 Gy γ radiation and mated as shown. Progeny that exhibited wings larger than the progenitor vg^W or vg^U stock were crossed to females from the original dominant stock and retained for further analysis.

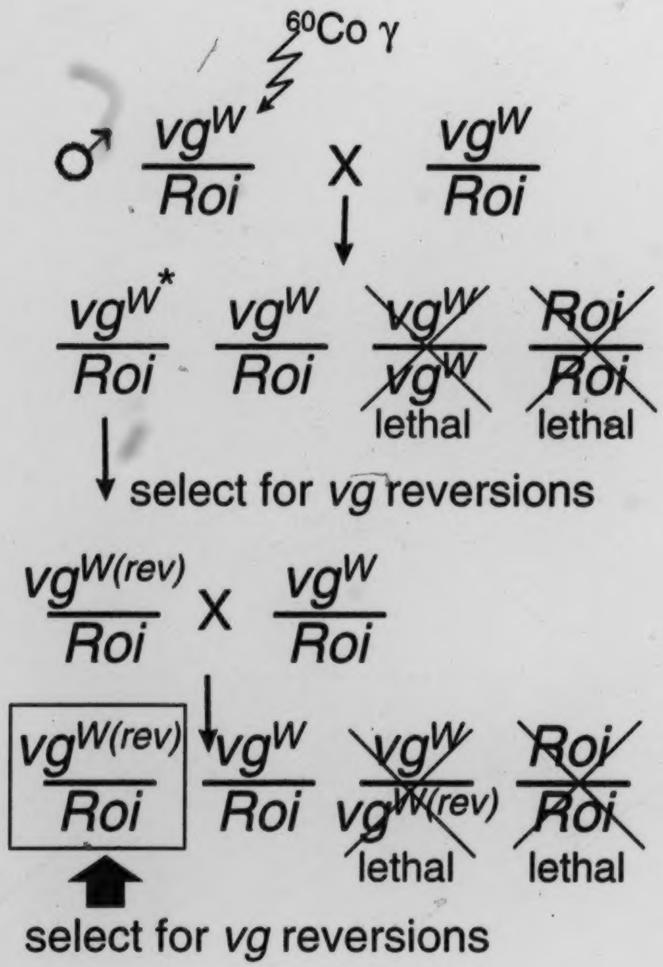
60Co γ
♂ vgW/Roi X vgW/Roi
vgW*/Roi vgW/Roi vgW/vgW lethal Roi/Roi lethal
select for vg reversions
vgW(rev)/Roi X vgW/Roi
vgW(rev)/Roi vgW/Roi vgW/vgW(rev) lethal Roi/Roi lethal
select for vg reversions

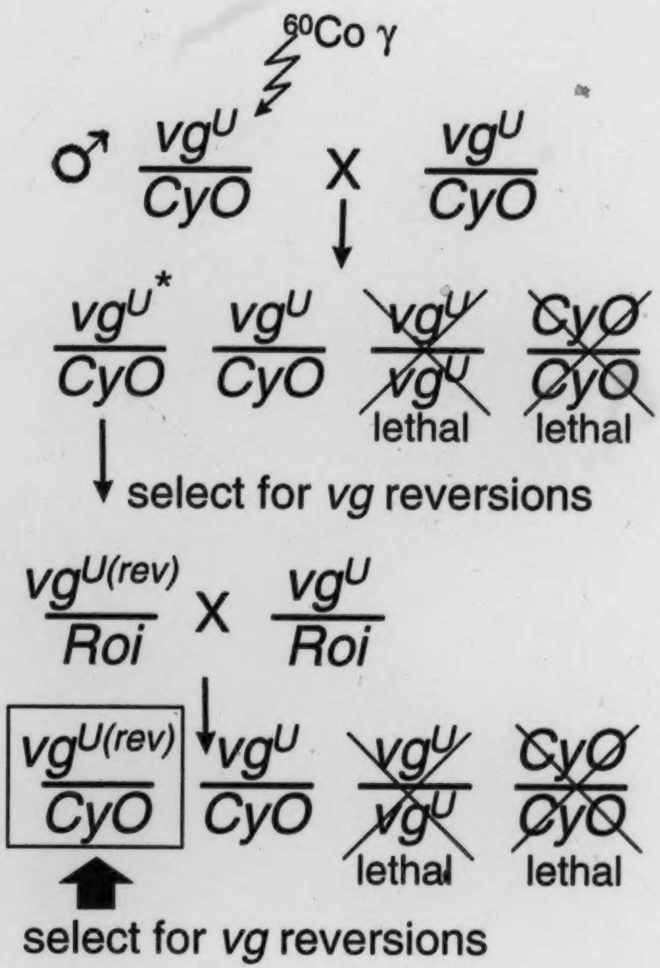
60Co γ
♂ vgU/CyO X vgU/CyO
vgU*/CyO vgU/CyO vgU/vgU lethal CyO/CyO lethal
select for vg reversions
vgU(rev)/Roi X vgU/Roi
vgU(rev)/CyO vgU/CyO vgU/vgU lethal CyO/CyO lethal
select for vg reversions

Table VI-1 Genotypes of stocks used in this study.

Stock genotype	Source
Df(2R)$vg^{Wingless}$/*CyO; *vg^{W}/*CyO*	(Shukla, 1980)
Df(2R)$vg^{Ultravestigial}$/*CyO; *vg^{U}/*CyO*	(Ives, 1956)
Df(2R) vg^{B} / CyO	Mid America Stock Centre
vg^{83b27}	(Alexandrov and Alexandrova, 1988)
vg^{83b27R}	(Williams et al., 1990a)
vg^{WR1}	(Williams et al., 1990b)
vg^{1}	Bloomington Stock Centre
ap-lacZ	(Cohen et al., 1992).
ryXho25 (en-lacZ)/CyO	(Hama et al., 1990)
hh-lacZ/*TM3 Sb*	(Lee et al., 1992)
dpp-lacZ/*TM2 Ubx*; *cn*/*cn*	(Blackman et al., 1991)
wg-lacZ/CyO	(Kassis et al., 1992)
ptc-lacZ	Philip Ingham
ci-lacZ	(Eaton and Kornberg, 1990)
sd-lacZ	(Campbell et al., 1992)
vg intron-2 lacZ/*Bc Gla*	(Williams et al., 1994)
vg intron-4 lacZ/ *Bc Gla*	(Kim et al., 1996)
cn^{1} $E(Pc)^{1}$$bw^{1}$/*SM5*	Bloomington Stock Centre
ph	(DeCamillis et al., 1992)
en^{E}/CyO	(Tabata et al., 1995)
inv^{30}/*CyO*	(Tabata et al., 1995)
en^{SFX31}	(Kornberg, 1981b)
en^{1}	(Eker, 1929)
$en^{28\text{-}11\text{-}1}$	Mike Russell
en^{2}	(Kornberg, 1981b)
en^{57}	(Nüsslein-Volhard and Wieschaus, 1980)
$en^{LA\text{-}I0}$	(Kornberg, 1981b)

the imaginal discs attached to the body wall but exposed for further treatment. The total time between dissection and fixation was kept to less than thirty minutes to ensure that minimal tissue degradation occurred. Following dissection, the tissue to be stained was immediately placed in 140µl PBS on ice. Each tube contained between eight and ten larval heads. Fixation of the imaginal discs was performed by a modified procedure derived from Pattatucci and Kaufman . The discs were first fixed quickly by the addition of 60µl of freshly made ten percent paraformaldehyde solution in PBS and 250 µl heptane to each tube and then shaken vigorously for 45 seconds. This initial fixation solution was then drawn off using a drawn out pasteur pipette and replaced with a second fixation solution containing 260µl PBS, 120µl 10% paraformaldehyde and 20 µl dimethyl-sulfoxide (DMSO). DMSO used for disc fixation was taken from a fresh bottle, aliquotted into 500µl tubes and stored at -70°C. The tubes containing the larval heads in fixation solution were then placed on a gently rocking platform shaker for 20 minutes at room temperature. In cases where a secondary antibody conjugated to horse radish peroxidase (HRP) was going to be used, the fixed tissue was then rinsed quickly in 500µl methanol twice and then incubated in 500µl methanol containing 0.2% hydrogen peroxide on a rocking platform shaker for 30 minutes to quench endogenous peroxidase activity.

The tissue was then washed in PBN-B solution (1xPBS, 0.5% NP-40, 0.1% BSA) for ten minutes to remove the remaining fixation or quenching solution. This step was repeated three additional times using fresh PBN-B wash each time for a total of 40 minutes of washing time. Immediately following the final wash in PBN-B, the tissues were incubated 90 minutes on a rocking platform in 200 µl blocking solution (1xPBS, 0.5% NP40, 0.1%BSA, 0.5% Carnation non-fat skim milk powder and 0.1% normal goat serum), at 4°C. Longer blocking steps are possible and sometimes proved advantageous with antibodies that produce high background staining. An appropriate dilution of primary antibody was then added directly to the blocking solution. The tubes containing the tissues were then left on a rocking platform overnight (12 or more hours) at four°C. To determine the optimal concentration of primary antibody to use in each case, test staining was performed using a series of ten-fold dilutions from 10^{-1} to 10^{-5} on wild type larval imaginal discs. The source, concentration, working dilution and reference for each antibody used in this study is listed in Table VI-2. When two or more primary antibodies were used concurrently, antibodies from different hosts were employed to minimize cross-reactivity with the secondary antibody.

Following overnight incubation in primary antibody, the larval tissue containing the imaginal discs was washed in PBN-B solution for five minutes at room temperature. Four more washes in PBN-B of 10, 15, 20 and 25 minutes were then performed each time removing the majority of the previous PBN-B solution. The blocking solution containing the primary antibody can be recovered and reused up to three additional times. At this point 200 µl of fresh blocking solution was added to the tubes containing the tissues, which were then incubated for 45-60 minutes at 4°C. An appropriate secondary antibody was then added directly to the blocking solution at a dilution suggested by the manufacturer (Table VI-2). If a specific primary/directly conjugated-secondary antibody combination was found to give a weak signal, a two step secondary antibody detection method would be employed. Significant amplification of a weak primary antibody signal could be realized by the use of a biotinylated secondary antibody followed by incubation with a streptavidin conjugated detection reagent. This occurs through the binding of multiple conjugated streptavidin molecules to each biotinylated secondary antibody. However, if both directly conjugated and biotinylated secondary antibodies were needed for double staining then only the biotinylated secondary antibodies were added at this step and incubated at four°C for 90 minutes. The biotinylated secondary antibody solution was then removed and the tissue washed four times for ten minutes in PBN-B. Following incubation with primary antibody (or biotinylated secondary antibodies) and subsequent washing, 200µl of blocking solution containing appropriate dilutions of alkaline phosphatase (AP), horse radish Peroxidase (HRP) or fluorescent label directly conjugated to either a secondary antibody or to streptavidin was added and the tubes were then incubated at 4°C for 90 minutes. For fluorescent labels, all subsequent steps were performed in subdued light to prevent bleaching of the fluorescent signal. Following the incubation the larval tissue was washed twice for ten minutes in PBN-B followed by three washes in PBN (1xPBS, 0.5% NP-40). Following this final wash, AP labeled secondary antibodies were detected by the addition of 250µl of a stable nitro-blue tetrazolium chloride (NBT) / 5' bromo-4chloro-3indoylphosphate p-toluidine salt (BCIP) to the larval tissue in a 24 well tissue culture dish. The resulting blue product was monitored periodically until the desired intensity of staining was obtained. At this point, the reaction was stopped by quickly rinsing the tissue five times in 1xPBS. High levels of AP background staining could be suppressed by the addition of 0.8 mg/ml levamisole to the NBT/BCIP staining solution to suppress endogenous phosphatase activity. HRP conjugated secondary antibodies were detected as above but a solution consisting of 270µl PBS 30µl 10x diamino-benzine (DAB) and 1µl of a 0.3% hydrogen peroxide solution was used instead of NBT/BCIP. Background activity associated with the HRP enzyme was quenched with hydrogen peroxide during the fixation step as described above. The imaginal discs of interest were then dissected from the larval body wall and mounted on microscope slides in a mounting solution consisting of 70% glycerol, 1xPBS. To slow the fading of fluorescent labels, 0.02% DABCO was added to the mounting solution. AP or DAB stained imaginal discs were observed on a Zeiss Axioskop compound microscope under normal lighting and photographed using either Kodak Ektar 25ASA colour print film, Elite 100 ASA colour slide film or Technical Pan film using Nomarski optics. Single fluorescent labels were similarly observed using appropriate filters and a high energy UV lamp. Parallel detection of two or more fluorescent labels was simultaneously performed using a Molecular Dynamics Multiprobe 2000i laser scanning confocal microscope. Signals corresponding to each fluorescent label were combined using the attached Silicon Graphics Iris Indigo UNIX workstation and Molecular Dynamics Imageworks software. The resulting images were printed onto Kodak Elite 100ASA slide film or exported via TIFF compressed image files and further processed using a Pentium-PC workstation (Microsoft Windows95) and Adobe PhotoShop v3.05 software. For dual colour images a separate TIFF image corresponding to each signal was exported separately and overlaid using the PhotoShop layer function.

Embryos

Embryos were collected on apple juice agar plates covered in a paste of fresh yeast. The embryos were collected and dechorionated by immersion in 50% sodium hypochlorite solution. The embryonic vitelline membrane was removed by placing the embryos into a glass scintillation vial containing 50% methanol and heptane and shaking vigorously. The embryos were subsequently washed four times in 1xPBS and fixed in glass scintillation vials containing 2ml of 12% paraformaldehyde in 1xPBS and 2ml of heptane. The fixed embryos were then removed from the vial and washed 4 times in 1xPBS and stored in

Table VI-2 Antibodies and conjugates used for immunohistochemical studies

Antibody	Concentration	Dilution	Source
Primary Antibodies			
rabbit anti-*vestigial*	5µg/µl	1/200	(Williams et al., 1991)
rabbit anti-*vestigial* region 1	7.2µg/µl	1/50	(Williams et al., 1991)
rabbit anti-*vestigial* region 2	8.1µg/µl	1/50	(Williams et al., 1991)
mouse anti-*engrailed* 4D9	unknown	1/100	Pat O'Farrell
mouse anti-*engrailed* (affinity purified)	50µg/µl	1/500	Tom Kornberg
rat anti-*apterous*	unknown	1/500	Sean Carroll
rabbit anti-*cubitus-interruptus*	100µg/µl	1/10^{-4}	Tom Kornberg
mouse anti-β-*galactosidase*	100µg/µl	1/10^{-4}	Promega
rabbit anti-β-*galactosidase*	100µg/µl	1/4x10^{-5}	Vector Systems
rabbit anti-*actin*	0.5µg/µl	1/100	Sigma
Secondary Antibodies			
Biotin labeled anti-mouse	0.5µg/µl	1/100	KPL
Biotin labeled anti-rabbit	1µg/µl	1/250	GIBCO BRL
Streptavidin-FITC	0.768µg/µl	1/1000	GIBCO-BRL
Streptavidin-HRP	0.607µg/µl	1/1000	GIBCO-BRL
Streptavidin-TR	0.5µg/µl	1/1000	GIBCO-BRL
Anti-rabbit-HRP	0.5µg/µl	1/1000	KPL
Anti-mouse-TR	1µg/µl	1/1000	Caltag Laboratories
Anti-mouse-Cy3	1µg/µl	1/10^{-4}	Jackson Immunological
Anti-rabbit-Texas Red	1µg/µl	1/10^{-4}	Jackson Immunological
Anti-rabbit-FITC	0.5µg/µl	1/500	KPL

95% ethanol at -20°C. The ethanol was then removed and the embryos were re-hydrated by washing 4 times in 1xPBS for ten minutes each time. The conditions for incubation with the primary and secondary antibodies, mounting and visualization were identical to those used for imaginal disc staining except that the mounting media for embryos contains 90% glycerol.

Southern Hybridizations

DNA from adult flies was isolated using a method outlined in Roberts (1986) with the modifications as outlined below. Approximately 50-100 adult flies of the appropriate genotype were collected, frozen in liquid nitrogen and stored at -70°C. Each sample of flies was then homogenized in a 15ml ground glass tissue grinder containing 2ml of chilled HM buffer (100mM Tris pH 8.0, 80mM EDTA and 160mM sucrose). The homogenate was then transferred to a 15ml polypropylene conical centrifuge tube. To ensure maximal recovery of the homogenate, the pestle was rinsed with 1ml of additional HM buffer and this was combined with the solution in the 15ml tube. 750µl of 10% SDS and 25µl of a 20mg/ml proteinase K solution was added to each tube and this solution was then incubated for 2 hours at 65°C to lyse the cells and release the DNA. The solution containing the lysed cells was then cooled to room temperature and the proteins were extracted twice with an equal volume of a 1:1 mixture of phenol and chloroform/iso-amyl alcohol (49:1) and once with chloroform, iso-amyl alcohol (49:1). After protein extraction, 450µl of an 8M potassium acetate solution was added to each sample and mixed gently. The tubes were then incubated 30 minutes on ice and centrifuged 20 minutes at 10 000 rpm at 4°C. The resulting supernatant was then transferred to a fresh 15ml COREX glass centrifuge tube and the genomic DNA was precipitated by the addition of an equal volume of absolute ethanol. The samples were then centrifuged as above and washed twice in 70% ethanol ensuring that no ethanol was left in the tube after the last wash. The tubes were dried no more than 10 minutes in air to let the residual ethanol evaporate and the pellet was then resuspended in 400µl TE (pH 8.0). This solution was then transferred to a 1.5ml microcentrifuge tube containing 10µl of a 10mg/ml DNase free RNase A solution and then incubated 30 minutes at 37°C. Following RNase treatment, the DNA was phenol:chloroform extracted and precipitated in absolute ethanol as above. The genomic DNA was recovered from the ethanol by pipetting in a minimal volume and transferring it to a fresh microcentrifuge tube containing 70% ethanol. The DNA was then centrifuged at 12 000 *g* for five minutes and the ethanol was removed and the pellet dried for one hour at room temperature. This genomic DNA was then resuspended in 100µl TE at 65°C. Equal aliquots of genomic DNA were cut with relevant restriction enzymes, separated on a 0.8% agarose gel and blotted to Genescreen plus nylon membrane (NEN) as per the manufacturers directions. Probes that selectively hybridized to either *inv*, *mam* or *vg* sequences were labeled with α^{32}P dATP using random primers and DNA Polymerase I (Klenow Fragment). The *vg* probe was isolated from the first third and fourth *vg* exons, the *inv*-specific probe corresponds to the first exon of *inv*, (Coleman et al., 1987) and the *mam* probe was obtained from a 2 kb *Eco*RI/*Bam*HI clone that represents the region designated -16 to -14 on the *mam* restriction map (Smoller et al., 1990; Yedvobnick et al., 1988). Hybridization of the probes to the blots and subsequent washing was performed as per the Genescreen plus manual (NEN).

PCR analysis of genomic DNA

To map specific alterations within the *vg* portion of the reverted alleles more precisely, PCR primers were created to allow selective isolation of specific portions of the *vg* coding region. Primers were chosen in such a manner that only sequences from the dominant revertant allele would be amplified when heterozygous to a series of *vg* deficiencies: vg^{83b27}, vg^{nw} and vg^{B} (Lindsley and Zimm, 1992). A positive control reaction, containing DNA from wild type or known deficiencies was performed in each case. Each primer was 20 bp in length, with an approximate annealing temperature of 65ºC (Table VI-3). The resulting PCR products were separated on 0.8% agarose gels and compared to the bands from known samples and DNA size markers. Bands that were found to be of different sizes than those produced by the known samples were excised, and further analyzed by restriction enzyme digestion and DNA sequencing.

Western blot analysis

Western blot analysis of *vg* protein was performed using a modified method of Fessler et al. (1993). 500 µg of tissue isolated from staged animals was homogenized directly in sodium dodecyl sulphate (SDS) buffer containing 0.5% dithiothreitol, 0.1M sodium chloride, 1 mM aprotinin and 100 mM phenylmethylsulfonyl fluoride. 2x bromophenol blue running dye was added to aliquots containing a constant amount of protein of each of the samples. These were then boiled for 5 minutes and loaded onto a 8% SDS polyacrylamide gel. Proteins were blotted to supported nitrocellulose membranes and detected using *vg* primary antibody and an anti-rabbit horseradish peroxidase conjugated secondary antibody (1/2000), and a chemiluminescent substrate (KPL). The intensity of the band stained with *vg* protein in each lane was calculated using a

Table VI-3 Primers used for analysis of revertant alleles

Primer name	Sequence 5'→ 3'	Melting temperature (Tm)
JTS3	AAGAATCTGCCAGCACTGGA	68.4°C
JTS4	GGGTGCACGTAATTGCTGTT	68.2°C
JTS5	CCCGCTCAAGTGACAATACC	68.2°C
JTS6	GCCCGAGGAGGAGTACAAAT	68.8°C
JTS7	GCCCCGAAGTTATGTACGGT	68.0°C
JTS8	GTCTCCAGTGCTGGCAGATT	68.4°C
JTS9	AAATTTCCCACCGTCGTTCT	68.4°C
JTS10	TTGGGTTTTCTGCTTTGCTT	68.2°C

GS-670 imaging densitometer (Bio-Rad). The relative amount of total protein loaded in each lane was measured by comparison to the levels of actin protein as detected by an actin antibody (Sigma).

RT-PCR detection of *vg* transcripts

RT-PCR was performed using the method of Huet et al. (1993) employing the JTS4 and JTS5 primers. Primers were chosen such that they are on opposing sides of a large intron to preclude the amplification of any contaminating genomic sequence. PCR using these primers produces a 1.6kb fragment from reverse-transcribed wild type *vg* mRNA. The dominant vg^{U} and vg^{W} alleles were made heterozygous to the *vg* expression null allele vg^{83b27R} to ensure that if any *vg* transcripts were made they would be representative of those produced by the vg^{W} or vg^{U} chromosomes. The head portion, containing the wing and haltere imaginal discs, was removed from larvae of the required genotype and stored at -70°C until sufficient tissue had been collected. When ten larval heads of each genotype were collected the RNA was isolated and 5-10µl of the reverse-transcribed RNA sample was used per PCR reaction. A negative control containing no DNA and positive control containing the *vg* cDNA-3 plasmid (Williams et al., 1990a) were also included. Products were separated in 1.2% agarose gels and stained with ethidium bromide.

Acridine orange staining of imaginal discs

To examine cell death within imaginal discs, embryos were collected from freshly yeasted agar plates over a period of one hour and then maintained at 25°C for 60 to 80 hours. Exact staging of individual larvae was accomplished by examination of anterior spiracles and mouthparts (Ashburner, 1989). The larvae were subsequently dissected in insect Ringer's and stained with 0.5 mg/ml acridine orange in insect Ringer's as described in Massucci et al. (1990). The tissue was washed twice in insect Ringer's and mounted in 70% glycerol/insect ringers. Whenever possible, the discs were dissected away from the larval body wall. Photography of the stained discs was as described above except that spot metering was used to ensure proper exposure times.

β-galactosidase staining of imaginal discs

β-galactosidase activity produced by *lacZ* reporter constructs was assayed using a procedure modified from Ashburner (1989). X-gal staining solution (5 mM $K_3Fe^{2+}(CN)_6$, 5 mM $K_4Fe^{3+}(CN)_6$, 1x PBS, 0.3% Triton X-100) was prepared ahead of time and pre-warmed at 37°C for five minutes. Following this, 25 μl of an 8% X-gal dissolved in DMSO stock solution was added per ml of X-gal staining solution. This solution was left at 37°C for at least 30 minutes and centrifuged for five minutes at 14 000*g* immediately before use. Imaginal discs were dissected in 1xPBS and fixed for 20 minutes in a solution containing four percent paraformaldehyde in 1xPBS. The fixed tissue was washed twice in PBT for five minutes. After washing, 1ml of staining solution was added to each sample and incubated at 37°C for several hours or overnight. The intensity of the X-gal staining was monitored periodically and stopped when staining was judged to be of optimal intensity.

Mounting adult tissues

Adult wings were photographed following dissection from newly emerged adult females. Individual wings were directly mounted in Gary's Magic Mountant (Ashburner, 1989) and left for 12 hours to allow the associated non-cuticular tissue to dissolve. Wings were photographed using a Zeiss Axioskop compound microscope and Kodak Technical Pan film.

Preparation of specific anti-sense RNA probes and whole mount *in-situ* hybridization to imaginal discs

Due to the increased stability of RNA:RNA hybrids over that of DNA:RNA hybrids, specific portions of the *vg* and *inv* cDNAs were re-cloned into pBluescriptSK+ to facilitate the production of *in vitro* transcribed RNA probes. The vector pBluescriptSK+ was chosen as it allows for transcription in either direction using the T7 and T3 viral promoters at either end of the multiple cloning site. The *vg* cDNA-1 (Williams et al., 1990a) containing the majority of the *vg* ORF was excised from the original plasmid using *Bam*HI and cloned into the *Bam*HI site of pBluescriptSK+. Orientation of the inserted *vg* cDNA was determined by restriction enzyme digestion and a single clone was isolated that placed the start site of the *vg* cDNA downstream from the T3 promoter. Thus, anti-sense RNA could be in vitro transcribed from the T7 promoter at the 3' end of *vg* (Figure VI-2). To produce specific probes from *inv* the region of the *inv* cDNA that is not homologous to *en* was cloned into pBluescriptSK+. From previously published results (Coleman et al., 1987) and Southern hybridization to both the *en* and *inv* total cDNA clones, it was determined that the 5' 988bp *Eco*RI-*Bst*XI fragment of *inv* would selectively hybridize to *inv* and not *en* sequences. To introduce this fragment into pBluescriptSK+, an *Eco*RI fragment representing the entire *inv* cDNA was first cloned into the vector. The vector was then digested with *Eco*RV and *Bst*XI and the resulting 3' overhang at the *Bst*XI site was removed using the 3' to 5' exonuclease activity associated with T4 DNA polymerase. Ligation of this fragment produced a plasmid containing the *inv*-specific region in the anti-sense orientation from the T7 promoter (Figure VI-3)

Figure VI-2 *vg* cDNA-1 in pBluescriptSK+ for making full-length anti-sense *vg* RNA probes.

An anti-sense RNA probe that will detect *vg* transcripts can be made by cutting this vector with *Bam*HI and performing *in vitro* transcription using T7 RNA polymerase.

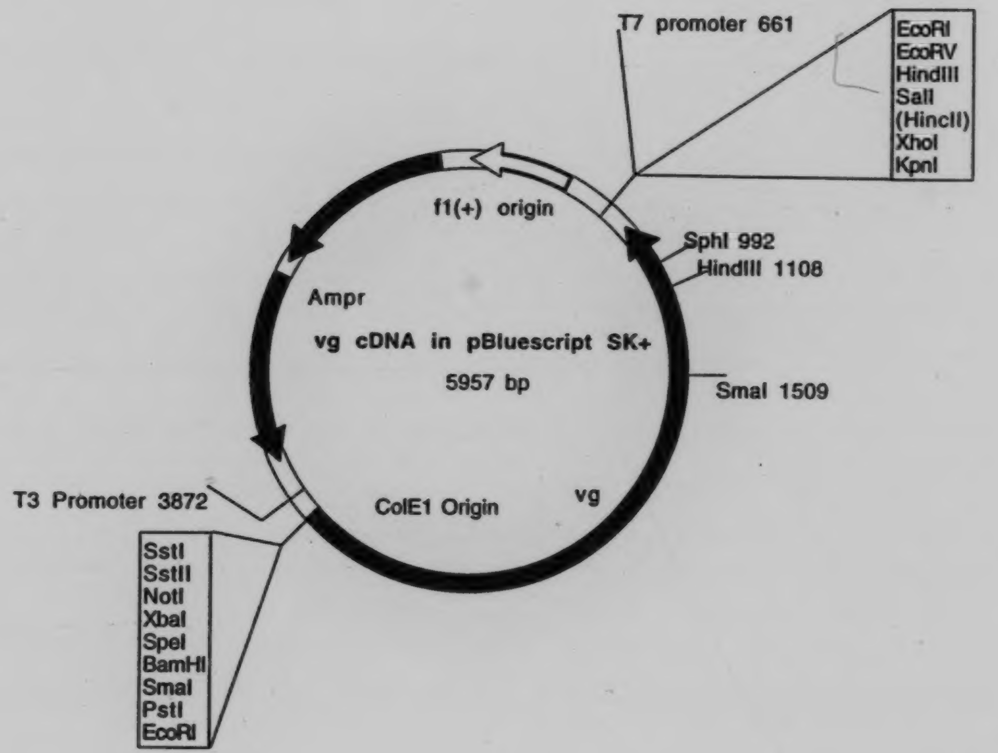
T7 promoter 661
EcoRI
EcoRV
HindIII
SalI
(HincII)
XhoI
KpnI
f1(+) origin
SphI 992
HindIII 1108
Ampr
vg cDNA in pBluescript SK+
5957 bp
SmaI 1509
T3 Promoter 3872
ColE1 Origin
vg
SstI
SstII
NotI
XbaI
SpeI
BamHI
SmaI
PstI
EcoRI

Figure VI-3 A plasmid for making *inv* RNA anti-sense probes that will recognize *inv* but not *en* transcripts *in-situ.*

The portion of *inv* sequence in this plasmid corresponds to the 5' 988bp *Eco*RI - *Bst*XI fragment of the *inv* cDNA (Poole et al, 1985).

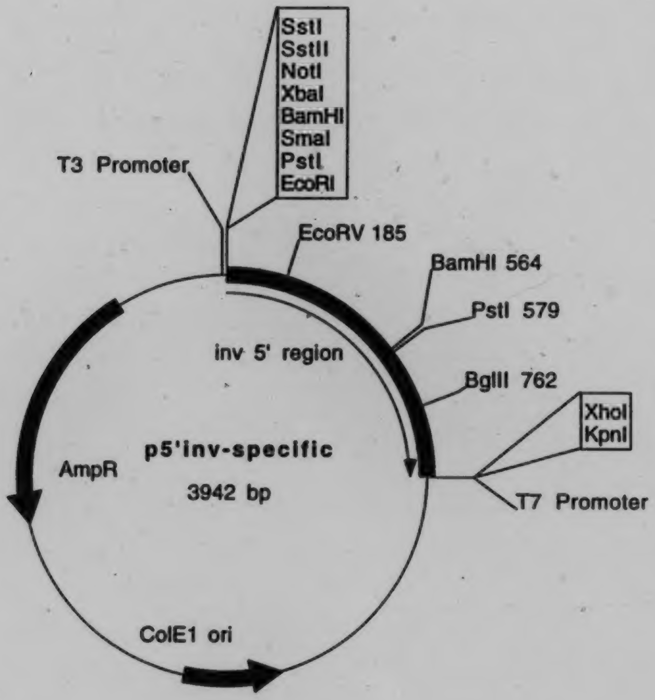
SstI
SstII
NotI
XbaI
BamHI
SmaI
PstI
EcoRI
T3 Promoter
EcoRV 185
BamHI 564
PstI 579
BglII 762
XhoI
KpnI
T7 Promoter
inv 5' region
p5'inv-specific
3942 bp
AmpR
ColE1 ori

The *in vitro* labeling procedure was adapted from that provided by the manufacturer of the DIG-11-dUTP (Boehringer Mannheim). To make DIG labeled RNA probes, 1µg of linearized plasmid was added to 2µl DIG NTP labeling mixture, 4µl 5x T7/T3 RNA polymerase reaction buffer, 1µl human placental RNase inhibitor (BRL) and 1µl T7 RNA polymerase (50U/µl) in a final volume of 20µl. This reaction was incubated at 37°C for 2 hours and subsequently stopped by the addition of 0.8µl of 500mM EDTA. The RNA probe was selectively precipitated from the DNA template by the addition of 5µl 4M LiCl and 75µl absolute ethanol and frozen at -70°C for 90 minutes. The RNA was pelleted by centrifugation at 14 000*g*, dried and resuspended in 100µl of RNase free water at 37°C for 1 hour.

Fixation and hybridization of the imaginal discs to the labeled probes was performed using an extensively modified procedure derived from that initially described by Massucci et al. (1990). All manipulations were performed in 0.7ml polypropylene microcentrifuge tubes. Dissection and initial fixation was identical to that employed for antibody staining of imaginal discs. However, after the second fixation in 4% paraformaldehyde + PBT, the dissected tissue was rinsed three times in PBT and then dehydrated by rinsing in 30% ethanol followed by sequential five minute washes in 30%, 50%, and 70% ethanol. At this stage, the dehydrated tissue samples could be stored at -20°C immersed in 70% ethanol for up to three months. The tissues were re-hydrated by a reverse series of five minute ethanol washes and then washed in PBT for fifteen minutes changing the PBT every five minutes. The tissues were then incubated approximately 45 seconds in a 50µg/ml solution of undigested Proteinase K (BRL) dissolved in PBT, which partially degrades the cellular proteins allowing greater access to the RNA probe The exact duration for Proteinase K digestion was determined empirically by testing the staining activity resulting from a range of incubation times. Most batches of Proteinase K required 45 seconds of digestion to allow optimal probe penetration without greatly affecting tissue morphology. The reaction was stopped by the removing the majority of the Proteinase K /PBT solution and immediately rinsing the tissue in PBT+2mg/ml glycine, followed by a 5 minute wash in PBT+2mg/ml glycine. At this point a further fixation in 10% paraformaldehyde in PBS + 0.2% glutaraldehyde was found to assist in preserving overall tissue integrity during the remaining hybridization steps.

Immediately following fixation the tissues were washed for a total time of 25 minutes, five times for five minutes in PBT. The tissue is then incubated in a solution containing 50% PBT and 50% hybridization buffer (50% formamide, 5x SSC, 100μg/ml sonicated denatured salmon sperm DNA, 200μg/ml yeast tRNA, 0.1% Tween-20, 50μg/ml heparin) for ten minutes followed by incubation for a further ten minutes in hybridization buffer at room temperature. Pre-hybridization was performed by the adding of fresh 500μl of hybridization buffer to each tube which were then placed on their side in a rotating hybridization chamber (Tyler Instruments) set at the slowest speed at 45°C for greater than one hour. In some cases, longer pre-hybridization times improved subsequent hybridization depending on the specific probe being used. After pre-hybridization, the majority of the buffer replaced with 100μl of fresh hybridization buffer, 2μl additional sonicated denatured salmon sperm DNA and approximately 2μl of either RNA or single stranded DNA probe labeled with digoxigenin-dUTP (DIG) giving a final probe concentration of 0.5ng/μl. The tubes containing the tissue were then returned to the incubator for 24-36 hours at either 58°C for RNA probes or 45°C for DNA probes. Following hybridization, the tissue was quickly rinsed three times with 500μl of pre-warmed hybridization buffer to remove the unbound probe. The tissues were then washed in 60% hybridization buffer/40% PBT for ten minutes at the hybridization temperature. This was followed immediately by a second wash in 40% hybridization buffer/60% PBT at the same temperature. Finally, the tubes containing the larval tissue were removed from the incubator and washed for a total of 40 minutes in 500µl PBT, adding fresh PBT approximately every ten minutes. The DIG labeled probe was detected by the addition of AP-conjugated anti-DIG antibody at a concentration of 1:2000 in PBT. A sharp reduction in non-specific background staining was realized if the anti-digoxigenin antibody was pre-absorbed against fixed but not-hybridized larval tissues for an hour at 4°C before use. After incubation with anti-DIG antibody, the tissues were washed four times ten minutes in 500µl PBT. Following washing, the tissue was incubated in a stable NBT/BCIP substrate mixture (BRL) and the reaction was monitored until the signal intensity was of optimal intensity. Depending upon the probes used and the abundance of the transcript being detected, the total staining times to produce the desired signal strength ranged from ten minutes to 12 hours. At this point the AP-NBT/BCIP reaction was stopped by quickly washing the tissue in PBT for five minutes for three or more times. To remove unbound coloured precipitate, the tissue was washed in 95% ethanol for five minutes and then 5 minutes in PBT. Imaginal discs of interest were removed from the larval carcass and mounted in 80% glycerol/PBS solution on Superfrost charged microscope slides. The discs were covered with a coverslip and photographed with Nomarski optics on a Zeiss Axioskop compound microscope using either Kodak Ektar 25 colour print film or Kodak Technical Pan black and white print film.

Cloning of the *vg* and *sd* ORF into the pET 16b bacterial expression vector

Segments containing the ORF of the *sd* and *vg* genes were cloned by selective amplification with PCR. For each gene, primers were designed such that they placed the respective ORF in frame with *Bam*HI sites at both the 5' and

3' ends. PCR was performed with a *Taq:Pfu* polymerase mixture (20:1) to avoid the high level of incorporation errors associated with lack of 3' exonuclease activity that is seen when *Taq* polymerase is used alone. PCR was performed in a Robocycler (Stratagene) or a Perkin Elmer GeneAmp 2400 thermal cycler using the following reaction conditions: 1 x 95°C (5 minutes), (add Taq), 10 x [95°C (35 seconds), 68-58°C (35 seconds) decreasing temperature by 1°C each cycle, 65°C (60 seconds per kb of target)], 5 x [5°C (35 seconds), 60°C (35 seconds), 65°C (60 seconds per kb of target)], 15 x [5°C (35 seconds), 55°C (35 seconds), 65°C (60 seconds per kb of target)]. The sequence of each of the primers designed for the *vg* and *sd* fragments is listed in Table VI-4.

Suitable restriction enzyme buffer was then added to one half of each sample followed by 40 units of *Bam*HI. The samples were incubated at 37°C for two hours. Excess enzyme and digestion times were necessary as the restriction enzyme sites are close to the ends of the DNA segment. The digested PCR fragment was ligated into the *Bam*HI site within pBluescriptSK- (Stratagene) or pET16b (Novagen). Simultaneously, a sample of undigested fragment was cloned into the *Eco*RV site of pBluescriptSK- using conditions that favoured blunt end ligation. Both approaches were found to be necessary as occasionally poor digestion of the *Bam*HI sites of the PCR derived fragment made cloning into the non-selectable pET16b plasmid difficult. If this occurred, The *Bam*HI fragment representing the ORF could be recovered from pBluescriptSK- and then easily cloned into pET16b (Figure VI-4 VI-5).

To generate deletions within *vg*, primers were designed facing outward from the segment to be deleted. Specific *Spe*I sites were engineered into each primer to allow for re-ligation in such a manner as to preserve the reading frame. *Spe*I was chosen as there is no endogenous site for this restriction enzyme within *vg*. PCR was then performed as above, amplifying both the remainder of the *vg* ORF and the pET16b plasmid as well. The PCR product was digested with *Spe*I, run out on a 1% agarose gel, purified, and 200ng of the resulting DNA was circularized by overnight incubation with T4 DNA ligase. The ligation mixture was then transformed into XL-Blue *E. coli* cells and plated onto LB-ampicillin plates. Multiple colonies were selected in case a specific product contained a cloning induced mutation within the *vg* ORF or critical sequences of the pET16b plasmid. During cloning of *vg*, a total of 16 colonies were tested and none contained mutations disrupting the *vg* ORF or pET16b sequences that could be detected by restriction enzyme digestion. To confirm there were no mutations within *vg* coding region, two separate *vg*/pET16b constructs were sequenced. The complete sequence of both *vg* ORFs was identical and also matched the published sequence of *vg* (Williams et al., 1991)

Preparation of plasmid DNA

Following ligation of the plasmids constructed above, mini-preparations of selected colonies were performed to isolate small amounts of DNA for further characterization. This method was modified from that provided by the supplier of the in vitro translation kit (Promega) that was ultimately used to produce probes from the sequences cloned into pET16b. Each colony was streaked on a second LB-ampicillin plate and inoculated into 5ml of LB medium containing ampicillin. The liquid cultures were left overnight at 37°C in a shaking incubator and the plates were also incubated overnight at 37°C. A 1.5ml aliquot of each culture was placed into a microcentrifuge tube and centrifuged at 12000 *g* for one minute. The remainder of each culture was stored at 4°C to inoculate a larger culture volume if needed. The LB medium was aspirated from the pellet of bacteria leaving it as dry as possible. The bacterial pellet was resuspended in

Table VI-4 Primers used to create expression constructs of *vg* and *sd*.

Primer name	Sequence 5' → 3'	Melting temperature (Tm)
sd 5' *Bam*HI	GGGGATCCGAAAAACATCACCAGCT	69°C
sd 3' *Bam*HI	GGCGGATCCATGCAGCTTTTGCTAT	69°C
sd C-term *Bam*HI #1	GGGGATCCAAATCCAGAGAGATGA	74°C
sd C-term *Bam*HI #2	GGGGATCCTCTGGATTTCCATGAA	74°C
vg cDNA 5' *Bam*HI	GCTGGATCCTGCGACAATGGCAGT	71°C
vg cDNA 3' *Bam*HI	CCAGGATCCGTTTAGAACCAGTAAA	71°C
*vg*ΔHA *Spe*I 3'	CGACTAGTGGAGTACTCCAGCTAT	68°C
*vg*ΔHA *Spe*I 5'	GCCACTAGTCCATACAAGTCGCTA	68°C
vg deletion primer#3	GGCACTAGTTCCTCGAGCATATGA	74°C
vg deletion primer #4	CCACTAGTGGAATCGTCGAAGGAT	74°C
vg deletion primer #5	CCACTAGTATCGGTGAGCGCAAAT	74°C
vg deletion primer #6	GCACTAGTACACACGCATACGCAT	74°C
vg deletion primer #7	GGACTAGTGGGACAGGCTCAATAT	74°C
vg deletion primer #8	CGCACTAGTATGAGGTCCTCTTCT	74°C
vg deletion primer#9	GGACTAGTTTACGTGCACCCCATA	74°C
vg deletion primer #10	CCCACTAGTGAGGCCGATAGATAT	74°C

Figure VI-4 Constructs containing the *vg* ORF that allow for bacterial or *in vitro* expression of full-length *vg* protein.

The fragment corresponding to the *vg* ORF begins at the newly introduced *Bam*HI site immediately 5' of the *vg* origin of translation.

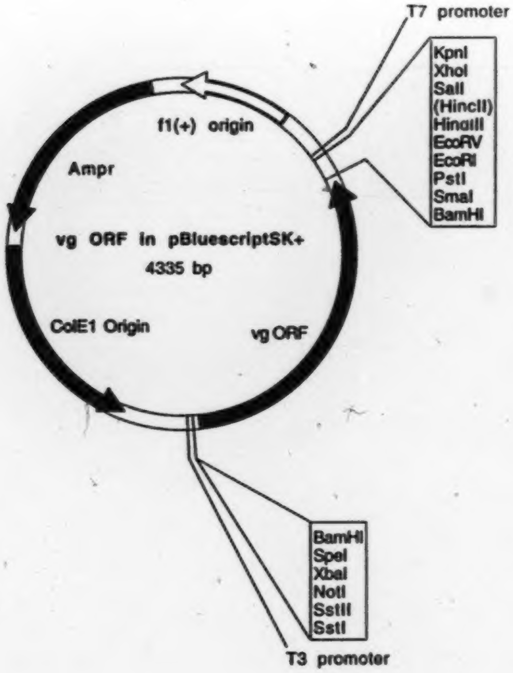
T7 promoter
KpnI
XhoI
SalI
(HincII)
HindIII
EcoRV
EcoRI
PstI
SmaI
BamHI
f1(+) origin
Ampr
vg ORF in pBluescriptSK+
4335 bp
ColE1 Origin
vg ORF
BamHI
SpeI
XbaI
NotI
SstII
SstI
T3 promoter

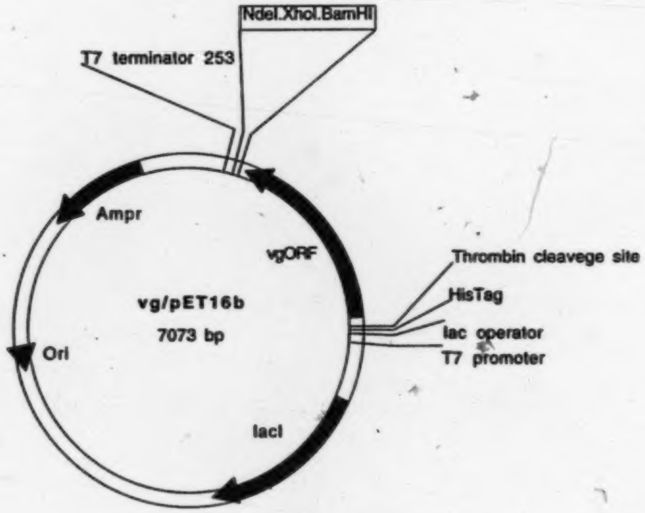
NdeI.XhoI.BamHI
T7 terminator 253
Ampr
vgORF
Thrombin cleavege site
HisTag
lac operator
T7 promoter
vg/pET16b
7073 bp
Ori
lacI

Figure VI-5 Constructs containing the *sd* ORF to allow for bacterial or *in vitro* expression of *sd* protein.

The fragment corresponding to the *sd* ORF begins at the newly introduced *Bam*HI site immediately 5' of the *sd* origin of translation.

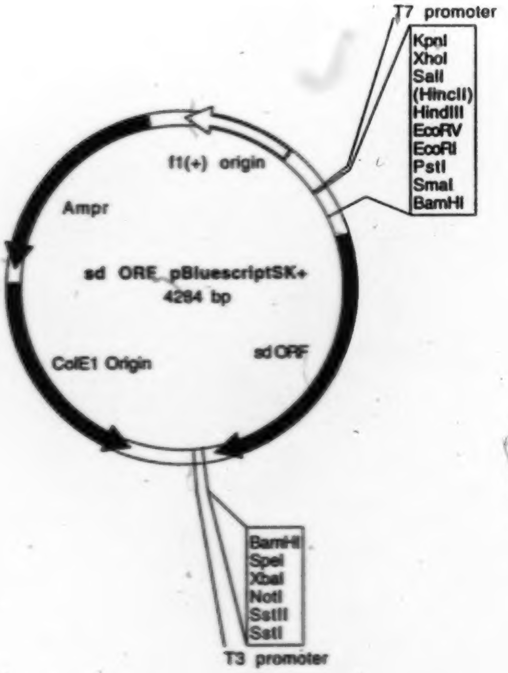
T7 promoter
KpnI
XhoI
SalI
(HincII)
HindIII
EcoRV
EcoRI
PstI
SmaI
BamHI
f1(+) origin
Ampr
sd ORF pBluescriptSK+
4284 bp
ColE1 Origin
sd ORF
BamHI
SpeI
XbaI
NotI
SstII
SstI
T3 promoter

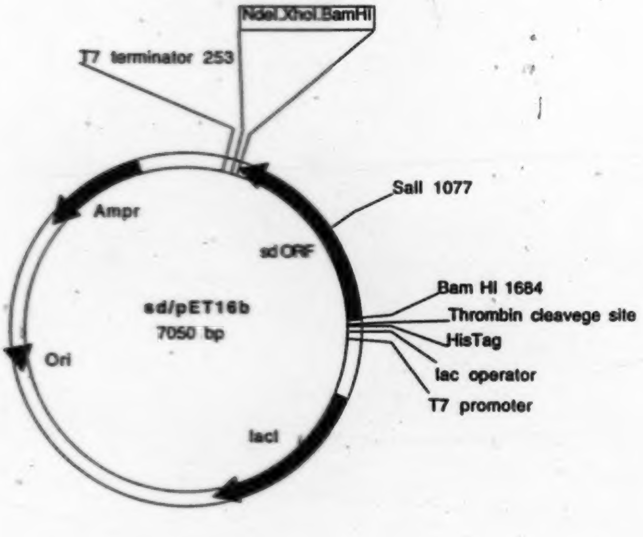
NdeI,XhoI,BamHI
T7 terminator 253
SalI 1077
Ampr
sd ORF
sd/pET16b
7050 bp
Bam HI 1684
Thrombin cleavege site
HisTag
Ori
lac operator
T7 promoter
lacI

100µl of ice-cold lysis buffer (25mM Tris-HCl pH 8.0, 10mM EDTA and 50mM glucose) and incubated five minutes at room temperature. Following this, 200µl of a freshly prepared 0.2N NaOH and 1% SDS, mixed by inversion and incubated 5 minutes on ice. 150µl of ice cold potassium acetate pH 4.8 solution was added and the tube was mixed by gentle inversion tube five or six times. The tubes were then centrifuged at 12 000 *g* for five minutes at 4°C. The supernatant was then transferred to a fresh tube. RNase A was then added to a final concentration of 20µg/ml and the samples were incubated for 20 minutes at 37°C.

The samples were extracted twice with phenol/chloroform:isoamyl alcohol (25/24:1) and once with 1volume of chloroform:isoamyl alcohol (24:1). Plasmid DNA was then precipitated by the addition of 2.5 volumes of absolute ethanol and incubated for five minutes on dry ice. The DNA was pelleted by centrifugation at 12 000*g* for five minutes, washed in 70% ethanol, dried five minutes, and resuspended in 30µl of TE. Aliquots of 3µl were incubated with appropriate restriction enzymes to determine the presence and orientation of the inserted DNA. Large-scale preparations of desired plasmids were performed using Quiagen Maxi-Prep columns following the manufacturer's instructions.

Far-Western Blot Analysis

Parallel induced and un-induced samples of bacterially expressed *vg* and *vg* protein was separated by electrophoresis on a 0.5mm 10% SDS-PAGE gel at 195V until the sample dye had completely run off. The proteins were then electrophoretically transferred to a supported nitrocellulose membrane in ice cold transfer buffer, (12.1g Tris-HCl, 57.7g glycine, 800ml methanol in a total volume of 4L in H_2O), for 45 min at 95V. The bound proteins were then immediately denatured in AC buffer containing 6M Guanidine-HCl and 1mM DTT and then renatured in a similar series of 3M, 1M and 0.1M Guanidine-HCl solutions. This allows proteins that are bound to the membrane to refold to a structure that more closely approximates their native form. Following this, the membrane was blocked overnight in AC solution (10% Glycerol, 100 mM NaCl, 20mM Tris pH 7.6, 0.5mM EDTA and 0.1% Tween-20) containing 2% skim milk powder (BLOTTO) on a shaking platform at 4°C.

A ^{35}S-methionine labeled protein probe was made using *in vitro* transcription and reticulocyte lysate translation. 1-2 µg of a plasmid containing the *sd* or *vg* pET16b expression vector was added to 25µl of rabbit reticulocyte lysate (Promega), 2µl of transcription buffer, 1 µl T7 RNA polymerase, 1µl amino acid mix (minus methionine), 1µl placental RNase inhibitor, 4µl of ^{35}S-methionine and water to 50µl total volume. This reaction was allowed to proceed 70 minutes at room temperature. Un-incorporated protein was removed by running each reaction through a Sephadex G25 spin column made in a 10cc syringe and washed three times in 100 µl AC buffer (spin 2000rpm for 3 minutes). The reaction mix is diluted to 100 µl in AC buffer and run through the column as above collecting the eluate in a 1.5 ml tube. This is then added to 10ml AC buffer containing 2% BLOTTO and 1mM DTT.

The blocking solution was removed from the blot, replaced with the probe solution and incubated on a rocking platform at 4°C for 3 hours. Following incubation in labeled probe, this solution was removed and the blot rinsed twice in AC-Wash buffer, (AC buffer, and 1mM DTT). The membrane was further washed in AC-Wash buffer plus 2% BLOTTO for 15 minutes. Finally the membrane was incubated four times for twenty minutes in AC-wash buffer for a total of 80 minutes. The membrane was dried at room temperature and exposed to Kodak BioMax X-Ray film for 12 to 48 hours depending upon the signal strength.

Bibliography

Abrams, J. M., White, K., Fessler, L. I., and Steller, H. (1993). Programmed cell death during *Drosophila* embryogenesis. Development *117*, 29-43.

Agrawal, N., Joshi, S., Kango, M., Saha, D., Mishra, A., and Sinha, P. (1995). Epithelial hyperplasia of imaginal discs induced by mutation in *Drosophila* tumor suppressor genes: growth and pattern formation in genetic mosaics. Developmental Biology *169*, 387-396.

Alexandrov, I. D., and Alexandrova, M. D. (1988). A new *nw* allele and interallelic complementation at the *vg* locus of *Drosophila melanogaster*. Drosophila Information Service *66*, 11.

Anand, A., Fernandes, J., Arunan, M. C., Bhosekar, S., Chopra, A., Dedhia, N., Sequiera, K., Hasan, G., Palazzolo, M. J., Raghavan, K. V., and Rodrigues, V. (1990). Drosophila "enhancer trap" transposants: Gene expression in chemosensory and motor pathways and identification of mutants affected in smell and taste ability. Journal of Genetics *69*, 151-168.

Anderson, D. T. (1972). The development of hemimetabolous insects. In Developmental systems: Insects, S. Counce and C. H. Waddington, eds. (New York: Academic Press), pp. 96-242.

Ashburner, M. (1989). *Drosophila*: A laboratory handbook (New York: Cold Spring Harbor Laboratory Press).

Basler, K., and Struhl, G. (1994). Compartment boundaries and the control of *Drosophila* limb pattern by the *hedgehog* protein. Nature *368*, 208-214.Bate, M., and Martinez Arias, A. (1991). The embryonic origin of imaginal discs in *Drosophila*. Development *112*, 755-761.

Bettler, D., Pearson, S., and Yedvobnick, B. (1996). The nuclear protein encoded by the Drosophila neurogenic gene *mastermind* is widely expressed and associates with specific chromosomal regions. Genetics *143*, 859-875.

Blackman, R. K., Sanicola, M., Raftery, L. A., Gillevet, T., and Gelbart, W. M. (1991). An extensive 3' *cis*-regulatory region directs the imaginal disc expression of *decapentaplegic*, a member of the TGF-β family in *Drosophila*. Development *111*, 657-665.

Blair, S. S. (1992). *engrailed* expression in the anterior lineage compartment of the developing wing blade of *Drosophila*. Development *115*, 21-33.

Blair, S. S. (1994). A role for the segment polarity gene *shaggy-zeste white 3* in the specification of regional identity in the developing wing of *Drosophila*. Developmental Biology *162*, 229-244.

Blair, S. S. (1995). Compartments and appendage development in *Drosophila*. BioEssays *17*, 299-309.

Blatt, C., and DePamphilis, M. L. (1993). Striking homology between mouse and human transcription enhancer factor-1 (TEF-1). Nucleic Acids Research *21*, 747-748.

Bownes, M., and Roberts, S. (1981a). Analysis of *vestigial*^{W} *vg(W)*: a mutation causing homeosis of haltere to wing and posterior wing duplications in *Drosophila melanogaster*. Journal of Embryology and Experimental Morphology *65(Sup)*, 49-76.

Bownes, M., and Roberts, S. (1981b). Regulative properties of wing discs from the *vestigial* mutant of *Drosophila melanogaster*. Differentiation *18*, 89-96.

Brand, A. H., and Perrimon, N. (1993). Targeted gene expression as a means of altering cell fates and generating dominant phenotypes. Development *118*, 401-415.

Bridges, C., and Morgan, T. H. (1919). *vestigial*. Carnegie Inst. Wash. Yearbook. *278*, 150.

Brower, D. L. (1984). Posterior-to-anterior transformation in *engrailed* wing imaginal disks of *Drosophila*. Nature *310*, 496-497.

Brower, D. L. (1986). *engrailed* gene expression in *Drosophila* imaginal discs. EMBO Journal *5*, 2649-2656.

Brower, D. L., Smith, R. J., and Wilcox, M. (1982). Cell shapes on the surface of the *Drosophila* wing imaginal disc. Journal of Embryology and Experimental Morphology *67*, 137-151.

Bryant, P. J. (1975). Pattern formation in the imaginal wing disc of *Drosophila melanogaster*: fate map, regeneration and duplication. Journal of Experimental Zoology *193*, 49-78.

Bryant, P. J. (1978). Pattern formation in imaginal discs. In The genetics and biology of *Drosophila*, M. Ashburner and T. R. F. Wright, eds. (New York: Academic Press), pp. 229-335.

Bryant, S. V., French, V., and Bryant, P. J. (1981). Distal regeneration and symmetry. Science *212*, 993-1002.

Bürglin, T. R. (1991). The TEA domain: a novel, highly conserved DNA-binding motif. Cell *66*, 11-12.

Busturia, A., and Morata, G. (1988). Ectopic expression of homeotic genes caused by the elimination of the *Polycomb* gene in *Drosophila* imaginal epidermis. Development *104*, 713-720.

Campbell, G., Orr-Weaver, T., and Tomlinson, A. (1993). Axis specification in the Developing *Drosophila* appendage: the role of *wingless*, *decapentaplegic*, and the homeobox gene *aristaless*. Cell *74*, 1113-1123.

Campbell, S., Inamdar, M., Rodrigues, V., Raghavan, V., Palazzolo, M., and Chovnick, A. (1992). The *scalloped* gene encodes a novel, evolutionarily conserved transcription factor required for sensory organ differentiation in *Drosophila*. Genes & Development *6*, 367-379.

Campbell, S. D., Duttaroy, A., Katzen, A. L., and Chovnick, A. (1991). Cloning and characterization of the scalloped region of Drosophila melanogaster. Genetics *127*, 367-380.

Capdevila, J., Estrada, M. P., Sanchez-Herrero, E., and Guerrero, I. (1994). The *Drosophila* segment polarity gene *patched* interacts with *decapentaplegic* in wing development. EMBO Journal *13*, 71-82.

Carroll, S. B., Weatherbee, S. D., and Langeland, J. A. (1995). Homeotic genes and the regulation and evolution of insect wing number. Nature *375*, 58-61.

Cohen, B., McGuffin, M. E., Pfeifle, C., Segal, D., and Cohen, S. M. (1992). *apterous*, a gene required for imaginal disc development in *Drosophila*, encodes a member of the LIM family of developmental regulatory proteins. Genes & Development *6*, 715-729.

Cohen, B., Simcox, A. A., and Cohen, S. M. (1993). Allocation of the imaginal primordia in the *Drosophila* embryo. Development *117*, 567-608.

Cohen, S. M. (1993). Imaginal disc development. In The development of *Drosophila melanogaster*, A. Martinez-Arias and M. Bate, eds. (New York: Cold Spring Harbor Laboratory Press), pp. 471-475.

Cohen, S. M. (1996). Controlling growth of the wing: Vestigial integrates signals from the compartment boundaries. BioEssays *18*, 855-858.

Cohen, S. M., Bronner, G., Kuttner, F., Jurgens, G., and Jackle, H. (1989). *Distal-less* encodes a homeodomain protein required for limb development in *Drosophila*. Nature *338*, 432-434.

Cohen, S. M., and Jürgens, G. (1989). Proximal-distal pattern formation in *Drosophila*: graded requirement for *Distal-less* gene activity during limb development. Wilhelm Roux's Archives of Developmental Biology *198*, 157-169.

Coleman, K. G., Poole, S. J., Weir, M. P., Soeller, W. C., and Kornberg, T. (1987). The *invected* gene of *Drosophila*: sequence analysis and expression studies reveal a close kinship to the *engrailed* gene. Genes & Development *1*, 19-28.

Couso, J. P., Bishop, S. A., and Martinez-Arias, A. (1994). The *wingless* signaling pathway and the patterning of the wing margin in *Drosophila*. Development *120*, 621-636.

Couso, J. P., Knust, E., and Martinez-Arias, A. (1995). *Serrate* and *wingless* cooperate to induce *vestigial* gene expression and wing formation in *Drosophila*. Current Biology *5*, 1437-1448.

de Cellis, J. F., de Cellis, J., Ligoxygakis, P., Preiss, A., Delidakis, C., and Bray, S. (1996a). Functional relationships between *Notch*, *Su(H)* and the bHLH genes of the *E(spl)* complex: the *E(spl)* genes mediate only a subset of *Notch* activities during imaginal development. Development *122*, 2719-2728.

de Cellis, J. F., Garcia-Bellido, A., and Bray, S. J. (1996b). Activation and function of *Notch* at the dorsal-ventral boundary of the wing imaginal disc. Development *122*, 359-363.

DeCamillis, M., Cheng, N., Pierre, D., and Brock, H. W. (1992). The *polyhomeotic* gene of *Drosophila* encodes a chromatin protein that shares polytene chromosome binding sites with *Polycomb*. Genes & Development *6*, 223-232.

Demerec, M. (1965). *Biology* of *Drosophila* (New York: Hafner Publishing Co.).

Diaz-Benjumea, F. J., and Cohen, S. M. (1993). Interaction between dorsal and ventral cells in the imaginal disc directs wing development in *Drosophila*. Cell *75*, 741-752.

Diaz-Benjumea, F. J., and Cohen, S. M. (1995). Serrate signals through Notch to establish a Wingless-dependent organizer at the dorsal/ventral compartment boundary of the *Drosophila* wing. Development *121*, 4215-4225.

Doherty, D., Feger, G., Younger-Shephard, S., Jan, L. Y., and Jan, Y. N. (1996). *Delta* is a ventral to dorsal signal complementary to *Serrate*, another *Notch* ligand, in *Drosophila* wing formation. Genes & Development *10*, 421-434.

Dolecki, G. J., and Humphreys, T. (1988). An engrailed class homeobox gene from sea urchins. Gene *64*, 21-31.

Dominguez, M., Brunner, M., Hafen, E., and Basler, K. (1996). Sending and receiving the Hedgehog signal: control by the *Drosophila* Gli protein Cubitus interruptus. Science *272*, 1621-1625.

Eaton, S., and Kornberg, T. B. (1990). Repression of *ci-D* in posterior compartments of *Drosophila* by *engrailed.* Genes & Development *4*, 1068-1077.

Eker, R. (1929). The recessive mutant *engrailed* in *Drosophila melanogaster.* Hereditas *12*, 217-222.

Ekker, M., Wegner, J., Akimenko, M. A., and Westerfield, M. (1992). Coordinate embryonic expression of three zebrafish *engrailed* genes. Development *116*,1001-1010.

Fessler, L. I., Condic, M. L., Nelson, J., Fessler, J. H., and Fristrom, J. W. (1993). Site-specific cleavage of basement membrane collagen IV during *Drosophila* metamorphosis. Development *117*, 1061-1069.

Fields, S., and Song, O. (1989). A novel genetic system to detect protein-protein interactions. Nature *340*, 245-246.

Fjose, A., Njølstad, P. R., Nornes, S., Molven, A., and Krauss, S. (1992). Structure and early embryonic expression of the zebrafish engrailed-2 gene. Mechanisms of Development *36*, 51-62.

Fleming, R. J., Scottgale, T. N., Diederich, R. J., and Artavanis-Tsakonas, S. (1990). The gene *Serrate* encodes a putative EGF-like transmembrane protein essential for proper ectodermal development in *Drosophila melanogaster.* Genes & Development *4*, 2188-2201.

French, V., Bryant, P. J., and Bryant, S. V. (1976). Pattern regulation in epimorphic fields. Science *193*, 969-981.

Fristrom, D. (1968). Cellular degeneration in wing development of the mutant *vestigial* of *Drosophila melanogaster.* Journal of Cell Biology *39*, 488-491.

Fristrom, D. (1969). Cellular degeneration in the production of some mutant phenotypes of *Drosophila melanogaster.* Molecular & General Genetics *103*, 363-391.

Fuse, N., Hirose, S., and Hayashi, S. (1996). Determination of wing cell fate by the *escargot* and *snail* genes in *Drosophila.* Development *112*, 1059-1067.

Garcia Bellido, A. (1975). Genetic control of wing disc development in *Drosophila.* Ciba Foundation Symposia *29,* 161-182.

Garcia Bellido, A. (1977). Homeotic and atavic mutation in insects. American Zoologist *17*, 613-630.

Garcia Bellido, A., and Merriam, J. (1969). Cell lineage of the imaginal discs in *Drosophila* gynadromorphs. Journal of Experimental Zoology *170*, 61-76.

Garcia Bellido, A., Ripoll, P., and Morata, G. (1973). Developmental compartmentalization of the wing disc of *Drosophila.* Nature New Biology *245*, 251-253.

Garcia Bellido, A., Ripoll, P., and Morata, G. (1976). Developmental compartmentalization in the dorsal mesothoracic disc of *Drosophila.* Developmental Biology *48*, 132-147.

Garcia Bellido, A., and Santamaria, P. (1972). Developmental analysis of the wing disc in the mutant *engrailed* of *Drosophila melanogaster.* Genetics *72*, 87-104.

Girton, J. R., and Bryant, P. J. (1980). The use of cell lethal mutations in the study of *Drosophila* development. Developmental Biology *77*, 233-243.

Goldschmidt, R. (1937). Gene and character. V. Further data on the *vg* dominigenes in *Drosophila melanogaster.* University of California: Zoology Publications *41*, 285-296.

Green, M. M. (1946). A study in gene action using different dosages and alleles of *vg* in *Drosophila melanogaster.* Genetics *31*, 1-20.

Green, M. M., and Oliver, C. P. (1940). The action of certain mutants upon the penetrance of heterozygous vestigial wing in *Drosophila.* Genetics *25*, 584-592.

Gubb, D. (1985). Further studies on *engrailed* mutants in *Drosophila melanogaster*. Roux's Archives of Developmental Biology *194*, 236-246.

Gúillen, I., Mullor, J. L., Capdevila, J., Sanchez-Herrero, E., Morata, G., and Guerrero, I. (1995). The function of *engrailed* and the specification of *Drosophila* wing pattern. Development *121*, 3447-3456.

Hadorn, E. (1978). Transdetermination. In The genetics and biology of *Drosophila*, M. Ashburner and T. R. F. Wright, eds. (New York: Academic Press), pp. 555-617.

Halder, G., Callaerts, P., and Gehring, W. J. (1995). Induction of ectopic eyes by targeted expression of the *eyeless* gene in *Drosophila*. Science *267*, 1788-1792.

Hama, C., Ali, Z., and Kornberg, T. B. (1990). Region-specific recombination and expression are directed by portions of the Drosophila *engrailed* promoter. Genes & Development *4*, 1079-1093.

Hartenstein, V. (1993). Atlas of Drosophila development (Plainsview, N.Y.: Cold Spring Harbor Laboratory Press).

Heemskerk, J., and DiNardo, S. (1994). Drosophila *hedgehog* acts as a morphogen in cellular patterning. Cell *76*, 449-460.

Hemmati-Brivanlou, A., de la Torre, J., Holt, C., and Harland, R. M. (1991). Cephalic expression and molecular characterization of *Xenopus En-2*. Development *111*, 715-724.

Hidalgo, A. (1994). Three distinct roles for the *engrailed* gene in *Drosophila* wing development. Current Biology *4*, 1087-1098.

Hodgkin, J. (1993). Doses and poisons: molecular perspectives on dominance. Trends in Genetics *9*, 1-2.

Holland, P. W. H., and Williams, N. A. (1990). Conservation of *engrailed*-like sequences during vertebrate evolution. FEBS Letters *227*, 250-252.

Huet, F., Ruiz, C., and Richards, G. (1993). Puffs and PCR: the in vivo dynamics of early gene expression during ecdysone responses in *Drosophila*. Development *118*, 613-627.

Hui, C. C., Matsuno, K., Ueno, K., and Suzuki, Y. (1992). Molecular characterization and silk gland expression of Bombyx *engrailed* and *invected* genes. Proceedings of the National Academy of Sciences of the United States of America *89*, 167-171.

Inamdar, M., Vajayraghavan, K., and Rodrigues, V. (1993). The Drosophila homologue of human transcription factor, TEF-1, scalloped is essential for normal taste behaviour. Journal of Neurogenetics *9*, 123-139.

Irvine, K. D., and Wieschaus, E. (1994). *fringe*, a boundary-specific signaling molecule, mediates interactions between dorsal and ventral cells during *Drosophila* wing development. Cell *79*, 595-606.

Ives, P. T. (1956). vgU: Ultravestigial. Drosophila Information Service *30*, 72-73.

Jack, J., and DeLotto, Y. (1992). Effect of wing scalloping mutations on cut expression and sense organ differentiation in the Drosophila wing margin. Genetics *131*, 353-363.

James, A. A., and Bryant, P. (1981). Mutations causing pattern deficiencies and duplications in the imaginal wing disc of *Drosophila melanogaster*. Developmental Biology *85*, 39-54.

Jiang, J., and Struhl, G. (1995). Protein kinase A and *hedgehog* signaling in *Drosophila* limb development. Cell *80*, 563-572.

Joyner, A. L., Kornberg, T., Coleman, K. G., Cox, D. R., and Martin, G. R. (1985). Expression during embryogenesis of a mouse gene with sequence homology to the Drosophila engrailed gene. Cell *43*, 29-37.

Joyner, A. L., and Martin, G. R. (1987). En-1 and En-2, two mouse genes with sequence homology to the *Drosophila engrailed* gene: expression during embryogenesis . Genes & Development *1*, 29-38.

Kassis, J. A., Noll, E., VanSickle, E. P., Odenwald, W. F., and Perrimon, N. (1992). Altering the insertional specificity of a *Drosophila* transposable element. Proceedings of the National Academy of Sciences of the United States of America *89*, 1919-1923.

Kim, J., Irvine, K. D., and Carroll, S. B. (1995). Cell recognition, signal induction and symmetrical gene activation at the dorsal-ventral boundary of the developing *Drosophila* wing. Cell *82*, 795-802.

Kim, J., Sebring, A., Esch, J. J., Kraus, M. E., Vorwerk, K., Magee, J., and Carroll, S. B. (1996). Integration of positional signals and regulation of wing formation and identity by *Drosophila vestigial* gene. Nature *382*, 133-138.

Kim, S. J., Lee, C. C., and Paik, S. G. (1987). The effects of temperature on the developmental profiles of glycerol-3-phosphate dehydrogenase and lactate dehydrogenase during the development of *vestigial* mutant of *Drosophila melanogaster*. Korean Journal of Genetics *9*, 153-162.

Kornberg, T. (1981a). Compartments in the abdomen of *Drosophila* and the role of the *engrailed* locus. Developmental Biology *86*, 363-372.

Kornberg, T. (1981b). *Engrailed*: a gene controlling compartment and segment formation in *Drosophila*. Proceedings of the National Academy of Sciences of the United States of America *78*, 1095-1099.

Kornberg, T., Siden, I., O'Farrell, P., and Simon, M. (1985). The *engrailed* locus of *Drosophila*: in situ localization of transcripts reveals compartment-specific expression. Cell *40*, 45-53.

Laloux, I., Dubois, E., Dewwecgub, M., and Jacobs, E. (1990). *TEC1*, a gene involved in the activation of *Ty1* and *Ty1*-mediated gene expression in *Saccharomyces cerevisiae*: Cloning and molecular analysis. Molecular and Cellular Biology *10*, 3541-3550.

Lasko, P. F., and Pardue, M. L. (1988). Studies of the genetic organization of the *vestigial* microregion of *Drosophila melanogaster*. Genetics *120*, 495-502.

Lawrence, P. A., and Morata, G. (1976). Compartments in the wing of *Drosophila*: a study of the *engrailed* gene. Developmental Biology *50*, 321-337.

Lawrence, P. A., and Sampedro, J. (1993). Drosophila segmentation: after the first three hours. Development *119*, 971-976.

Lawrence, P. A., and Struhl, G. (1982). Further studies of the *engrailed* phenotype in *Drosophila*. EMBO Journal *7*, 827-833.

Lecuit, T., Brook, W. J., Ng, M., Calleja, M., Sun, H., and Cohen, S. M. (1996). Two distinct mechanisms for long-range patterning by Decapentaplegic in the *Drosophila* wing. Nature *381*, 387-393.

Lee, J. J., von Kessler, D. P., Parks, S., and Beachy, P. A. (1992). Secretion and localized transcription suggest a role in positional signalling for products of the segmentation gene *hedgehog*. Cell *71*, 33-50.

Lewis, E. B. (1978). A gene complex controlling segmentation in *Drosophila*. Nature *276*, 565-570.

Lindsley, D. L., and Zimm, G. G. (1992). The genome of *Drosophila melanogaster* (San Diego: Academic Press).

Logan, C., Hanks, M. C., Noble-Topman, S., Nallainathan, D., Provart, N. J., and Joyner, A. L. (1992). Cloning and sequence comparison of the mouse, human and chicken *engrailed* genes reveal potential domains and regulatory domains. Developmental Genetics *13*, 345-358.

Lohs-Schardin, M., Sander, K., Cremer, C., Cremer, T., and Zorn, C. (1979). Localized ultraviolet laser microbeam irradiation of early Drosophila embryos: Fate maps based on localization and frequencies of adult defects. Developmental Biology *68*, 533-545.

Madhavan, M., and Schneiderman, H. A. (1978). Histological analysis of the dynamics of growth of imaginal discs and histoblast nests during the larval development of *Drosophila melanogaster*. Wilhelm Roux's Archives of Developmental Biology *183*, 269-306.

Manzanares, M., Marco, R., and Garesse, R. (1993). Genomic organization and developmental pattern of expression of the *engrailed* gene from the brine shrimp *Artemia*. Development *118*, 1209-1219.

Mardon, G., Solomon, N. M., and Rubin, G. M. (1994). *dachshund* encodes a nuclear protein required for normal eye and leg development in *Drosophila*. Development *120*, 3473-3486.

Massucci, J. D., Miltenberger, R. J., and Hoffman, F. M. (1990). Pattern-specific expression of the Drosophila *decapentaplegic* gene in imaginal discs is regulated by 3' cis-regulatory elements. Genes & Development *4*, 2011-2023.

Maves, L., and Schubiger, G. (1995). wingless induces transdetermination in developing Drosophila wing discs. Development *121*, 1263-1272.

Meinhardt, H. (1982). Generation of structures in a developing organism. In Developmental Order: Its Origin and Regulation, S. Subtelny and P. Green, eds. (New York: Alan R. Liss).

Meinhardt, H. (1983). Cell determination boundaries as organizing regions for secondary embryonic fields. Developmental Biology *96*, 375-385.

Merrill, V. K., Diederich, R. J., Turner, F. R., and Kaufman, T. C. (1989). A genetic and developmental analysis of mutations in *labial*, a gene necessary for proper head formation in *Drosophila melanogaster*. Developmental Biology *135*, 367-391.

Merrill, V. K., Turner, F. R., and Kaufman, T. C. (1987). A genetic and developmental analysis of mutations in the *Deformed* locus in *Drosophila melanogaster*. Developmental Biology *122*, 367-391.

Mglinetz, V. A., and Balakireva, M. D. (1982). Notum duplication: a homeotic effect of *vestigial* in Drosophila? Genetika, Moscow *18*, 1481-1488.

Mirabato, P. M., Adams, T. H., and Timberlake, W. E. (1989). Interactions of three sequentially expressed genes control temporal and spatial specificity in *Aspergillus* development. Cell *57*, 859-868.

Morata, G. (1993). Homeotic genes of Drosophila. Current Opinion in Genetics and Development *3*, 606-614.

Morata, G., and Lawrence, P. A. (1975). Control of compartment development by the engrailed gene of *Drosophila*. Nature *255*, 614-617.

Morcillo, P., Rosen, C., and Dorsett, D. (1996). Genes regulating the remote wing margin enhancer in the Drosophila *cut* locus. Genetics *144*, 1143-1154.

Morgan, T. H. (1911). The origin of nine wing mutations in *Drosophila*. Science *33*, 496-498.

Morgan, T. H., Bridges, C. B., and Schultz, J. (1938). Constitution of the germinal material in relation to heredity. Carnegie Institute (Washington) Year Book *37*, 298-309.

Mortin, M. A., and Lefevre, G. (1981). An RNA polymerase II mutation in *Drosophila melanogaster* that mimics *Ultrabithorax*. Chromosoma *82*, 237-247.

Nakashima-Tanaka, E. (1968). The effect of temperature and genetic background on the phenotypic expression of several *vestigial* strains of *Drosophila melanogaster*. Genetica *38*, 447-458.

Nash, D., and Bell, J. B. (1968). Larval age and the pattern of DNA synthesis in polytene chromosomes. Canadian Journal of Genetics and Cytology *10*, 82-92.

Nellen, D., Burke, R., Struhl, G., and Basler, K. (1996). Direct and long-range action of a Dpp morphogen gradient. Cell *85*, 387-393.

Neumann, C. J., and Cohen, S. M. (1996a). Distinct mitogenic and cell fate specification functions of *wingless* in different regions of the wing. Development *122*, 1781-1789.

Neumann, C. J., and Cohen, S. M. (1996b). A hierarchy of cross-regulation involving *Notch*, *wingless*, *vestigial* and *cut* organizes the dorsal/ventral axis of the *Drosophila* wing. Development *122*, 3477-3485.

Ng, M., Diaz-Benjumea, F. J., and Cohen, S. M. (1995). nubbin encodes a POU-domain protein required for proximal-distal patterning in the Drosophila wing. Development *121*, 589-599.

Ng, M., Diaz-Benjumea, F. J., Vincent, J., Wu, J., and Cohen, S. M. (1996). Specification of the wing by localized expression of *wingless* protein. Nature *381*, 316-318.

Nöthiger, R. (1972). The larval development of imaginal discs. In The biology of imaginal discs, H. Ursprung and R. Nöthiger, eds. (New York: Springer-Verlag), pp. 1-34.

Nüsslein-Volhard, C., and Wieschaus, E. (1980). Mutations affecting segment number and polarity in Drosophila. Nature *287*, 795-801

O'Brochta, D. A. (1980). Cell degeneration in *vestigial* mutant of *Drosophila melanogaster*. American Zoologist *20*, 913.

O'Brochta, D. A., and Bryant, P. J. (1983). Cell degeneration and elimination in the imaginal wing disc caused by the mutations *vestigial* and *Ultravestigial* of *Drosophila melanogaster*. Roux's Archives of Developmental Biology *192*, 285-294.

Orenic, T. V., Slusarski, D. C., Kroll, K. L., and Holmgren, R. A. (1990). Cloning and characterization of the segment polarity gene *cubitus interruptus Dominant* of *Drosophila*. Genes & Development *4*, 1053-1067.

Pan, D., and Rubin, G. (1995). cAMP-dependant protein kinase and *hedgehog* act antagonistically in regulating *decapentaplegic* transcription in *Drosophila* imaginal discs. Cell *80*, 543-552.

Panganiban, G., Nagy, L., and Carroll, S. B. (1994). The role of the *Distal-less* gene in the development and evolution of insect limbs. Current Biology *4*, 671-675.

Patel, N. H., Martin-Blanco, E., Coleman, K. G., Poole, S. J., Ellis, M. G., Kornberg, T. B., and Goodman, C. S. (1989). Expression of engrailed proteins in arthropods, annelids and chordates. Cell *58*, 955-968.

Pattatucci, A., and Kaufmann, T. (1991). The homeotic gene *sex combs-reduced* of *Drosophila melanogaster* is differentially regulated in the embryonic and imaginal stages of development. Genetics *129*, 443-461.

Phillips, R., and Whittle, R. (1993). *wingless* expression mediates determination of peripheral nervous system elements in late stages of *Drosophila* wing disc development. Development *118*, 427-438.

Phillips, R. G., Roberts, I. J. H., Ingham, P. W., and Whittle, J. R. S. (1990). The *Drosophila* segment polarity gene *patched* is involved in a position-signalling mechanism in imaginal discs. Development, 105-114.

Poole, S. J., and Kornberg, T. B. (1988). Modifying expression of the *engrailed* gene of Drosophila melanogaster. Development, 85-93.

Rabinow, L., and Birchler, J. A. (1990). Interactions of *vestigial* and *scabrous* with the *Notch* locus of *Drosophila melanogaster*. Genetics *125*, 41-50.

Roberts, D. B. (1986). Drosophila : a practical approach (Oxford: IRL Press).

Sanicola, M., Sekelsky, J., Elson, S., and Gelbart, W. M. (1995). Drawing a stripe in *Drosophila* imaginal disks: negative regulation of *decapentaplegic* and *patched* expression by engrailed. Genetics *139*, 745-756.

Schmid, A. T., Tinley, T. L., and Yedvobnick, B. (1996). Transcription of the neurogenic gene *mastermind* during *Drosophila* development. Journal of Experimental Zoology *274*, 207-220.

Schwartz, C., Locke, J., Nishida, C., and Kornberg, T. B. (1995). Analysis of *cubitus interruptus* regulation in *Drosophila* embryos and imaginal discs. Development *121*, 1625-1635.

Serrano, N., Brock, H. W., Demeret, C., Dura, J., Randsholt, N., Kornberg, T. B., and Maschat, F. (1995). *polyhomeotic* appears to be a target of Engrailed regulation in *Drosophila*. Development *121*, 1691-1703.

Shukla, P. T. (1980). *Vestigial wingless*: A dominant allele of *vestigial* in *D. melanogaster*. Drosophila Information Service *55*, 210.

Simcox, A. A., Herpsperger, E., Shearn, A., Whittle, J. R. S., and Cohen, S. M. (1991). Establishment of imaginal discs and histoblast nests in Drosophila. Mechanisms of Development *34*, 11-20.

Simmonds, A. J., Brook, W. J., Cohen, S. M., and Bell, J. B. (1995). Distinguishable functions for *engrailed* and *invected* in anterior-posterior patterning in the *Drosophila* wing. Nature *376*, 424-427.

Simpson, P., Lawrence, P. A., and Maschat, F. (1981). Clonal analysis of two wing-scalloping mutants of *Drosophila*. Developmental Biology *84*, 206-211.

Smoller, D., Freidel, A., Schmid, A., Bettler, D., Lam, L., and Yedvobnick, B. (1990). The *Drosophila* neurogenic locus *mastermind* encodes a protein unusually rich in amino acid homopolymers. Genes and Development *4*, 1688-1700.

Tabata, T., Eaton, S., and Kornberg, T. (1992). The *Drosophila hedgehog* gene is expressed specifically in posterior compartment cells and is a target of *engrailed* regulation. Genes & Development *6*, 2635-2645.

Tabata, T., and Kornberg, T. B. (1994). Hedgehog is a signaling protein with a key role in patterning *Drosophila* imaginal discs. Cell *76*, 89-102.

Tabata, T., Schwartz, C., Gustavson, E., Ali, Z., and Kornberg, T. B. (1995). Creating a Drosophila wing de novo, the role of *engrailed*, and the compartment border hypothesis. Development *121*, 3359-3369.

Thomas, U., Jonsson, F., Speicher, S. A., and Knust, E. (1995). Phenotypic and molecular characterization of *Ser*^{D}, a dominant allele of the *Drosophila* gene *Serrate*. Genetics *139*, 203-213.

Tiong, S., Nash, D., and Bender, W. (1995). *Dorsal wing*, a locus that affects dorsoventral wing pattering in *Drosophila*. Development *121*, 1649-1656.

Tiong, S. Y. K., and Nash, D. (1990). Genetic analysis of the *adenosine 3* (*Gart*) region of the second chromosome of *Drosophila melanogaster*. Genetics *124*, 889-897.

Vachon, G., Cohen, B., Pfeifle, C., McGuffin, M. E., Botas, J., and Cohen, S. M. (1992). Homeotic genes in the bithorax complex repress limb development in the abdomen of the *Drosophila* embryo through the target gene *Distal-less*. Cell *71*, 437-450.

Verheyen, E., Purcell, K. J., Fortini, M., and Artavanis-Tsakonas, S. (1996). Analysis of dominant enhancers and suppressors of activated *Notch* in *Drosophila*. Genetics *144*, 1127-1141.

Vincent, J. P., and O'Farrell, P. H. (1992). The state of *engrailed* expression is not clonally transmitted during early *Drosophila* development. Cell *68*, 923-931.

Waldorf, U., Fleig, R., and Gehring, W. J. (1989). Comparison of the homeobox-containing genes of honeybee and *Drosophila*. Proceedings of the National Academy of Sciences of the United States of America *86*, 9971-9975.

Wedeen, C. J., Price, D. J., and Weisblat, D. A. (1991). Cloning and sequencing of a leech homologue to the *Drosophila engrailed* gene. FEBS Letters *279*, 300-302.

Wieschaus, E., and Gehring, W. (1976). Gynandromorph analysis of the thoracic disc primordia in *Drosophila melanogaster*. Wilhelm Roux's Archives of Developmental Biology *180*, 31-46.

Wilkins, A. S., and Gubb, D. (1991). Pattern formation in the embryo and imaginal discs of *Drosophila*: what are the links? Developmental Biology *145*, 1-12.

Williams, J. A., Atkin, A. L., and Bell, J. B. (1990a). The functional organization of the *vestigial* locus in *Drosophila melanogaster*. Molecular & General Genetics *221*, 8-16.

Williams, J. A., and Bell, J. B. (1988). Molecular organization of the *vestigial* region in *Drosophila melanogaster*. EMBO Journal *7*, 1355-1363.

Williams, J. A., Bell, J. B., and Carroll, S. B. (1991). Control of *Drosophila* wing and haltere development by the nuclear *vestigial* gene product. Genes & Development *5*, 2481-2495.

Williams, J. A., Paddock, S. W., and Carroll, S. B. (1993). Pattern formation in a secondary field: a hierarchy of regulatory genes subdivides the developing *Drosophila* wing disc into discrete sub-regions. Development *117*, 571-584.

Williams, J. A., Paddock, S. W., Vorwerk, K., and Carroll, S. B. (1994). Organization of wing formation and induction of a wing-patterning gene at the dorsal/ventral compartment boundary. Nature *368*, 299-305.

Williams, J. A., Pappu, S. S., and Bell, J. B. (1988). Molecular analysis of hybrid dysgenesis-induced derivatives of a P-element allele at the *vg* locus. Molecular & Cellular Biology *8*, 1489-1497.

Williams, J. A., Scott, I. M., Atkin, A. L., Brook, W. J., Russell, M. A., and Bell, J. B. (1990b). Genetic and molecular analysis of vg^U and vg^W: two dominant *vg* alleles associated with gene fusions in *Drosophila*. Genetics *125*, 833-844.

Wurst, W., Auerbach, A. B., and Joyner, A. L. (1994). Multiple developmental defects in *Engrailed-1* mutant mice: an early mid-hindbrain deletion and patterning defects in forelimbs and sternum. Development *120*, 2065-2075.

Xiao, J. H., Davidson, I., Matthes, H., Garnier, J., and Chambon, P. (1991). Cloning, expression and transcriptional properties of the human enhancer factor TEF-1. Cell *65*, 551-568.

Xu, T., Rebay, H., Fleiming, R., Scottgale, N., and Artavanis-Tsakonas, S. (1990). The *Notch* locus and the genetic circuitry involved in early *Drosophila* neurogenesis. Genes and Development *4*, 464-467.

Yedvobnick, B., Smoller, D., Young, P., and Mills, D. (1988). Molecular analysis of the neurogenic locus *mastermind* of *Drosophila melanogaster*. Genetics *118*, 483-497.

Zecca, M., Basler, K., and Struhl, G. (1995). Sequential organizing activities of engrailed, hedgehog and decapentaplegic in the *Drosophila* wing. Development *121*, 2265-2278.